Bolaamphiphiles

Jürgen-Hinrich Fuhrhop* and Tianyu Wang

Institut für Organische Chemie, Freie Universität Berlin, Takustrasse 3, D-14195 Berlin, Germany

Received October 22, 2003

Contents

1. Introduction

Bolaamphiphilic molecules contain a hydrophobic skeleton (e.g., one, two, or three alkyl chains, a steroid, or a porphyrin) and two water-soluble groups on both ends.[1−6] Bolaamphiphiles are related to and often combined with "edge amphiphiles", where one flank of a hydrophobic core carries hydrophilic groups whereas the other edge is hydrophobic (Figure 1). The terms "bolaform amphiphiles" or "bolaphiles" have also been used but do not make much sense. "Form" does not appear elsewhere in organic nomenclature, and a connection with "phile = friendly" makes sense with respect to a solvent ("amphiphile") or reaction center ("nucleophile") but not in connection with a noun describing a substitution pattern. If the 14-letter word "bolaamphiphile" becomes too cumbersome when it is repeated several times in an article, the abbreviation "bola" is appropriate. Charged bolas may be called "bolytes"; bolas with an α-glucose and an ω-lysine headgroup may be named "glucose−lysine bolas" in short; dyes with water-soluble substituents on opposite edges are "bola dyes", etc.

Synthetic bolaamphiphiles try to reproduce the unusual architecture of monolayered membranes found in archaebacteria but commonly do not use the same building blocks, which are difficult to synthesize.[7−9] The ester bonds found in membrane lipids of most other organisms as well as in common model bolas are replaced there by ether bonds, which let the archaebacteria survive in a volcanic environment, e.g., in hot sulfuric acid. The hydrophobic core usually contains several chiral methine groups with methyl substituents. They help to stiffen the membrane by helix formation within the macrocycles. If more fluid membrane parts are needed, contemporary biological organisms as well as synthetic chemists introduce cis-configured C=C double bonds into the hydrophobic core. This is not allowed for volcano inhabitants who

* To whom correspondence should be addressed. Phone: 49 030 83855394. Fax: 49 030 83855589. E-mail: fuhrhop@chemie.fu-berlin.de.

Jürgen-Hinrich Fuhrhop (right) was born in Berlin, Germany, in 1940 as a Kriegskind (warchild). Since his first review in this journal in 1993, p 1566, he has written three books on Organic Synthesis (1994, 2003), Membranes and Molecular Assemblies (1995), and Molecular and Supramolecular Chemistry of Natural Products and their Model Compounds (2000) as well as more than 100 additional scientific papers and managed a Sonderforschungsbereich on "Vectorial Membrane Processes". He tried to contribute to the development of useful models for single steps in biological photosynthesis and thoroughly enjoyed the corresponding experimental endeavors of his 126 co-workers over a 35-year period and his technician Mrs. Andrea Schulz over 16 years. Typical scientific subjects were the reactivity and assembly of porphyrins and bolaamphiphiles, spherical and planar monolayer lipid membranes (MLMs), chiral bilayer effects in micellar fibers, long-distance heterodimers, and, most recently, nanowells and the sorting of molecules within them. The overall keyword was reversible, noncovalent synthesis or synkinesis, as he calls it, of photo- and redox-active systems. He is thoroughly grateful for the fact that he was allowed to live for almost 60 years in Berlin without a war, which was not possible in the 400 years before. A happy marriage in this peaceful period produced three wonderful daughters and, as a follow-up, seven equally perfect grandchildren.

Tianyu Wang (left) was born in 1971 in Tianjin, China. He completed his Ph.D. degree at the Institute of Chemistry, Chinese Academy of Science, in 2001 with Professor Jinshi Ma, where he was working on porphyrin synthesis. He is currently carrying out postdoctoral research on porphyrin polymers and nanowells made of bolaamphiphiles in the laboratory of Prof. Dr. J.-H. Fuhrhop at the Free University, Berlin. He married recently in Berlin.

10.1021/cr030602b CCC: $48.50
Published on Web 03/12/2004

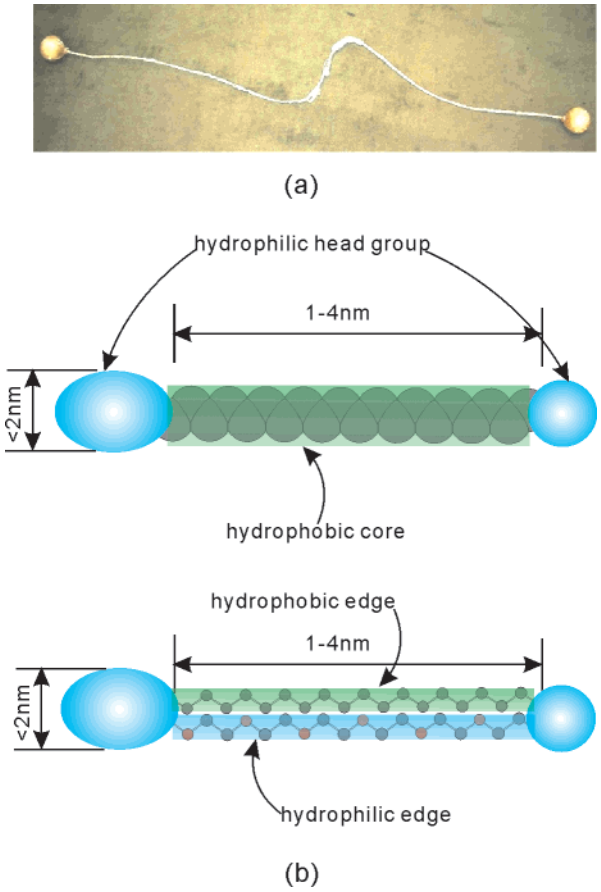

Figure 1. (a) Photograph of an argentine bola with leather balls; (b) schematic drawings of a bolaamphiphile (abbreviation, bola). Green coloring indicates hydrophobic parts; blue means hydrophilic. Red will be used for conjugated systems, usually dyes, as well as for oxygen atoms in structural formula.

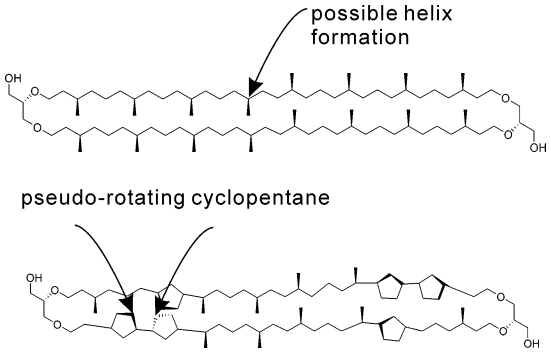

Figure 2. Structural formula of typical bolas from archaebacteria. Acid-stable ether linkages let them survive in acidic media; chiral methylated centers induce twistings to form helical structures; pseudo-rotating cyclopentane units replace the chemically sensitive cis-double bonds, which are used to fluidize biological bilayer lipid membranes.

have to survive in highly acidic environments. Archaebacteria chose flexible cyclopentane units instead. In terms of sophisticated syntheses, the archaebacteria are thus far more ambitious than higher organisms when they devised their membranes. Total syntheses of such macrocyclic tetraethers have been tried but have not been achieved so far, Figure 2.[7−9]

Synthetic bolas tend to form extended planar monolayers on the surface of water or of smooth

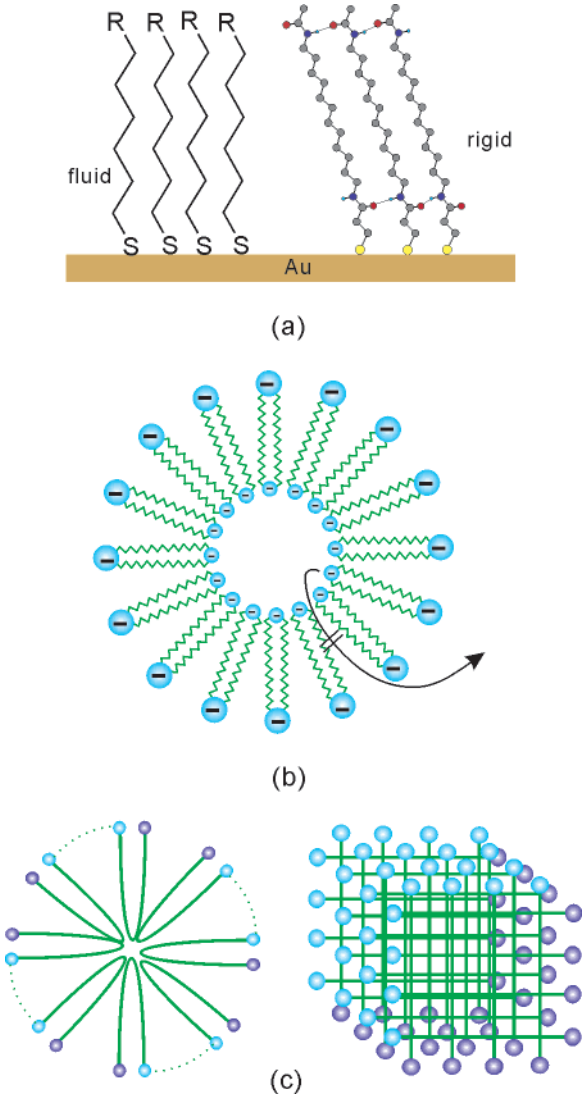

Figure 3. (a) Once ordered, a monolayer lipid membrane of a vesicle with charged headgroups does not rearrange (no flip-flop). (b) In micelles, bilayer bent bolas or alternating monolayers of straight bolas may occur.

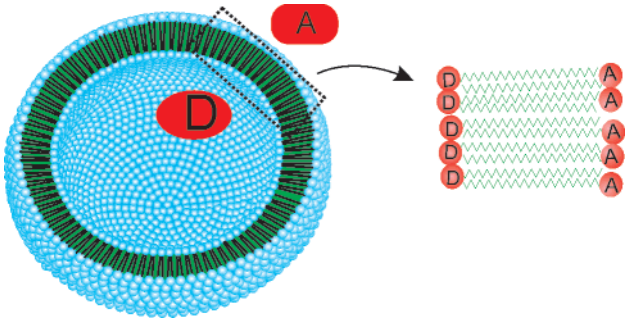

Figure 4. Typical asymmetric MLM vesicle may contain electron donors (D) as small inner headgroups and acceptors (A) as large outer headgroups, or water-soluble donors may be isolated in the entrapped water volume from acceptors in the bulk water volume. Both arrangements may, for example, be achieved with hydroquinones only, which are oxidized with $FeCl_3$ only on the outside.

solids (Figure 3a).[5,6,10] Multilayers may be formed by the combination of two bolas with two cationic or two anionic headgroups or, more common, by combination of a dianionic bola and a cationic polymer or vice

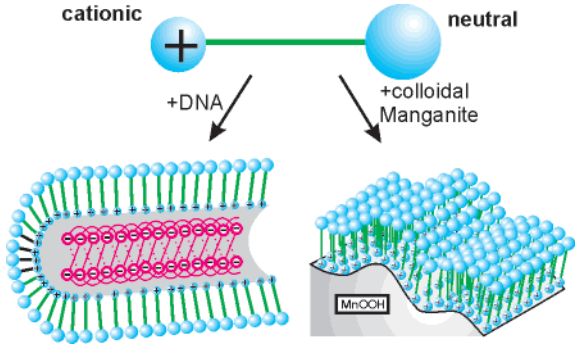

Figure 5. Bolas with an electroneutral and a positively charged headgroup may be used to neutralize surface charges of polyelectrolytes or colloids as anticorrosive monolayers or a solvent for hydrophobic molecules.

versa. Ultrasonication of aqueous dispersions of bola monolayers yields spherical lipid particles made of monolayer lipid membranes (MLMs). Long-chain bolas produce vesicles (liposomes; Figure 3b). Short-chain, water-soluble bolas give micelles (Figure 3c).

When the synthetic work on bolas started in the early 1980s, the main targets were asymmetric membranes for light-induced charge separation. Asymmetric lipid membranes with electron donors on the inner side of the vesicle membrane and acceptors outside were rapidly achieved, and charge separation was indeed shown to occur (Figure 4). It then turned out, however, that charge recombination was equally fast. Fluid lipid membranes are inefficient as barriers

Scheme 1

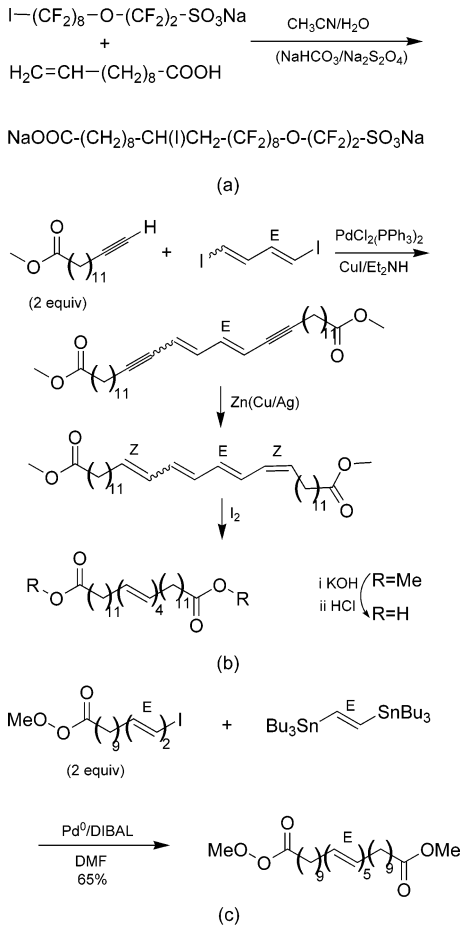

Scheme 2

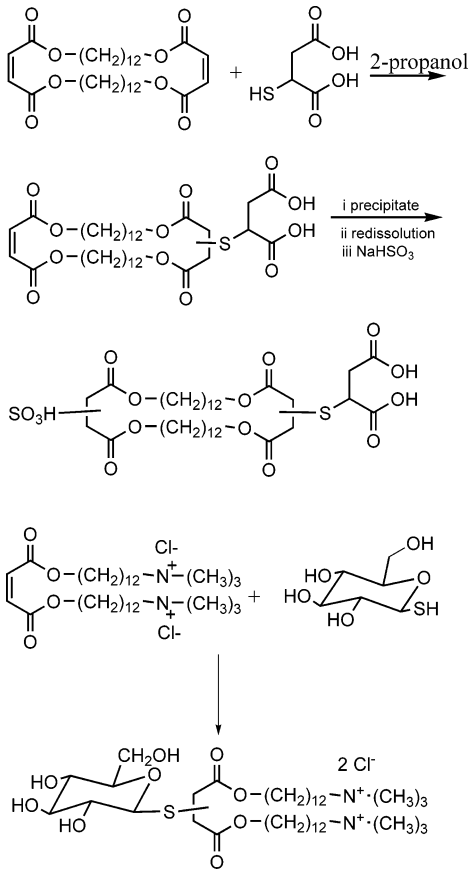

for rapid electron flow. The magic of energy conversion dissipated from artificial lipid membrane systems, but the chemistry of unsymmetric bolas had been established.[1,2,11]

Bolas were then preferably used as coatings of smooth solid materials: one end of the bolas was covalently attached to the surface of electrodes (Figure 3a), polyelectrolytes, or nanoparticles (Figure 5) whereas the other headgroups were used for solubilization in water and for interactions with solutes. Fluid or rigid monolayers covered with reactive end groups were thus obtained and applied to yield electron-conducting materials or machinery based on molecular recognition processes.[6,10]

2. Synthesis

Most bolas are made from commercial α,ω-diols, -dihalides, -diamines, and dicarboxylates by condensation and substitution reactions. Here we discuss only a few nontrivial syntheses of bolas which have been successfully applied in the construction of supramolecular assemblies or provide easily accessible pathways in this direction. This implies that sufficient quantities (≥100 mg) have been made. Milligram quantities are, in general, unacceptable as starting materials for the preparation and characterization of monolayers, vesicles, and fibers.

Single-chain bolas have been obtained from α,ω-diiodides. $sp-sp^2$. Cross-coupling of polyene diiodides and alkynes and the Stille reaction between two polyene iodide molecules and a bis(tributylstannyl)-ethane were reasonably successful in syntheses of

Scheme 3

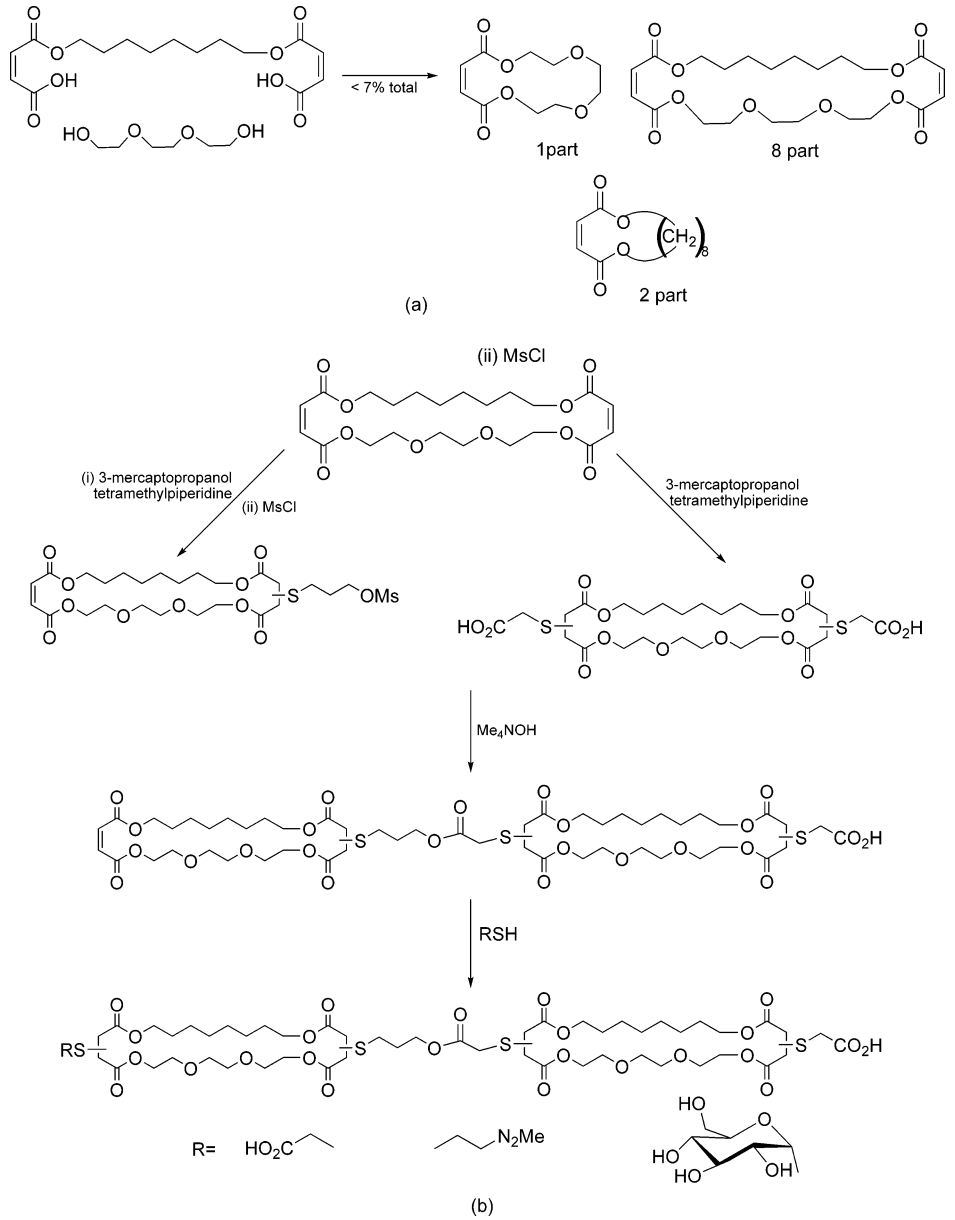

long-chain bolas. A C28 bola was, for example, isolated in a 60% overall yield.[12] Asymmetric coupling of hydro- and fluorocarbon segments was achieved by simple mixing of an ω-iodofluorocarbon sulfonate and 10-undecenoic acid in an acetonitrile/water mixture in the presence of dithionite.[13] The iodide on a CF_2 group was reactive enough to add to the C=C double bond (Scheme 1).

Asymmetric bolas are best made by two successive Michael additions to macrocyclic bis-maleic tetraesters. 2-Thio-succinic acid in ethanol led to a monosubstituted macrocycle, which precipitated. Redissolution in more polar solvents, e.g., DMF, allowed a second Michael addition at the other end. Asymmetric bolas were thus obtained in high yield and purity without any chromatography (Scheme 2), if one does not care about the exact regio- and stereochemistry of the end groups.[14−16]

Fyles et al. have been following this trail.[17−25] At first they introduced oligoethylene-glycols (OEGs) as the second alcohol, which produced membrane-soluble edge amphiphiles. The yield of the macrocycles dropped to 0.2−7%. Transesterification as well as instability were the main problems (Scheme 2).[17−19] These edge bola amphiphiles were applied to form ion channels in spherical vesicle and planar black lipid membranes. For pores in bilayer lipid membrane (BLMs), two macrocyclic edge amphiphiles had to be coupled. This was done by esterification of a macrocyclic carboxylate with a macrocyclic mesylate in DMSO and in the presence of tetramethylammonium hydroxide (Scheme 3). Chromatography yielded 12% of a yellow oil with a perfect elemental analysis.[24]

A more simple bis-macrocyclic system was based on the esterification of *m*-phthalic acid dichlorides with long-chain diols.[26] The tetraester cyclophane was obtained in 16% yield from ω-hydroxy-diesters and the *m*-phthaloyl dichloride. Connection of two such macrocycles was achieved via the amidation of

Scheme 4

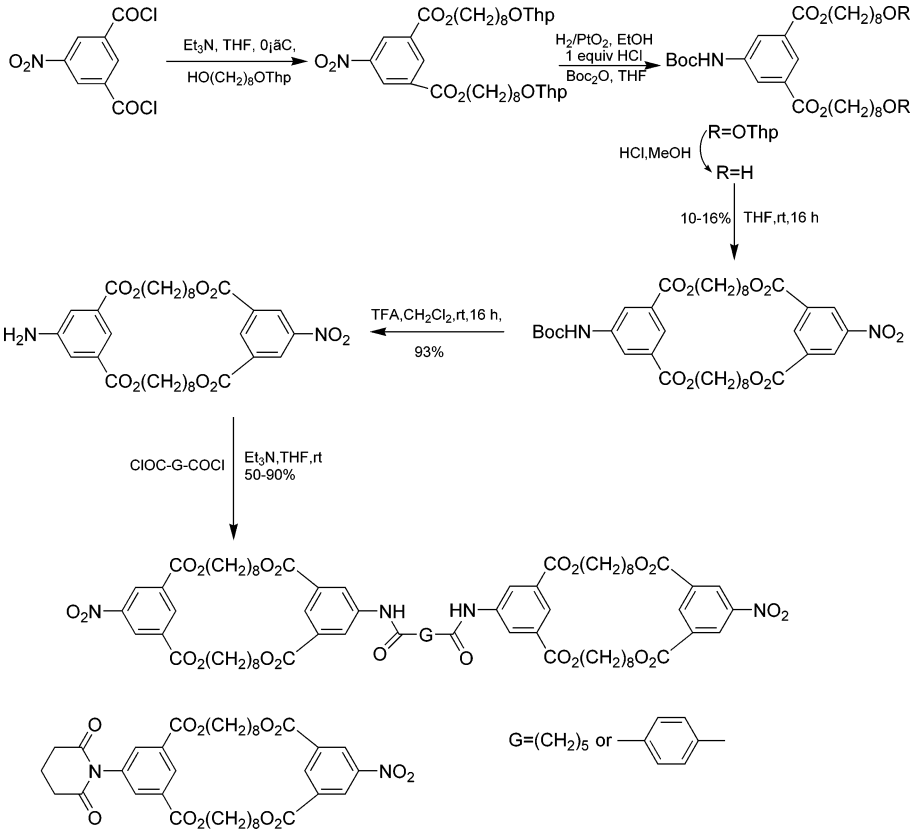

p-phthaloyl dichloride with the *p*-amino groups located on the macrocycle (Scheme 4).[27]

Close analogues to the archaebacterial bolas (see Figure 2) are macrocyclic thioacetals, which are obtainable in quantitative yield from benzaldehyde and α,*ω*-dithiols,[28,29] as well as sulfide macrocycles with four ether links, which are produced from 2,2-dithioethanol and diols in the melt in 50% yield (Scheme 5).[30]

Thompson et al. prepared symmetrical α,*ω*-phosphate bolas with one C_{20} linker and two C_{10} chains from a dibromide and two protected glycerol molecules using sodium hydride in tetrahydrofuran as a base. The terminal phosphate group was introduced after protection of the primary alcohol group of glycerol with trityl chloride, deprotection with BF_3, and phosphorylation with $POCl_3/Et_3N$. Asymmetric diether moieties were obtained by Sharpless epoxidation of allylic alcohols and nucleophilic addition of aliphatic diols to the resulting epoxides under a variety of conditions. Yields were around 80%; dithioether formation was much less efficient. The α,*ω*-introduction of cholin phosphorylates was achieved by esterification of the primary alcohol groups with 3-nitrobenzenesulfonoyl chloride and transesterifications with 2-chloro-2-oxo-1,3,2-dioxyphospholane (Scheme 6).[31a,b] Engberts reported on biphosphate diester bolas.[32]

Acylation of a secondary amine with the mercaptothiazoline derivative yielded a tertiary amide after 1 week. Neither sugar hydroxyl groups nor the carboxyl groups needed protection. Spermine was, for example, condensed with a free acid in DMF in the

Scheme 5

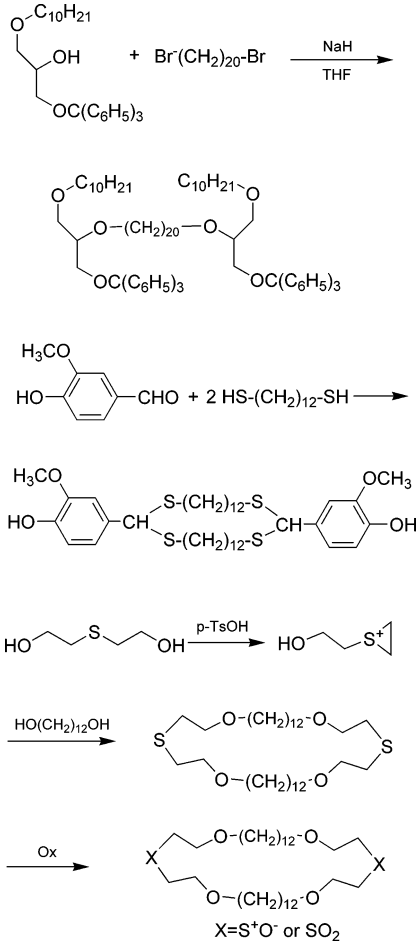

Scheme 6

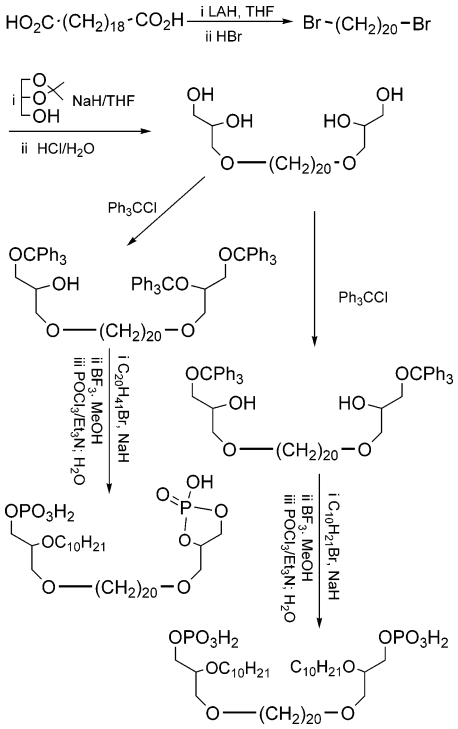

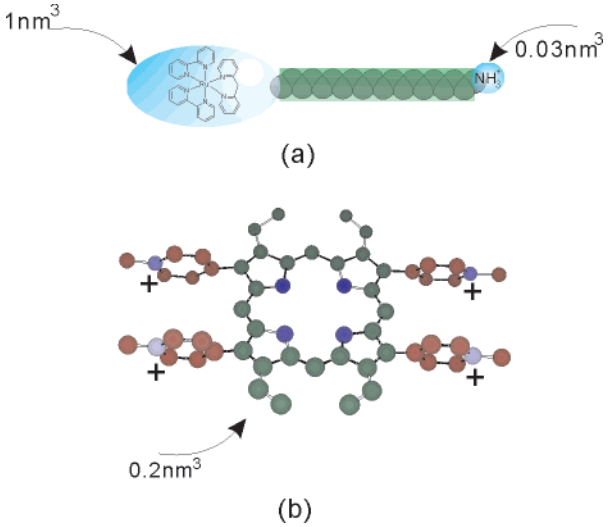

Figure 6. (a) Largest headgroup of an amphiphile known to the authors is a ruthenium−tris-bipyridinate (10^3 Å^3) and the smallest one an amino group (30 Å^3). Connecting alkyl chains provides a fluid hydrophobic core. (b) The most popular rigid hydrophobic core is made of a porphyrin (7 × 7 × 4 Å = 200 Å^3). Substituents, in particular four *p*-substituted phenyl groups, may blow up the volume to 30 × 30 × 4 = 3600 Å^3 or more.

presence of NEt_3 and BOP as coupling agent (Scheme 7).[33] Metathesis of olefinic glycosides has also been applied in syntheses of carbohydrate bolas.[34]

3. Intra- and Intermolecular Arrangements of Bola Headgroups

Bolas are used to build up monolayered lipid membranes (MLMs) in bulk aqueous media or on smooth solid surfaces. For these purposes the width of the bola's headgroups should be smaller or about the same as that of the hydrophobic core. Interdigitation, which is commonly applied in bilayers of single-headed amphiphiles in order to accommodate for bulky headgroups, does seldom occur in bolas. The smallest hydrophilic headgroup is the primary amino group with a diameter of about 0.3 nm and a volume of 0.03 nm^3; the largest known headgroups were made of a ruthenium−tris(bipyridyl) complex with a diameter of 1.0 nm and a volume of 1 nm^3. Larger hydrophilic headgroups are usually polymeric and transform bolas into copolymers. The width of the hydrophobic core in known bolas lies between 0.5 and 3 nm, corresponding, for example, to two alkyl chains or one tetraphenylporphyrin unit (Figure 6). The third dimension, namely, thickness of bola units, is

Scheme 7

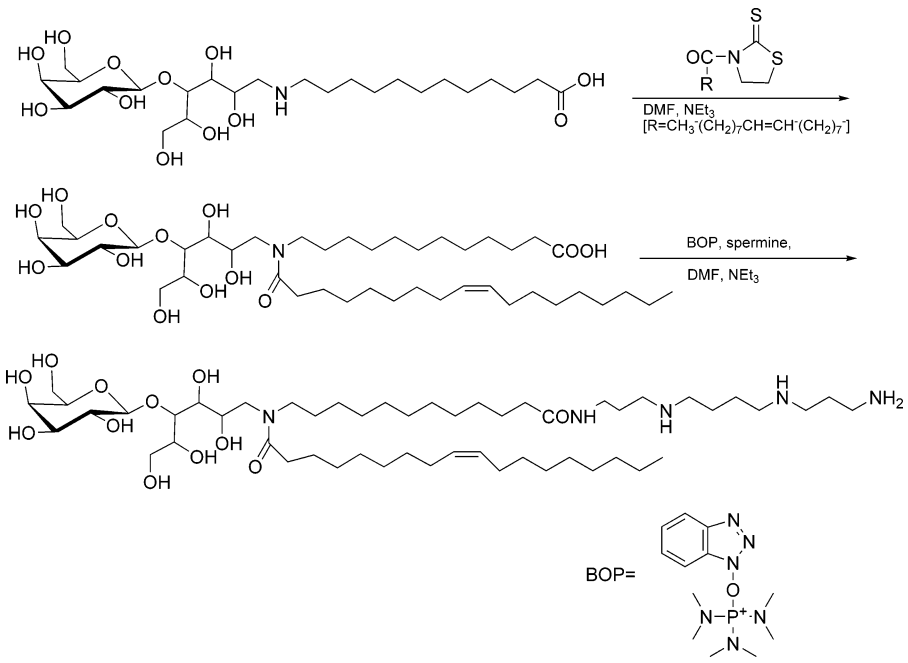

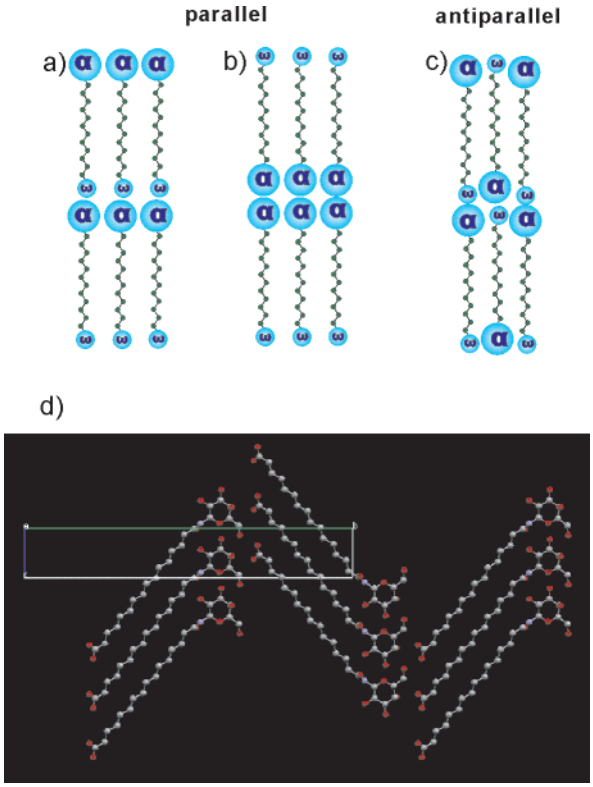

Figure 7. Possible arrangements of bolas in crystals: (a) parallel α,ω, (b) parallel α,α, and (c) alternating or antiparallel α,ω and α,α. (d) α,ω-Crystal packing of an α-carboxy-ω-glucosamide bola.

limited to less than 1.0 nm. More bulky molecules tend to arrange in crystals rather than in isolated monolayers.

3.1. Crystal Structures

In crystals, several packing orders for planar monolayers are possible, and some of them have been verified experimentally. At first parallel packing may occur if the size difference between α- and ω-headgroups is not too large. These unsymmetrical MLMs may then pack either in an α−ω or α−α manner ("tail-to-tail" or "head-to-tail" in the original paper, Figure 7a).[35] The third alternative is alternating packing. Standard α−ω packing was observed with 1-galactosamide groups as large α-heads and smaller carboxyl groups at the ω-end. The carboxyl groups bind to the primary OH group of galactose, which is fixated by bifurcated hydrogen bonds, as well as to the oxygen in the pyranose ring, thus producing a hydrogen-bond chain. The galactose and carboxyl planes are almost parallel when viewed along the *a*-axis and perpendicular to each other in the *c*-axis view. No water molecules are needed to stabilize the structure; the alkyl chain is all-trans-configured and has an inclination of 52° to the normal of the layer plane (Figure 7b). The axial 0−4 hydroxy group is buried in the hydrophilic surface and binds better to the small acidic carboxyl group then to another sugar moiety.

The situation is quite different in symmetrical α,ω-bis-1-galactosamides, where a water molecule binds to the axial 0−4 and connects it to neighbors.[36] In

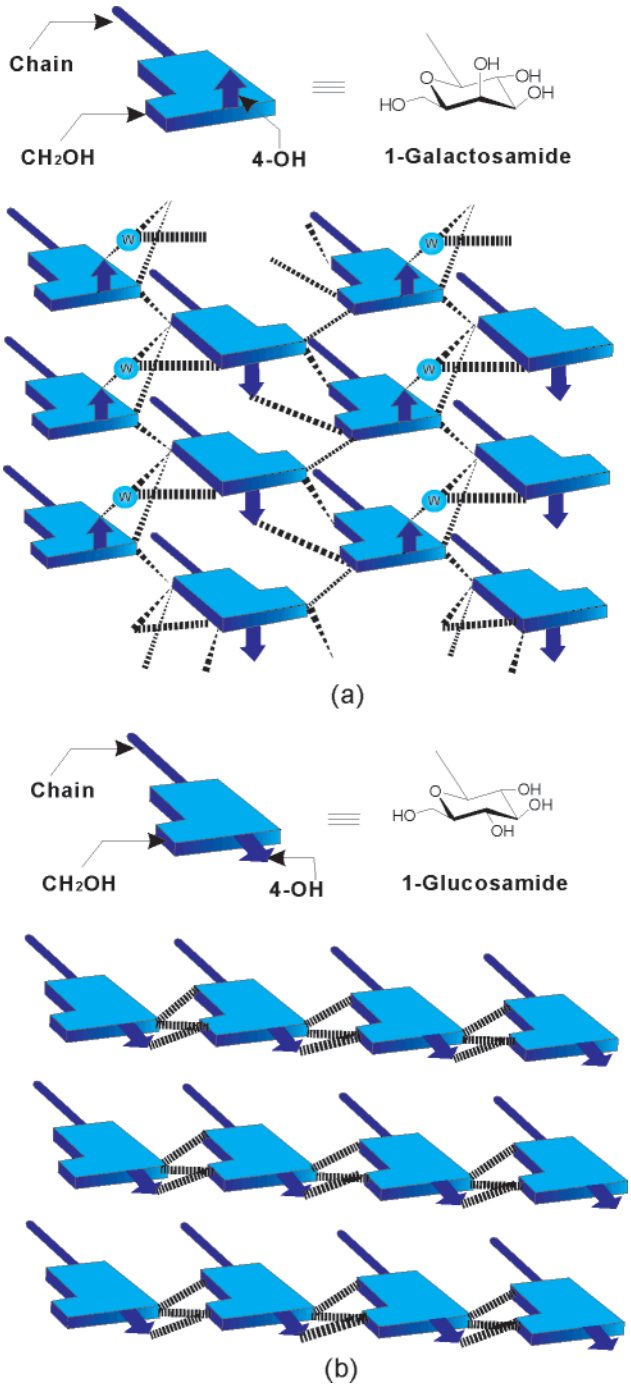

Figure 8. Comparison of the packings of α,ω-galactosamide and α,ω-glucosamide headgroups in crystals of symmetric bolas. (a) The axial OH groups of the galactosamide catch a connecting water molecule in steps. (b) Equatorial OH groups of glucosamide bind to each other directly with hydrogen bonds in a plain.

the related α-glucosamide-ω-galactosamide, water is not needed and side-by-side amide interaction via the secondary amide group becomes dominant (Figure 8).[37] Since glucose and galactose have a similar diameter, pairing of the same headgroups leading to α−α and ω−ω packing is now also observed.[36−38]

The number of methylene groups in the connecting chains influences the crystal packing drastically. Even-numbered 1-glucosamide bolas could, for example, not be crystallized. Only the axial OH group of the C-12 galactonamide bola allowed a close

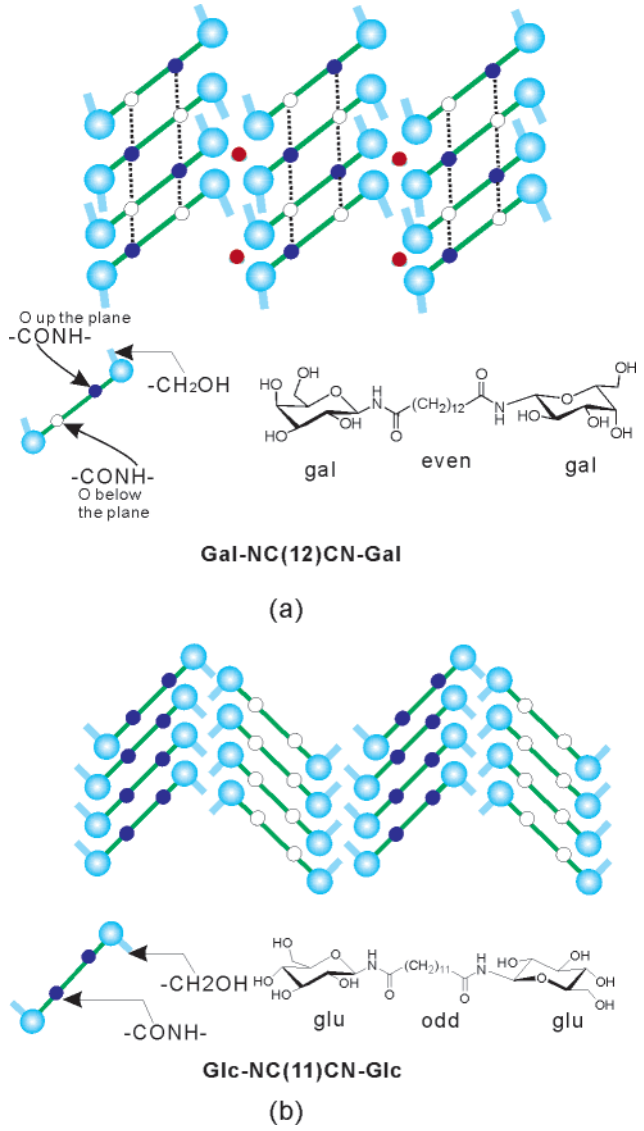

Figure 9. Similar arrangements of the headgroups occur in odd- and even-numbered bolas with 1-amino-galactose and -glucose headgroups. Arrangements of hydrogen bonds and crystal planes are, however, different. In the even case water is needed to connect the headgroups by hydrogen bonds, which is not necessary in the odd case. Hydrogen bonds between the amide groups occur in the paper plane in the even case and perpendicular to that plane in the odd case.

contact of the CH_2OH-6 groups in hydrogen bonds, allowing for construction of a macrocycle made of two pyranose units, and it produced crystals. In the odd $(CH_2)_{11}$ case, the CH_2OH groups point into different directions and have no difficulty to bind to the next glucose moiety, thus forming nonproblematic chains (Figure 9). Antiparallel packing is more common in single-headed amphiphiles, where it allows voids to fill beneath bulky headgroups by the alkyl chains.

Infrared spectra for the glucosamide headgroups also showed strong changes of the amide I bond depending on odd−even-numbered alkyl chains between two secondary amide groups within the hydrophobic core. It was close to 1640 cm^{-1} for 11 and 13 CH_2 links, indicating immobilization by strong hydrogen bonds with 12 and 14 CH_2 groups. The

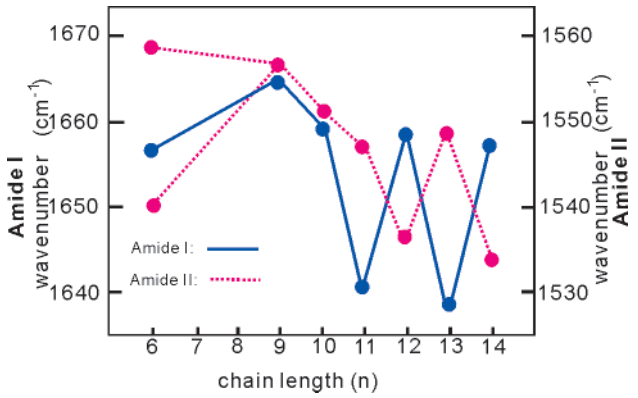

Figure 10. Amide I and II infrared absorptions of bis-glucosamides with even- and odd-numbered oligomethylene chains. Odd-numbered bolas have stronger hydrogen bonds corresponding to low-energy amide I and high-energy amide II absorption bands.

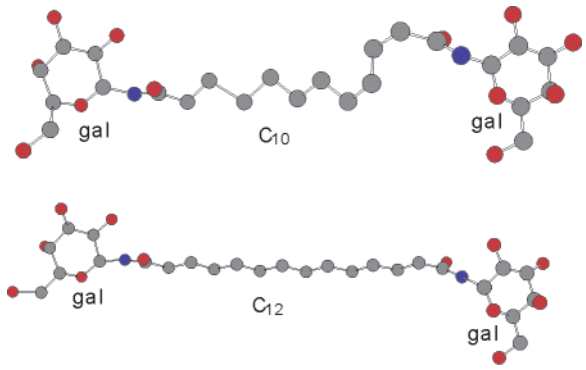

Figure 11. Short connecting chains ($<C_{10}$) tend toward gauche-conformation; in very short ones α- and ω-headgroups may touch each other in a cyclic conformer ($>C_{12}$). Long connecting chains are usually *all*-trans or only bent at the ends.

same band occurred close to 1660 cm^{-1}, which corresponds to more mobile CO groups (Figure 10).[38]

This is in contrast to bolas which are fixed on gold and contain two secondary amide linkages. An odd number of methylene groups between them causes fluid monolayers, whereas an even-numbered oligomethylene chain allows two parallel-running hydrogen-bond chains and rigidity (see Figure 21).

Short alkyl chains ($\leq(CH_2)_{10}$) have, furthermore, the tendency to coil up at room temperature and to contain gauche-conformers beyond C_{12}, and they more likely to be all-trans (Figure 11). In C_{18} bolas disturbances of the all-trans configuration are only known to occur at the very last bond before the headgroups.[36] The strength of van der Waals bonding between the alkyl chains and their tendency to adjust their conformation to allow for optimal packing of the headgroups are of similar importance around C-10.

Crystal structures of α,ω-bis-L-alanine bolas made from L-alanine bolas show a sheet in the case of an odd $(CH_2)_{11}$ connecting chain and a helical arrangement of the ala headgroups in the case of an even-numbered $(CH_2)_{10}$ link. This difference also appeared in the overall arrangement of the bolas: they formed a wedge in the even case and a slightly curved plane. In both crystals the terminal NH_2 and COOH group are connected within the same crystal plane and to

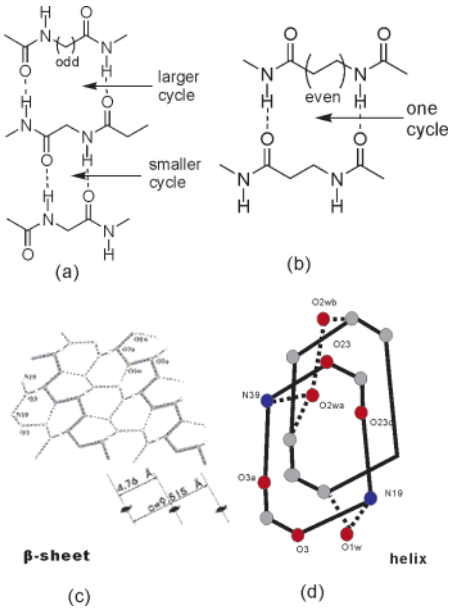

Figure 12. Diamido bolas with alanine headgroups form intermolecular hydrogen-bond cycles in crystals. Even-membered connecting chains lead to the formation of one type of cycles superposing as helices; odd-numbered chains lead to two different cycles and sheet formation.

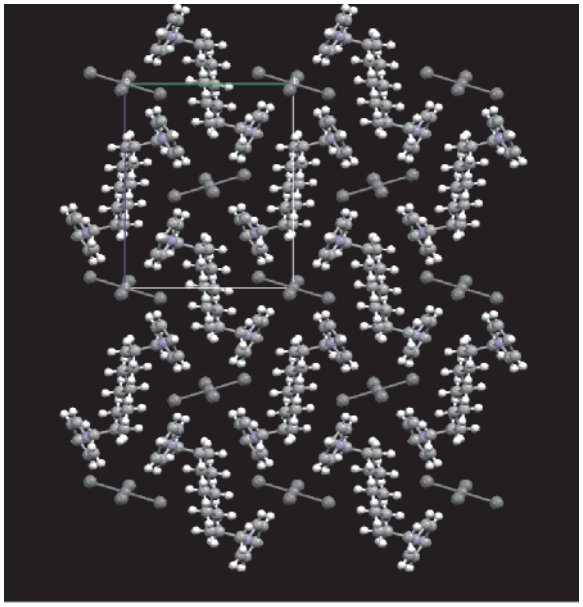

Figure 13. $PdBr_4^-$ anions form salts with α,ω-bis-pyridinium bolas, Br^- − atoms are in close contact with pyridine CH protons.. The big headgroup salt segregates the connecting alkyl chains of neighboring molecules from each other.

the neighboring plane (Figure 12). One of the resulting hydrogen-bond cycles is, small and rigid in the odd case. This cycle may be responsible for crystallization. The flexible cycle in even-chain bolas is obviously not helpful. They are therefore more difficult to crystallize and tend to form fibers and gels in aqueous solution, whereas odd-chain homologues do not form gels but precipitate as crystals under the same conditions.[39]

Symmetric bolas with two charged end groups provide the possibility of playing with counterions. X-ray structures are rare. The free acids do not reveal any abnormalities. All-trans alkyl chains are connected by the usual hydrogen-bond cycles between two COOH groups, in odd- as well as even-numbered diacids.[40,41] Crystal structures of silver(I),[42] manganese(II),[43] and cobalt(II)[42,43] soaps of dicarboxylic acids are known. The alkyl chains are again all-trans and lie quasi-perpendicularly to the polar COO metal sheets. Weak antiferromagnatism of manganese and cobalt chains was found.[43−45] Urea forms hexagonal tunnels around disordered 1,10-decanedicarboxylic acid molecules;[46] β-cyclodextrin entraps the 1,12-dodecane homologue;[47] pyridyl calixarene gives 2:1 complexes, which appear as hydrogen-bonded chains in crystals.[48] α,ω-Diamines crystallize in a similar simple manner as dicarboxylic acids. They have a much lower melting point and must be analyzed at low temperature.[49] NH−N intra- and interlayer hydrogen bridges (length = 3.2 and 3.5 Å) are again found; all-trans alkyl chains lie perpendicular to the amine plane. The even-numbered 1,12-diaminododecane crystallized only as a dihydrochloride monohydrate; fusion enthalpies were found to be higher for diamines with an even-numbered oligomethylene linker,[50] which is rarely found in bola crystal. α,ω-Diamines have also been crystallized in the form of bis-cyclodextrin pseudorotaxane[52] and crown ether[53,54] complexes.

An interesting example of a "bola metal complex" was reported for an α,ω-bipyridinium salt. The counterions were $Pd(II)Br_4$ dianions in which the bromide ions interacted with methine protons of the pyridinium rings. Square grids of bolas were formed, which were even stable in aqueous solution. The most important effect of the large counterions was the total segregation of the oligomethylene chains connecting the pyridinium rings (Figure 13).[55] In aqueous solutions one may suspect entrapment of a hydrophobic water volume. Several other applications of bolas in crystal engineering have been reviewed.[56,57]

In the case of the important monomer of Nylon 11, namely, 11-amino-undecanoic acid, two crystal structures have been reported.[58,61] They were obtained as hydrobromides from aqueous HBr[59] and from water as a hydrate.[60] In both cases sheets of linear conformers in an α,α-arrangement were obtained (Figure 14a). The C_{12} homologue could not be crystallized. A cyclic dimer of odd 11-amino-undecanoic acid showed a β-turn type III as found in proteins.[60] A corresponding trimer was also obtained as crystalline byproduct in the industrial synthesis of Nylon 11 (Rilsan).[61] In the latter trimer the C-11 spacer between two amide groups allowed a strong intramolecular hydrogen bond between two amide groups as well as intramolecular hydrogen-bond chains (Figure 14b).[61] In even m,n-Nylons made of diamines and diacids, similar patterns of hydrogen bonds lead to equally stable crystallites. Intermolecular hydrogen bonding may occur in progressive intrasheet patterns (p-sheets) with acid and amine regions, which leads to a shear by 13° parallel to the chain axis. Another possibility is linear hydrogen bonding of the type which is only possible when the neighboring sections

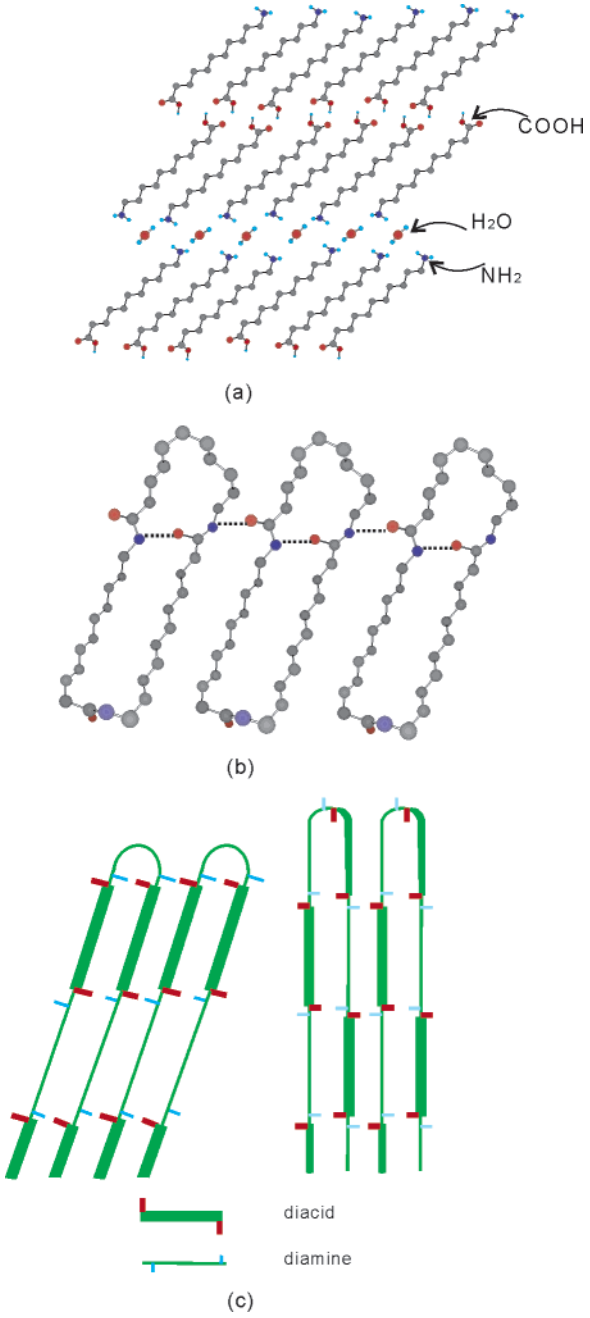

Figure 14. (a) 11-Amino-undecanoic acid forms α,α-connected crystals (compare with Figure 7a). The carboxyl groups face each other directly; the amino groups are connected by water molecules. (b) The corresponding lactam trimer shows a typical structure found in Nylon 11: two amide groups from hydrogen-bond chains, the third is located at a bend and remains lonely. (c) Schematic diagram of Nylon-12. Alternating or progressive sheets made of diamine and dicarboxylate segments are connected by hydrogen-bond chains.

follow in the order (diacid−diamine; alternating arrangement; a-sheets; Figure 14c).[62,63]

Odd-numbered nylons show strong ferroelectric to paraelectric transitions which originate from the cooperative switching of β-crystallite dipoles.[64] Pressure or stretching of Nylon-11 films produces electric fields, because reorientation of double crystallites leads to a polarization reversal. It is the polar hydrogen-bonded sheet crystal structures that are responsible for the piezoelectric effect and "ferroelectricity" of Nylon-11 films. The piezoelectric constants are low but can be strengthened in blends with poly(vinylidene fluoride), where $-CONH\cdots F_2C-$ hydrogen bonding connects both polymers.[65] Heating of even-numbered nylons lead to crystal modifications known as Brill transition.[66a,b] No significant change of physical properties occurs, however. Noncovalent sheets and fibers made of bolas should produce similar effects but have not been reported so far.

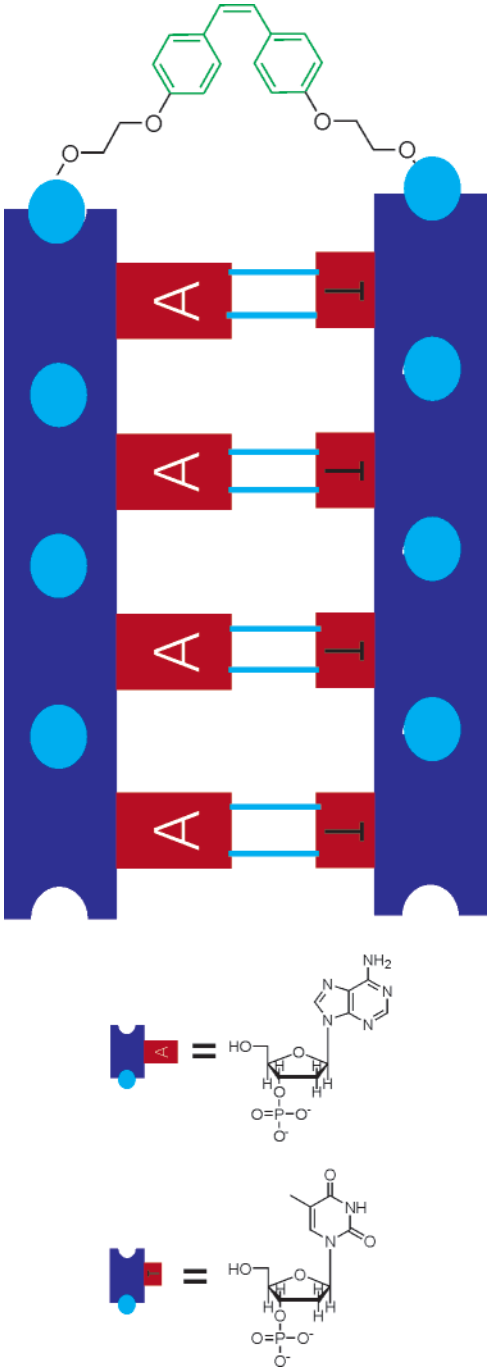

Figure 15. Model of the cis-isomer of an $\alpha(T)_4$–$(A)_4$ bola. Intramolecular hydrogen bonding prevents its photoisomerization to the *trans*-stilbene.

Our final bola structure is a model only, not a crystal structure. A stilbene α,ω-diol was connected with α-$(T)_4$ and ω-$(A)_4$ headgroups. The trans-isomer was photoisomerized one way to yield a stable hairpin structure with a quantum yield of 0.17. The inter-

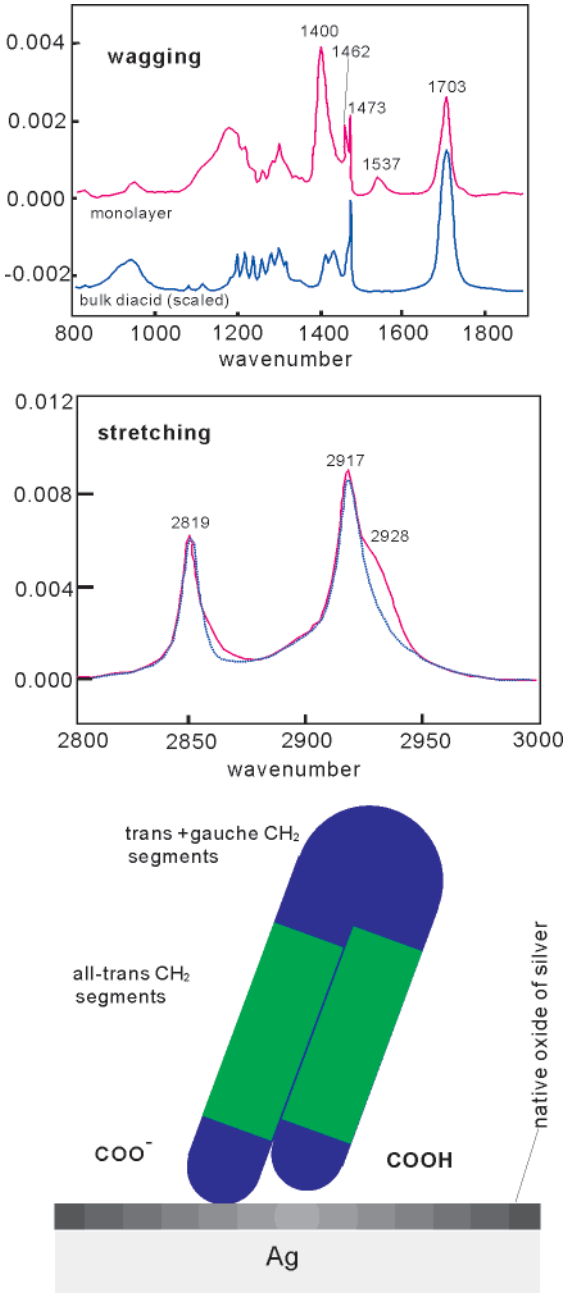

Figure 16. α,ω-Dicarboxylate bolas are bent on silver surfaces. A comparison with infrared spectra of the all-trans-configured bulk acid (lower and dotted traces) indicates the gauche bend in the monolayer.

action of the thymine with the adenine end groups is strong enough to prevent any photochemical back reaction (Figure 15).[67] This is a good example for α,ω interactions in a bola, which steers an equilibrium mixture to one component only, namely, the macrocycle. For columnar liquid crystals, see section 6, Figure 61.

3.2. Planar Molecular Monolayers

The reactivity and structure of bolas open an easy way to change the properties of surfaces with a minute amount of material: the α-headgroup can be used to bind a lipid chemically to a fluid (mercury),[68] colloidal,[69,70] or solid surface;[70−76] the hydrophobic core may serve as a barrier or solvent; the second

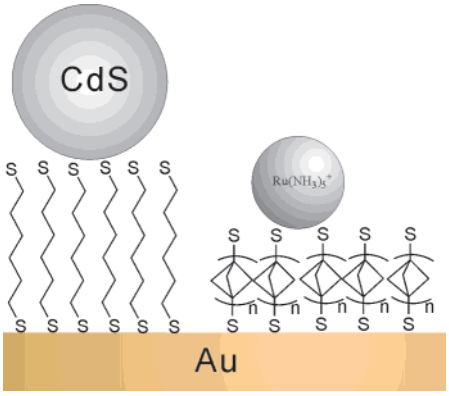

Figure 17. Long-chain α,ω-dithiols bind only with one SH group to gold. The remaining outer SH group can then be used to fixate colloids (e.g., CdS), transition-metal ions, or electrophilic organic molecules.

headgroup will be in contact with the environment and allow for molecular recognition of solutes in the volume water. The hydrophobic core finally may form a fluid monolayer and dissolve organic molecules or it may be rigid and provide an efficient protective layer against corrosion.

The lipid monolayers may be spread on the surface of water in a drop of an organic solution (Pockels, Langmuir), and this monolayer may be transferred to solid substrates (Langmuir−Blodgett technique). Self-assembled monolayers (SAMs) are made by plunging a solid plate directly into a bola solution containing a headgroup, which reacts chemically with the surface of the solid.[10] In all cases the bola may react with only one end or with both ends, namely, the α- and ω-headgroups with the fluid or solid substrate and form a ∩-shaped monolayer or the ω-headgroup may be in contact with the environment as stated in the first paragraph. Only the latter type is of general interest. The ∩ produces the same hydrophobic surface, which can be obtained with single-headed amphiphiles.

The only example of a uniformly folded bola on solid surfaces is provided by $HOOC-(CH_2)_{30}-COOH$ on silver. Ellipsometry yielded a surface film thickness of 20 ± 2 Å. In the reflection infrared spectra the 2928 cm^{-1} shoulder as well as the lack of sharp bands between 1130 and 1350 cm^{-1} for the progression of wagging modes indicated low all-trans sequence lengths (Figure 16).[73]

In all other cases a linear conformation of the bola was found. $HS-(CH_2)_6SH$ has been employed in the binding of metal ions to the surface of gold electrodes and fixated cadmium sulfide nanocrystals.[75] Rigid staffane bolas bound Ru^{2+} complexes to the monolayer's surface, and the properties of the electroactive film were strongly dependent on pH (Figure 17).[76]

The hydrophilicity of these monolayer-protected surfaces was determined by measurements of the contact angle θ_a of water or hexadecane (= HD) droplets (Table 1).[72] Mixed monolayers with partly buried hydroxyl groups switched from hydrophobic to hydrophilic at a CH_3/CH_2OH range of 1:10. Mixed ω-CH_3/CH_2OH monolayers of thiols on gold show no hydrogen bonding between the OH groups; domain

Table 1. Advancing Contact Angles θ_a on Thiol Monolayers Adsorbed on Gold

RSH	$H_2O^{\theta_2}$	HD	RSH	$H_2O^{\theta_2}$	HD
$HS(CH_2)_2(CF_2)_5CF_3$	118	71	$HS(CH_2)_{11}$	74	35
$HS(CH_2)_{21}CH_3$	112	47	$HS(CH_2)_{12}$	70	0
$HS(CH_2)_{17}CH{=}CH_2$	107	39	$HS(CH_2)_{10}$	67	28
$HS(CH_2)_{11}Osi(CH_3)_2C(CH_3)_3$	104	30	$HS(CH_2)_8$	64	0
$HS(CH_2)_{11}Br$	83	0	$HS(CH_2)_{11}$	0	0
$HS(CH_2)_{11}Cl$	83	0	$HS(CH_2)_{15}$	0	

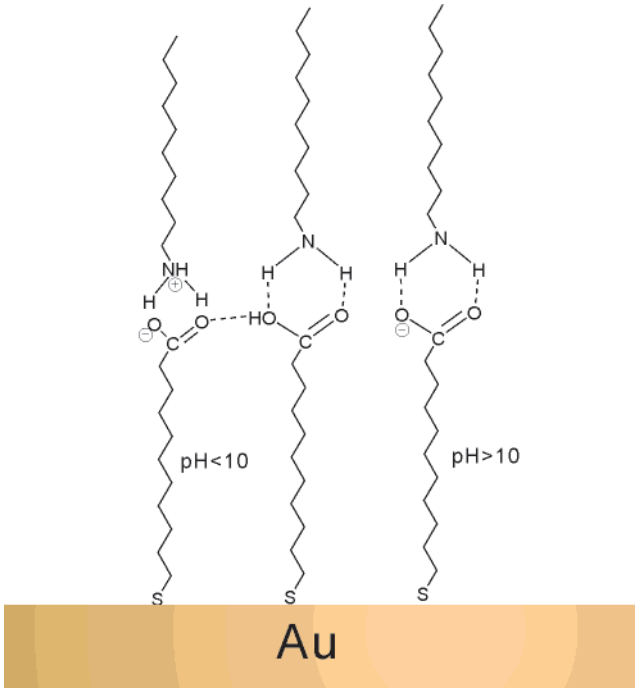

Figure 18. Surface carboxylate groups adsorb amines at low (left) and high (right) pH.

formation does not occur.[75] Ether linkages were solvated down to 0.5 nm beneath the surface.[71]

CN, OH, and COOH at the inner ends of bolas bind to copper, silver, and gold surfaces. The scant angles of trans-extended alkyl chains are 28° on gold and 13° on copper and silver.[48] Carboxylate groups on the outer surface absorb long-chain amines. Some of the amine molecules are bound as ammonium salts and others by hydrogen bonding without removing the proton from the carboxyl group (Figure 18).[77]

Fluid and rigid bolas were also applied on gold and silicon electrodes to fixate redox systems and to separate them by a defined distance from the electrode surface as well as to introduce an insulating monolayer. Colloids (see Figures 5 and 36), proteins (see Figures 19 and 62), quinones,[78,79] fullerene,[80−82] and porphyrins[83] have thus been attached and reduced or oxidized from a distance (Figure 19).

Silicate particles were best stabilized and solubilized in water as well as in solvents by silylethoxypropyl-amino coating.[84a] Mesoporous silica was obtained with long-chain α,ω-diamines.[84b] In water such particles were best soluble at pH 11, where most amino groups are electroneutral. Acid−base titrations caused precipitation at low pH and full redissolution at pH 11. Adsorption of porphyrins characterizes the surface properties of these particles in

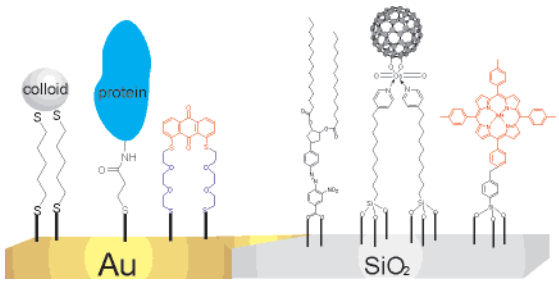

Figure 19. Various reactive headgroups which have been covalently bound to the surface of SAMs.

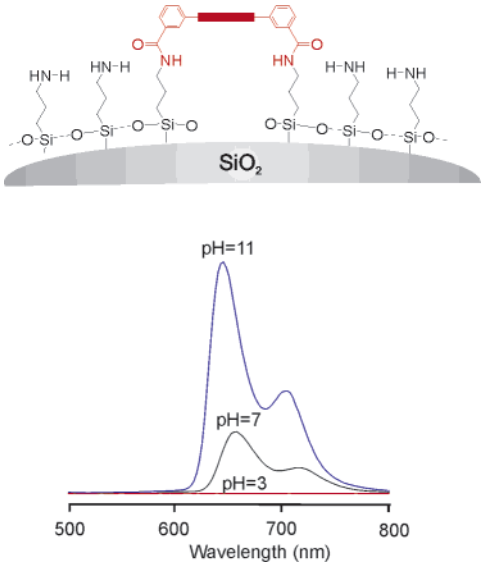

Figure 20. Fluorescence spectra of aminated silica particles with covalently bound, flat-lying porphyrins (= red stick). A drop in pH leads to precipitation of the NH_2 particles after protonation; the porphyrin absorption peaks disappear slowly. Upon increasing the pH to 11 again, the original spectrum is restored.

showing distinct changes of fluorescence spectra (Figure 20).[70]

Rigid membranes on smooth surfaces have been reviewed under the title of "Molecular Landscapes".[85] The stiffness may be reached by either two parallel-running hydrogen-bond chains between two secondary amide groups at the ends of hydrophobic cores made of oligomethylene chains[39,86−88] or stiff hydrophobic units such as bridged carbocycles, stilbene, or biphenylene[89−96] (Figure 21a−d).

An α-hydrosulfide-ω-trimethylsilyl (TMS) bola was used to prepare patterned surfaces on gold by lithography with 3-nm gold particles. The gold particles were first covered with 5-mecapto-2-benzimidazole-sulfonate sodium salt, converted to the sulfonic acid by ion exchange, and then used as a catalyst in microcontact printing. Wherever the sulfonic acid gold particle touched the TMS groups, they hydrolyzed the silyl ether, leading to a deposit ion of the particles on the SAMs. After rinsing with water, the flat gold surface was recovered but now contained hydrophilic OH stripes next to the hydrophobic TMS stripes (Figure 22), which led to high contrast in the AFM phase image.[98]

The onset of superconductivity at a critical temperature T_c is caused by the formation of electron

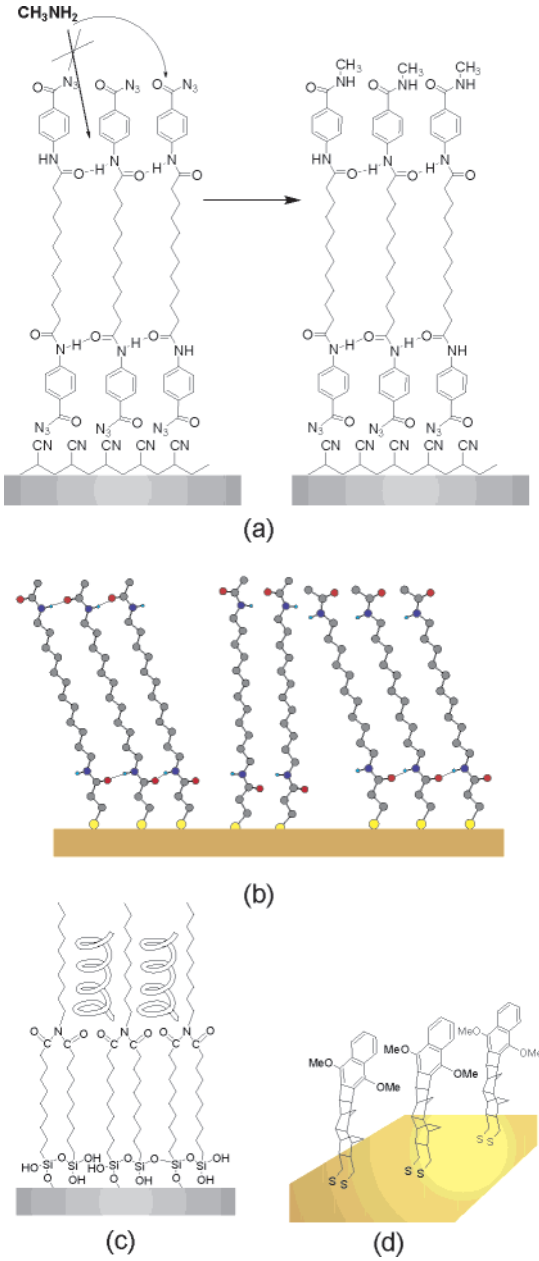

Figure 21. (a) A 15-nmm lipid bilayer is totally impermeable to methylamine, if two parallel running amide hydrogen-bond chains rigidify the monolayer. Outside azide groups are quantitatively aminated; inside azide groups are not changed within the following hours. (b) The formation of two parallel-running amide hydrogen-bond chains depends on the scant angle of about 20° and an even-numbered connecting oligomethylene chain. Upright-standing and odd-numbered diamido bolas form fluid monolayers because only one amide-hydrogen-bond-chain can be formed. (c) Porous fluid monolayers can be made by connecting two bola headgroups with a headgroup of a single chain amphiphile. Addition of water-insoluble hydrocarbons of equal length, indicated by a helix, may then fill up the cleft and thereby rigidify the nonpolar surface. (d) Rigid hydrophobic cores produce porous monolayers. The distance between a gold electrode and redox-active centers, e.g., hydroquinones, can be set accurately.

pairs and creation of an energy gap around the Fermi level for the remaining electron. An Hg-based superconducting electrode with a T_c of 134 K was coated with a 3.1 nm Ag layer by sputtering and coated with a mixed monolayer of $CpFeCpOOC(CH_2)_{8-}SH$ and

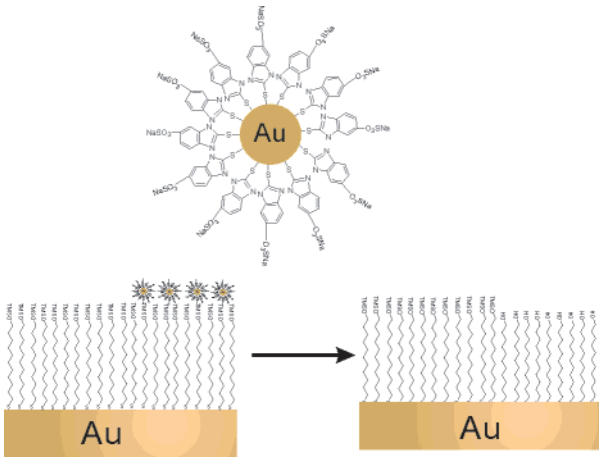

Figure 22. Gold colloids coated with monolayers ending in sulfonate groups hydrolyze trimethylsilyl ethers upon contact. Microcontact printing has been executed using this bola−bola reaction.

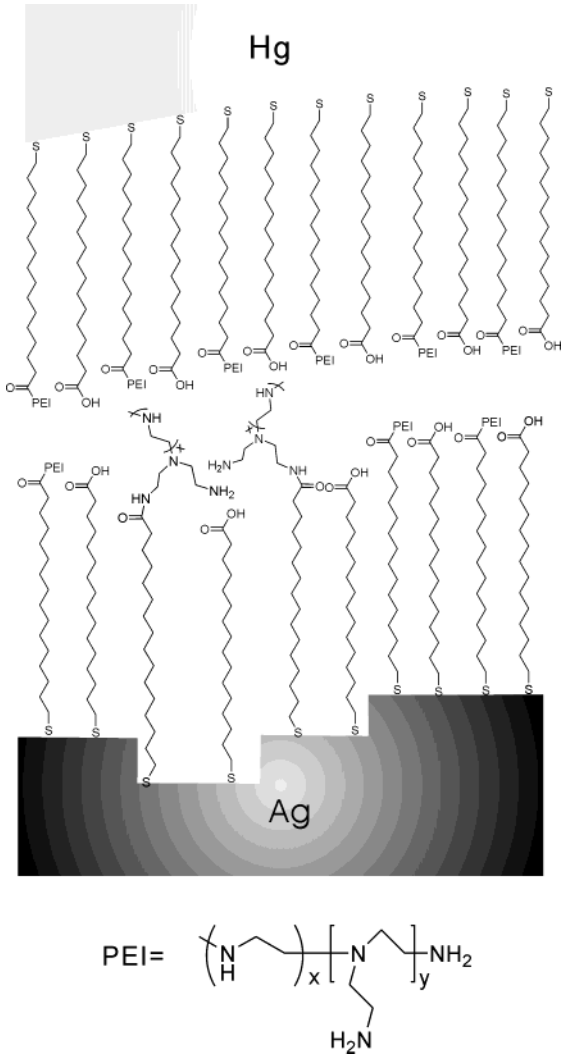

Figure 23. Hg−bola SAM−metal junctions allow the construction rectifiers of molecular size and the measurement of breakdown voltages of MLMs. Polyamines which fill up surface irregularities of the solid electrode are most efficient.

$CH_3(CH_2)_7SH$. The fluid monolayer interface allowed the transfer of paired electrons. It acquired the superconductivity of the high-temperature supercon-

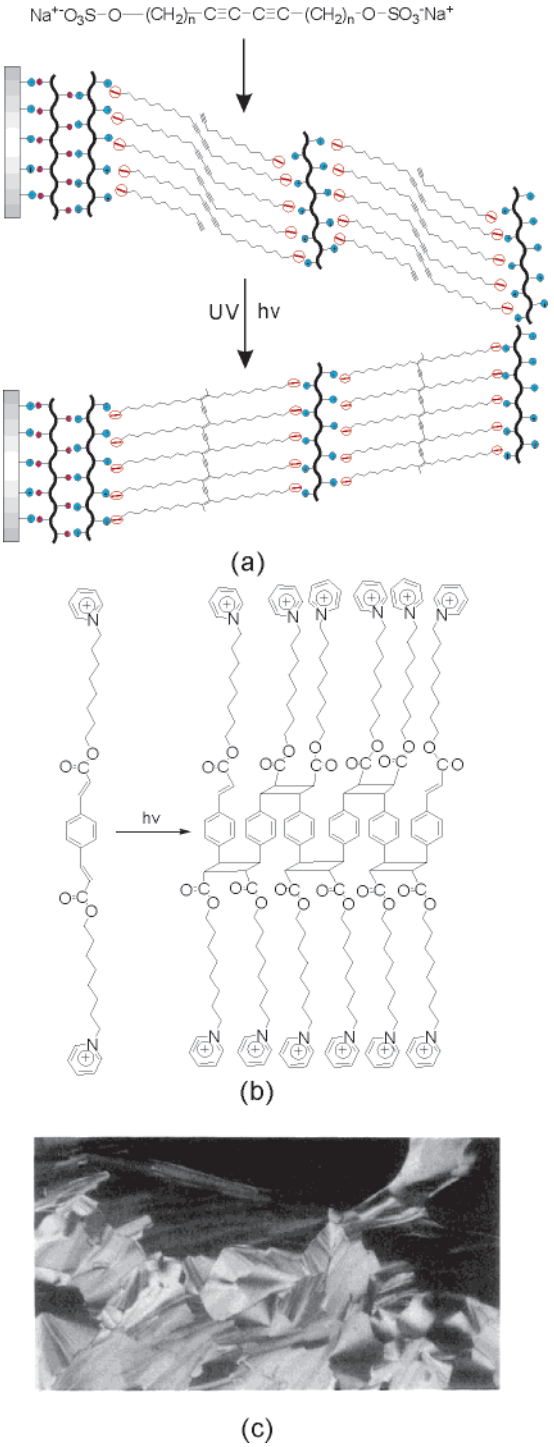

Figure 24. Schemes of UV-polymerization in a self-assembled multilayer (a) diacetylene and (b) vinyl cyclization. (c) The AFM picture shows a typical surface view after irradiation and polymerization.

ductor via the proximity effect. The CV curves of the monolayer were measured at temperatures from 125 to 145 K, and the separations of the anodic and cathodic peaks were used to calculate the difference in energy between the transferring electron and the energy level of the superconducting electrode material.[99]

Mercury−SAM/SAM−silver junctions (Figure 23) are useful in the electrical characterization of SAMs. They behave as capacitors with plates separated by a nanometer-thick dielectric. The low conductivity

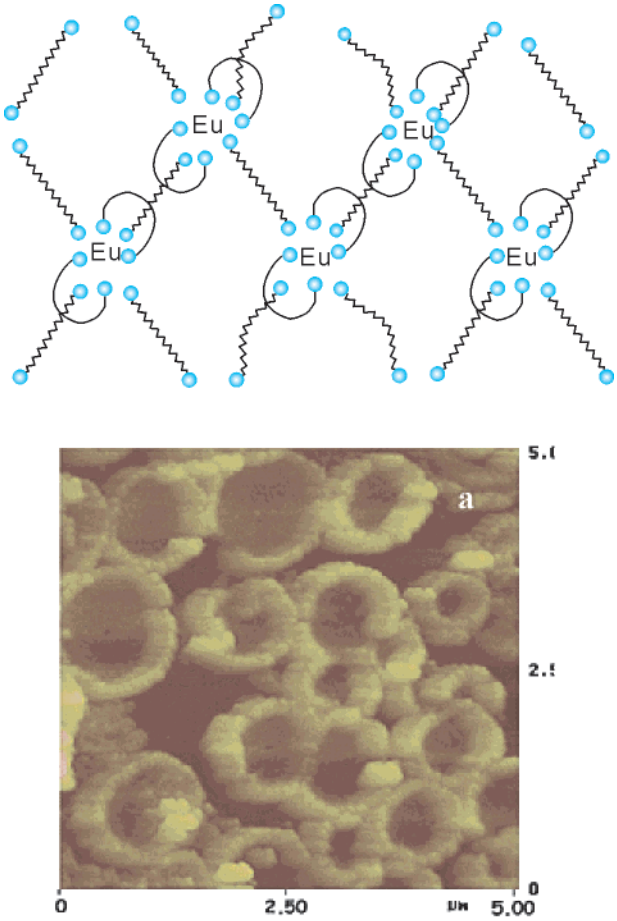

Figure 25. AFM image and a model of an octadecane dicarboxylate multilayer after reactions with europium(III) ions in the subphase.

($\sigma = 10^{-15}$ S cm^{-1}) of monolayers makes them excellent nanoscale insulators and dielectrics.[100] The most stable SAM/SAM bilayer was made of HS−$(CH_2)_{15}$COOH. It survived voltages of up to 5 V before breakdown.[101] Oligophenylene bilayers helped in electron-tunneling attenuation. Factors β of the molecular bridges were measured to be around 0.5−1.0 Å^{-1}. Electron transfer across a range of molecular bilayers and monolayers could be easily measured with the mercury system.[101,102]

3.3. Multilayers

A major difficulty in multistep self-assembly procedures lies in possible substitution reactions of bola A by bola B. Bola A should be bound as tightly as possible to the substrate, and it should be poorly soluble in the medium, which is used for the second self-assembly step. Most important, there must be a reliable method of detection for A on the substrate. Strongly fluorescing dye is optimal; a strong infrared absorption of A may also be sufficient.

Multilayer formation is a standard result of the LB technique but has, to the best of our knowledge, not been performed with bolas. The Decher method to assemble cationic and anionic polyelectrolytes in an alternating fashion[103−105] has, however, been transferred to bolas.[104] Only one of the components was monomeric, e.g., diacetylenic-α,ω-disulfonate, which

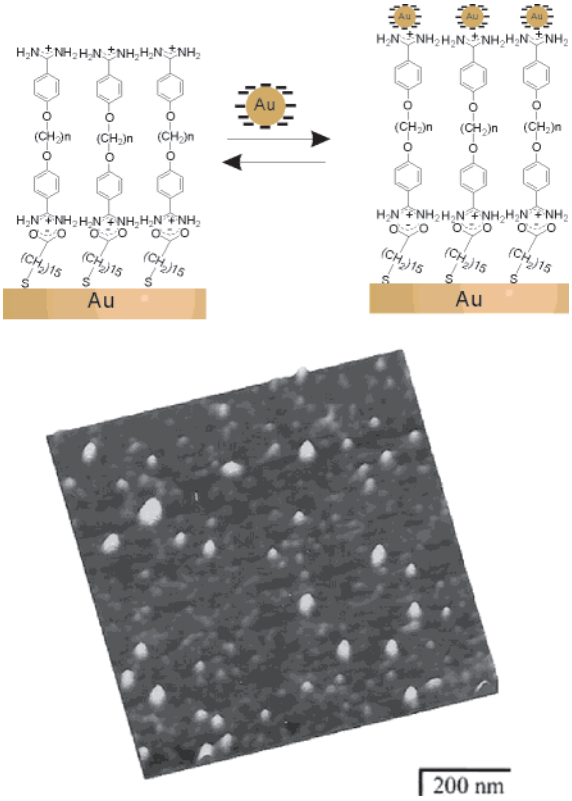

Figure 26. (top) Schematic representation of the consecutive build up of a nanoparticle composite by electrostatic benzamidine−carboxylate interactions and final attachment of the gold dots. (bottom) AFM of the gold particles.

alternated with polyallylamine (Figure 24a).[106] The diacetylene unit in the hydrophobic core was then polymerized to yield rigid monolayers between fluid ones.

Other multilayers of bolas were formed with covalent polyelectrolytes. The direct transfer of polymeric amphiphiles to solid substrates by LB techniques is generally not advisable as polymeric films tend to be too viscous and their transfer rates are slow. Self-assembly of monomers and subsequent polymerization is more promising. The dicationic bola and the anionic polymer bola, for example, formed perfect multilayers. Eight alternating layers of the dicationic bola and the anionic polyelectrolytes were assembled and stabilized by photopolymerization using UV light.[107,108] Tirrell et al. synthesized α,ω-di(methylpyridinium) bolas with a phenylene−diacrylic ester group in the center and coupled it with poly(2-acrylamido-2-methyl-1-propanesulfonic acid) (PAMPSA) on mica. Twenty dipping cycles gave a uniform rise of the phenylene absorption at 320 nm, and UV irradiation led to quantitative bleaching, indicating polymerization via cyclobutane formation (Figure 24b).[75] It took less than 5 min to remove the first monomeric film from mica with chloroform; the polymerized film dissolved only partially after 2 h. Nevertheless, the first few layers proved to be mechanically fragile; the multilayer (Figure 24c) as a whole could not be used as a solid coating.[107,108]

1,20-Octadecanedicarboxylic acid was spread on water-containing Ag(I) or Eu(III) ions. Stripe formation was observed for Ag(I), whereas Eu(III) produced

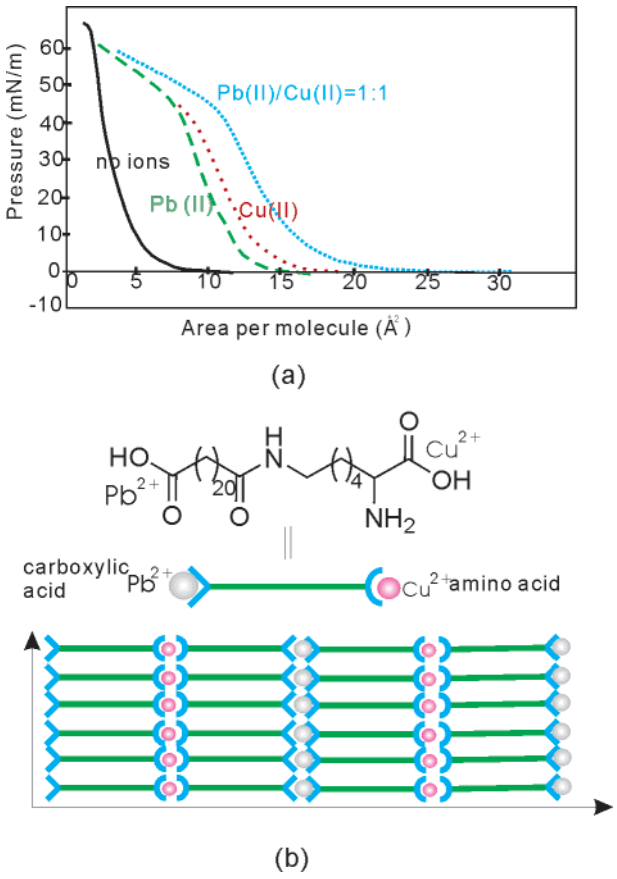

Figure 27. Bola with an α-carboxyl and an ω-amino acid (AA) group assembles via COO−Pb^{2+}−OOC and AA−Cu^{2+}−AA bonds. On a water surface this leads surprisingly to the largest molecular area, when both ions are present in the subphase.

large disks upon compression of the monolayer.[109] The stripes ("nanofibers") were traced back to linear head−Ag(I)−head assemblies, the disks were explained with hydrophobic interactions between U-shaped molecules fixed at both ends by an Eu(III) ion (Figure 25).

The most straightforward way to construct a bola bilayer is covalent fixation of an α-hydrosulfide-ω-carboxylate on gold and addition of α,ω-bis(benzamidines) in aqueous solution.[110] A second bola layer made of α,ω-dicarboxylates has so far not been achieved. It would presumably arrange in a flat monolayer and not allow any further built-up processes. The terminal layer on the benzamidine surface was made of spherical gold particles with an ω-mercaptohexadecanoic acid coat, which were detectable in AFM pictures (Figure 26).

Bolas with carboxylic acid and α-amino acid headgroups at opposite ends were spread on water or on a solution containing a mixture of Cu^{2+} and Pb^{2+} metal ions. Copper(II) was exclusively attracted to the amino acid groups, whereas lead(II) was bound to carboxyl only. Without ions the surface area measured by the LB technique was less than 5 Å² per molecule, with Pb(II) it rose to 12 Å², and with Cu(II) to 13 Å² per molecule (Figure 27a). The low values of molecular areas point to multilayer formation of presumably flat-lying molecules (Figure 28b). Both metal ions Pb^{2+} and Cu^{2+} then partly decompose

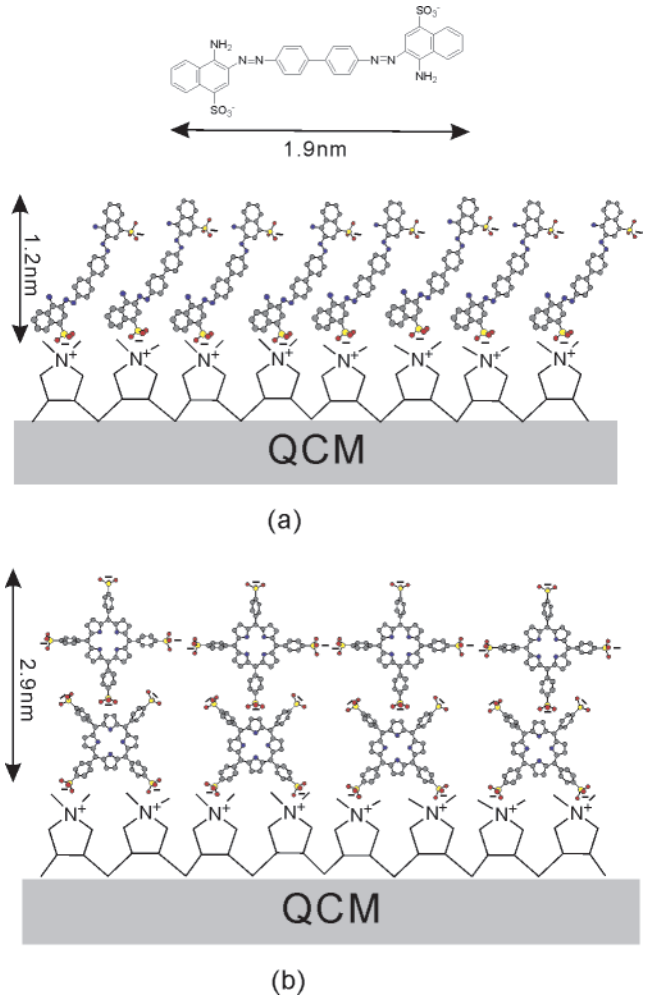

Figure 28. Quartz balance (QCM) frequencies decrease with nanogram sensitivity upon addition of dye−polyion films. The most tightly bound dyes are those with a hydrophobic core and two hydrophilic end groups or, in other words, bola dyes. (a) A good example is congo red. It is tightly adsorbed to poly(diallyl-dimethylammonium chloride; PDDA) on the quartz ($\Delta F = -80$ Hz) and then adsorbs itself the same PDDA polymer ($\Delta F = -46$ Hz; not shown). (b) Porphyrins are adsorbed as bilayers.

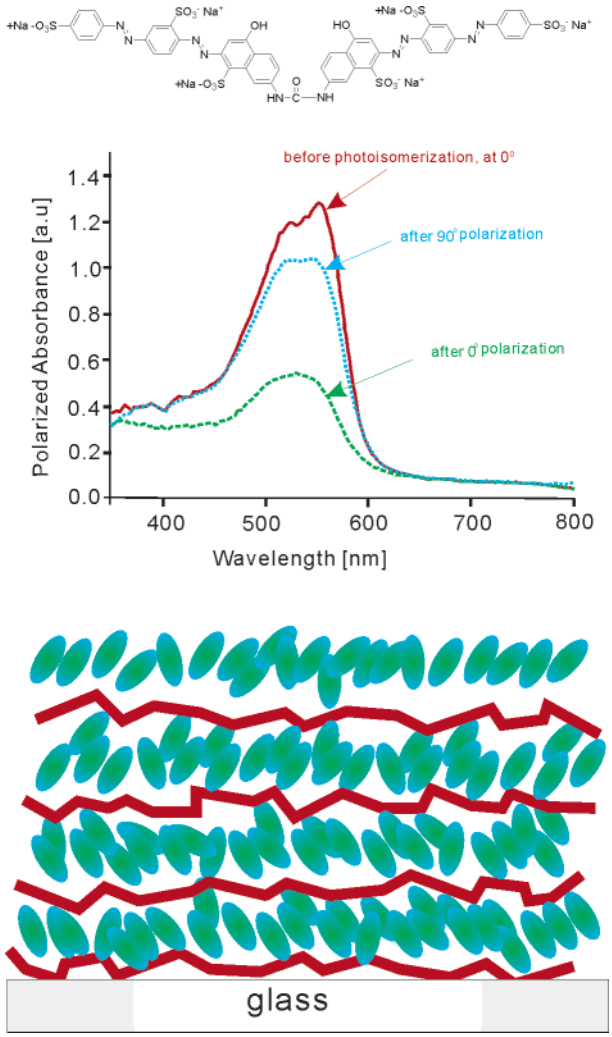

Figure 29. In Direct Red 80−PDDA multilayers the dye can be photoaligned by polarized visible light. The multilayer becomes dichroitic as suggested by the model given.

the multilayers. Crystalline monolayer films with α-spacings in grazing-incidence X-ray diffraction (GIXD) of 76 Å for Pb(II) and 71 Å for Cu(II) were obtained. XPS data confirmed the assumed ratio of two bolas to one Pb(II) and one Cu(II). The GIXD studies show the self-assembly of a bimetallic film, where the long molecules are arranged head-to-head intercalating the two different ions in an alternating manner (Figure 27b). The same metal ions are arranged in "wires" within the crystalline sheets.[111]

Bola dyes have also frequently been coupled with polyelectrolytes in alternating multilayers to give mono- or bilayers.[112,113] Anionic Congo Red (CR) copper phthalocyaninetetrasulfonic acid (PhtTS) assembled with cationic poly(L-lysine). Up 100 bilayers were thus assembled. The 100-bilayer-film thickness was estimated to be 1930 or 19 Å per bilayer in the phthalocyanine−poly(L-lysine) case; the number of dye molecules was estimated at 8.6×10^{13} per cm^2. The alternating adsorption procedure was also followed by quartz balance measurements. Polydiallyldimethylammonium chloride (PDDA) was used together with PhtTS (Figure 28b) or CR (Figure 28a). It was found that both dyes were desorbed from quartz platelets after addition of PDDA if the dyes were applied in highly concentrated solutions ($>10^{-4}$ M), where dye aggregates occur. If the dyes, in particular Congo Red, were adsorbed from more dilute solutions ($<10^{-5}$ M), they stick much tighter. The phthalocyanines or corresponding porphyrins appear in the form of nitrogen dianions within two PDDA layers, whereas the free-base porphyrin dominates on the surface. The anions appear in the staggered arrangement producing strong exciton splitting of the Soret band; in the outermost layers this splitting is less pronounced (Figure 28).[113]

The paper of Kunitake[113] compares in detail the advantages and limitations of alternating self-assembly procedures from solution and stepwise Langmuir−Blodgett transfers of insoluble monolayers on water. The conclusion can be summarized as follows: self-assembled multilayers are only uniform if charge interactions between the headgroups dominate. 2D-crystallization of SAMs is rare. LB techniques are much more difficult to apply to surfaces, and they give more crystalline multilayers. In par-

ticular, they often show well-defined distances between the headgroups, which is not the case in SAMs.

Some photoreactive dicationic bolas contained a diazo dye in the center. The azobenzene units underwent cis−trans isomerization upon UV irradiation, and optical dichroism was induced if linearly polarized light was used.[114] The dichroism could be reversibly written, rewritten by irradiation of the multilayered film on silica with polarized 360 nm light or erased with unpolarized 450 nm light. The speed of writing strongly depended on the ionic strength of the medium (Figure 29). A comparison of diazo dye bolas of different molecular lengths showed that anionic dye−polycation pairs containing the longest dye, namely, Direct Red 80, underwent a pronounced photoalignment upon irradiation with linearly polarized UV light. A tilted J-aggregate was obtained under such irradiation (Figure 29). It showed a much lower extinction coefficient than the nonaligned probe. Useful photopatterns or holographic reliefs may be formed by such alignment processes.[115]

Triblock molecules with a hydrophilic−hydrophobic−hydrophilic bola arrangement interact strongly with multilayers. A significant decrease of lamellar spacing and membrane thickness was observed. This was traced back to a change of membrane thickness. A "GFM 13" triblock bola was, for example, inserted into the monolayers. This increased the membrane surface area and lowered the interlamellar spacing significantly, already at a ratio of one inclusion molecule per 1000 surfactant molecules.[116] For columnar liquid crystals, see section 6, Figure 61.

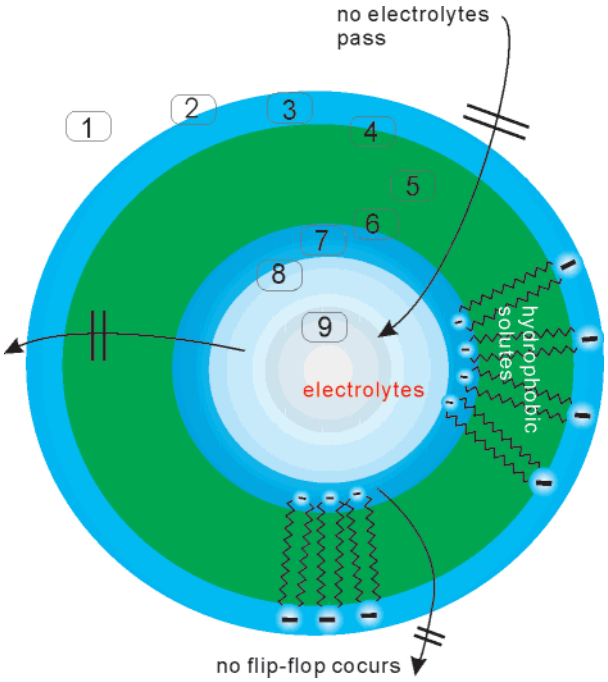

Figure 30. Utilizable regions for reaction centers in spherical monolayer lipid membranes (MLM vesicles). 1 and 9 are bulk and entrapped water phases for the build up of membrane potential; 3 and 7 are outer and inner headgroups, which may be functionalized for electron (or proton) donation and acceptance. 2, 8, 4, and 6 are the aqueous and membrane regions for the fixation of water or membrane-soluble dyes; membrane region 5 acts as fluid solvent with a solution capacity close to chloroform. The membrane is largely oversized with respect to the entrapped water volume (blue).

4. Monolayer Lipid Membrane (MLM) Vesicles

Solutes in aqueous solutions of bola vesicles may be concentrated in 1 out of 9 distinct regions. Region 1 is "outside water" and contains all ions, which are added to the vesicular solution. They do not cross the membrane within several hours. Region 9 is the inside water volume and is occupied by electrolytes, if the mixture is sonicated. Regions 2 and 8, the Gouy−Chapman layer, contain the counterions of the headgroup regions 3 and 7. If the headgroups are charged, very little flip−flop turnovers occur. Regions 4, 5, and 6 dissolve hydrophobic solutes, which usually concentrate at 4, because the alkyl chains are most flexible there (Figure 30).

The monolayer lipid membrane (MLM) has, in contrast to bilayer lipid membranes (BLM curve b), no distinct melting point (curve a in Figure 31), which renders it heat resistant. Addition of a 1:2 mixture of the bola sodium eicosanedioate (SEDA) and the single-headed amphiphile dodecyltrimethylammonium bromide (DODAB) produced vesicles which did not melt up to 80 °C (curves c and d).[117] Addition of sodium laurate to DODAB vesicles, leading to a catanionic bilayer, had a much smaller effect than the transmembrane bola.[118a] Flip−flop of bolas in bilayers was also observed (compare with Figure 3a and see Figure 38b).[118b]

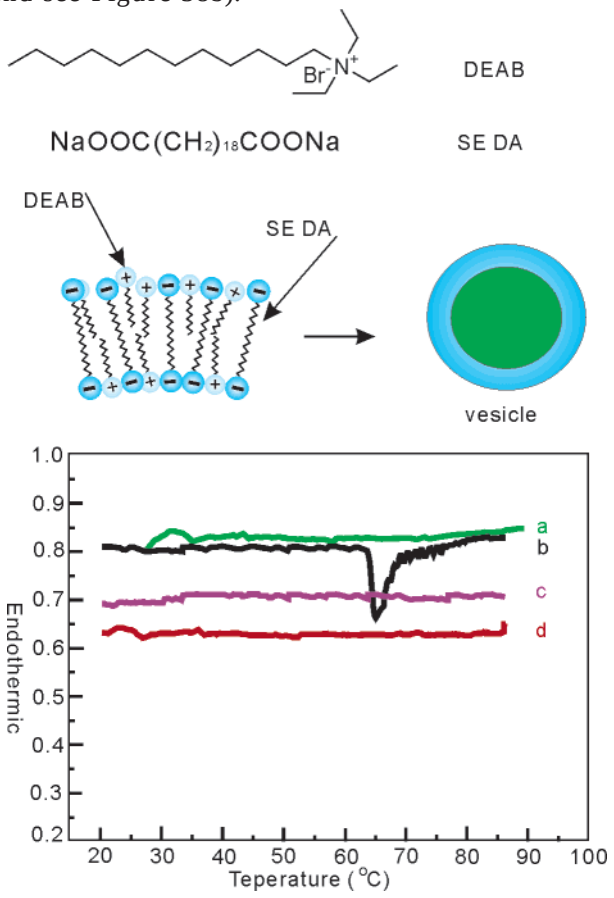

Figure 31. (a) Addition of a trans-membrane, dianionic bola to a cationic bilayer membrane increases the melting point of the latter by ≥40 °C. (a) DSC curve of SEDA monolayer, (b) of DEAB-bilayer, and (c, d) of mixtures of DEAB and SEDA.

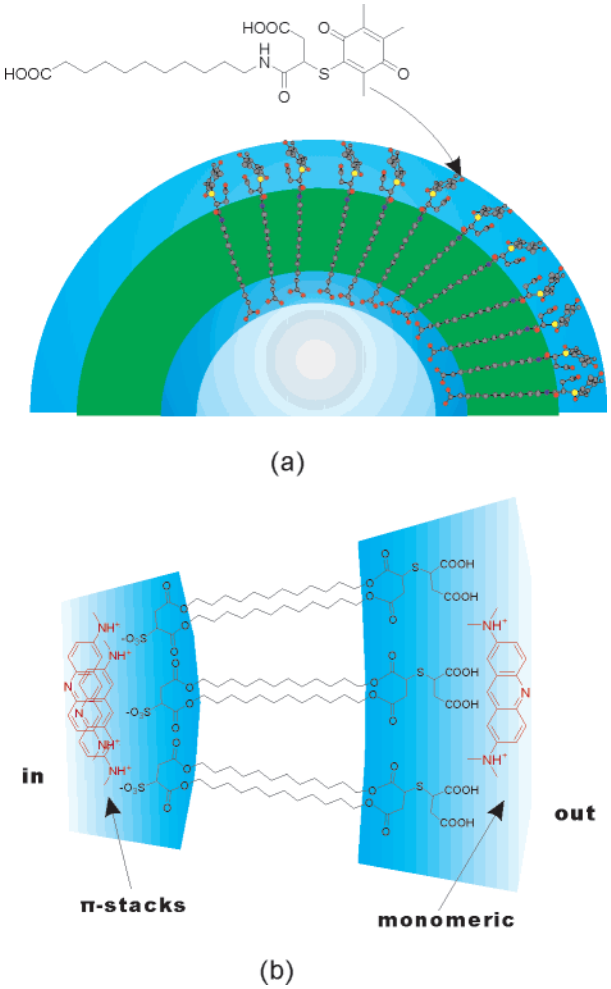

Figure 32. (a) In monolayer lipid membrane (MLM) vesicles made of the α-quinone-ω-carboxylate, >99% of the quinone was on the outer surface (= large headgroup). (b) An unsymmetric monolayered vesicle membrane with a large, electroneutral succinic acid surface does not lead to a stacking and metachromatic effect of methylene blue in the bulk water medium. The anionic sulfonate polyelectrolyte, however, produces such an effect with acridine orange inside the vesicle. It was thus shown that >1% of the small anionic headgroups appeared on the outer surface; >99% were inside.

In spherical MLM vesicles, the size of both headgroups may either be the same or different. Under favorable conditions, two headgroups of different size may assemble selectively on the inner or outer surface of vesicles to form asymmetric MLMs: all the large headgroups then go to the outer surface, whereas all the smaller headgroups occupy the inner surface (Figure 32).[1−4] This kind of topic asymmetry also occurs in mixed bilayer membranes, where two different one-headed amphiphiles are preferably localized in the inner or outer membrane.[5] The quantitative separation of some bola headgroups either in- or outside which is typical for MLM has, however, not been reported for BLMs. The smallest possible diameter of MLM vesicles is the same as for BLM vesicles, namely, 25 nm. The large curvature of vesicles leads to quite different outer and inner surfaces areas.[1,2,14] If, for example, the bola has a length of 2 nm, the ratio of both surface areas will be equal to 3^2:1.6^2 or 1.33:1. A bola with a large

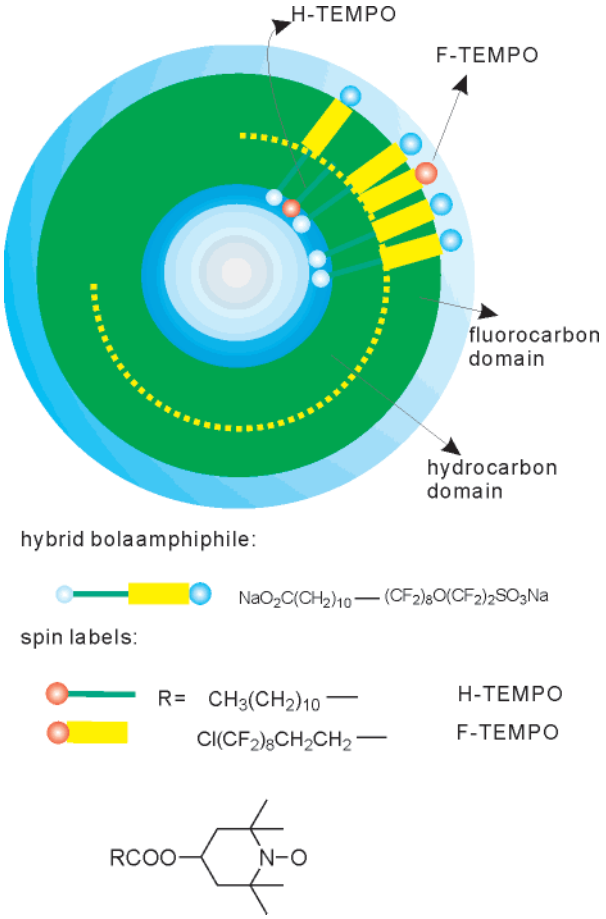

Figure 33. Region 5 (see Figure 30) is separated here in a $(CF_2)_2$ outer section and a $(CH_2)_2$ inner section. A radical with a fluorinated side chain (F-TEMPO) concentrates outside and is much more rapidly reduced by ascorbic acid in the bulk water phase than the inside analogue with a $(CH_2)_n$ side chain.

headgroup on one end, e.g., succinic acid, and a smaller headgroup on the other end, e.g., sulfonate, arranges in small vesicles in a way that the two carboxylate groups are all on the outer surface and the smaller sulfonate groups exclusively at the inner surface. Such separation may be proven by either ^{1}H NMR techniques using shift reagents in the bulk water phase or simply the metachromatic effect of surface-adsorbed methylene blue. It forms aggregates only in the presence of polyanions, e.g., sulfonate, but not on neutral surfaces, e.g., protonated carboxyl groups (Figure 32b). The quinone−carboxyl bola of Figure 32a has all the quinone on the outer surface.

A unique, single-chain hybrid bola was investigated by Hui.[13] It consisted of an "inside" undecanoic acid and "outside" C_{10} fluorocarbon segment with a sulfonate headgroup. Large vesicles with diameters between 200 and 500 nm and a membrane of monolayer thickness were found in TEMs. Spin labeling with hydrogenated (H-TEMPO) and fluorinated nitroxides (F-TEMPO) and their reduction with ascorbic acid showed that F-TEMPO was reached very quickly whereas H-TEMPO was much more inert (Figure 33).

Membrane asymmetry is more important because it may allow the localization of electron donor−

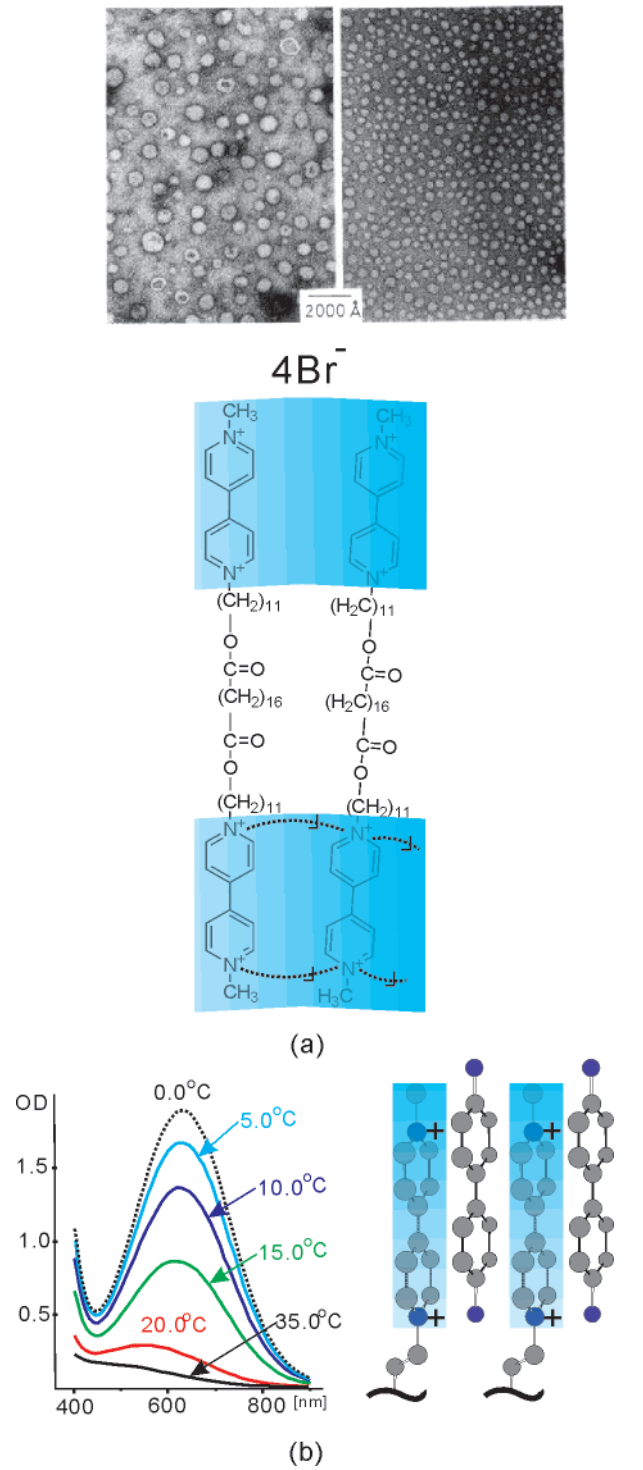

Figure 34. (a) One-sided connection of bipyridinium headgroups with iodide leads to a spontaneous vesiculation of the water-soluble tetrabromide. (b) Benzidine intercalates into the outer region of viologen vesicles and forms blue polymeric charge-transfer complexes at low temperature.

acceptor pairs at distances between 1 and 3 nm, which is ideal for light-induced charge separation and related energy conversions. In artificial systems bolas may allow photosynthetic processes from Nature to be copied without using membrane proteins.

If one adds 1 mol of α,ω-bis-viologen tetrabromide amphiphile to 1 mol of iodide ions, one induces a one-sided aggregation of the symmetrical bola and obtains again an unsymmetrical membrane: all pyridinium iodides are inside the vesicle and all pyridinium bromides are outside (Figure 34a).[119] Complexation of the viologen headgroup with benzidine has a similar effect: the blue benzidine−viologen will only form at the outer surface (Figure 34b).[120]

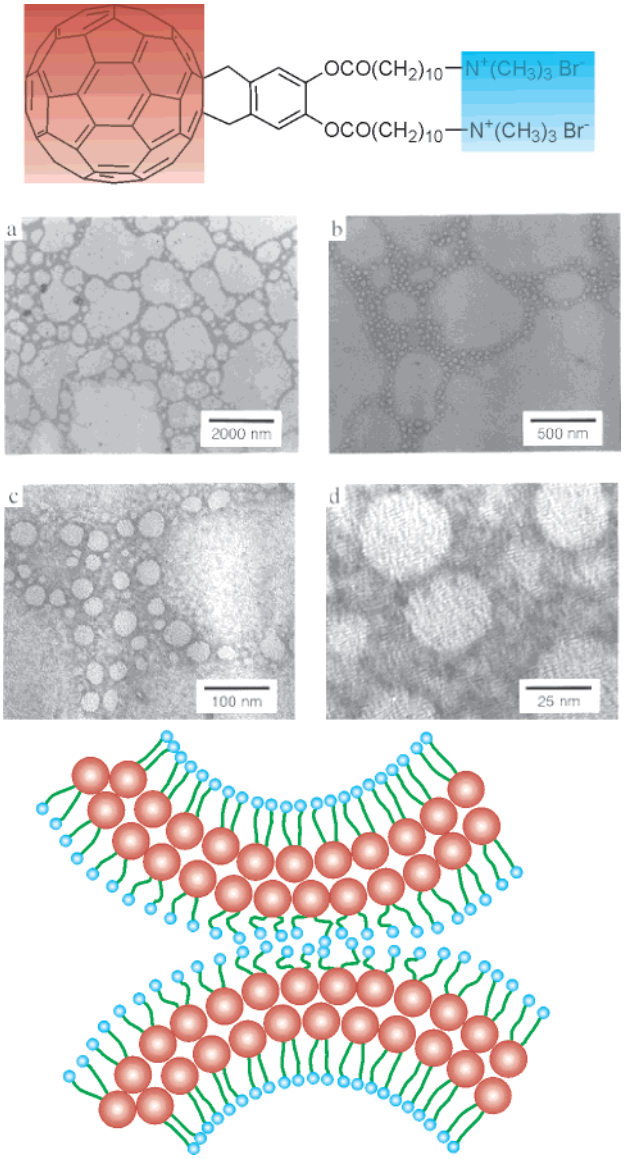

Figure 35. [60]-Fullerene bolas produce foamlike mesoscopic fractals (a−d). The hydrophobic fullerene moieties were partly exposed to water.

Scheme 8

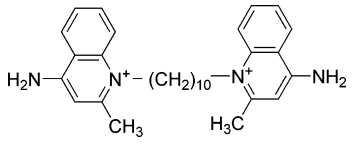

A bola with a fullerene core produced vesicles with a diameter of about 30−50 nm, which assembled to give frams upon sonication (Figure 35).[121]

The dicationic dequalinium dichloride bolas (Scheme 8) also give stable MLM vesicles, which work as perfect vehicles for DNA delivery to mitochondria. Hydrolyzable peptide bolas are also useful and nontoxic.[122a,b]

To summarize, MLM vesicles are unique with respect to the unsurpassed thinness of the membranes and can be organized very well with respect to the size and solubility of inner and outer headgroups. It should also be mentioned that a very cheap commercial bola, namely, "dimer acid", forms perfect MLM vesicles.[122c]

5. Nanowells, Ion Pores, Electron Conductors

5.1. Nanowells

Nanowells are form-stable gaps in rigid lipid monolayers which are bound to smooth solid surfaces or colloidal particles. They were produced by two-step self-assembly procedures: first, a flat porphyrin molecule was bound in an orientation parallel to the surface; second, upright-standing bolas were self-assembled to the remaining free reaction sites of the same surface. This leads to the formation of nanowells with the shape of a porphyrin and a height corresponding to the bola length. This will, however, only be the case if the hydrophobic bolas are rigid or if they are connected by two hydrogen-bond chains between secondary amide groups. Long-distance porphyrin heterodimers on silica particles have, for example, been realized. Porphyrin A was first deposited on aminated silica; a diamido bola containing an activated CC double bond followed and was aminated by Michael addition. Porphyrin B was then attached to the resulting ring of ammonium groups (Figure 36). Light-induced energy transfer was found when

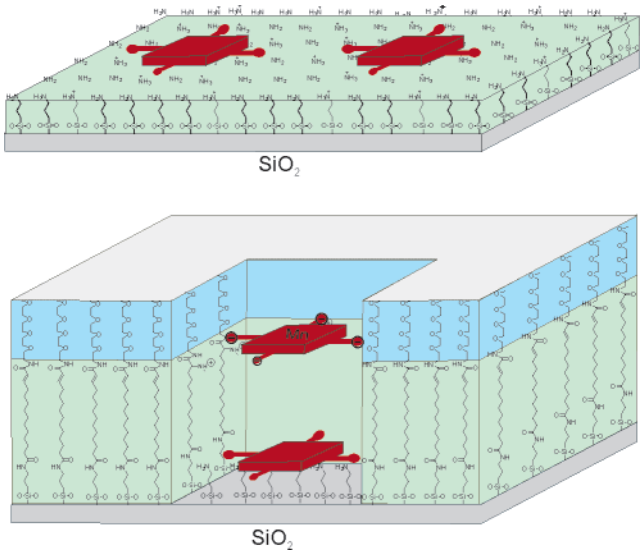

Figure 36. (a) Model of an amine-coated silica particle with covalently attached porphyrin molecules. The diameter of the smooth particles was 100 nm; their surface is, on a molecular scale, close to planar. (b) In a second self-assembly step a rigid bola wall was raised around the porphyrin. A nanowell with a porphyrin bottom was thus established. An ammonium ring was assembled by Michael addition of methylamine at the rim of the nanowell. A second tetraanionic porphyrin was then attached within this ring. Nanowells with oligoethylene glycol (OEG) headgroups were also built on the smooth surface of aminated silica particles or on old particles. These particles are soluble, and their nanowells can be filled in water as well as in chloroform.

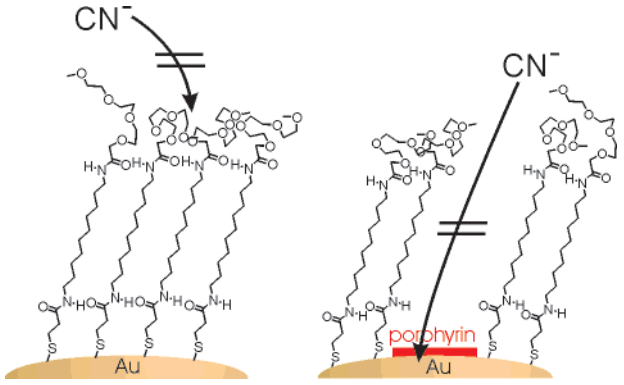

Figure 37. Models of diamido bola-coated gold particles. The rigid coating protected the gold from dissolution by sodium cyanide in the bulk solution, even if it contained nanowells with a porphyrin bottom.

A and B were 6 Å apart. The bolas are needed to fixate the monolayer on the substrate, e.g., SH for gold or −COX for aminated silicate as well as to functionalize the surface. The gaps can then be seen as simple models for reactive centers on biological protein and membrane surfaces; catalysis and charge separation may be realized here. The most useful outside headgroup is oligoethylene (OEG), which allows one to study the nanowells in water as well as in various organic solvents, e.g., chloroform.[69,87,88] The nanowells are the only means to order stacks of different single molecules on top of each other. Both water- and chloroform-soluble molecules can be used.

Rigid monolayers on smooth citrate gold particles provide perfect protection against corrosion by cyanide in the bulk solution. Even nanowells with a porphyrin bottom allow no passage of the cyanide ions to the gold surface (Figure 37).

5.2. Pores for Ion Transport

Pores are hydrophilic domains in vesicle membranes. The building blocks are usually bolas as well as edge amphiphiles. The hydrophobic core must be long enough to cross the lipid membrane, with polar headgroups on both ends and to help to enforce a stretched conformation. The bola core is then made of a macrocycle or of a row of several small cyclic molecules, which contain a polar and a nonpolar edge. Bacteria produce such amphiphiles in the form of protein helices, which will not be discussed here, or in the form of reduced carbohydrates, tetrahydrofuranes, and related oligomers. The hydrophobic edge will lead to dissolution within the membrane; the hydrophilic edges will lead to the formation of water-filled pores, which are also called "channels". In biological cells such edge amphiphiles lead to a breakdown of the membrane potential; they act as killing antibiotics. Synthetic analogues are often made to achieve ion-selective transport.

Nanowells and pores thus serve different purposes. Nanowells with hydrophobic walls with or without hydrophilic hooks and a reactive dye bottom are thus useful as organizing matrix for reactive systems. Pores are more on the disintegrating side of supramolecular chemistry. They abolish the separating

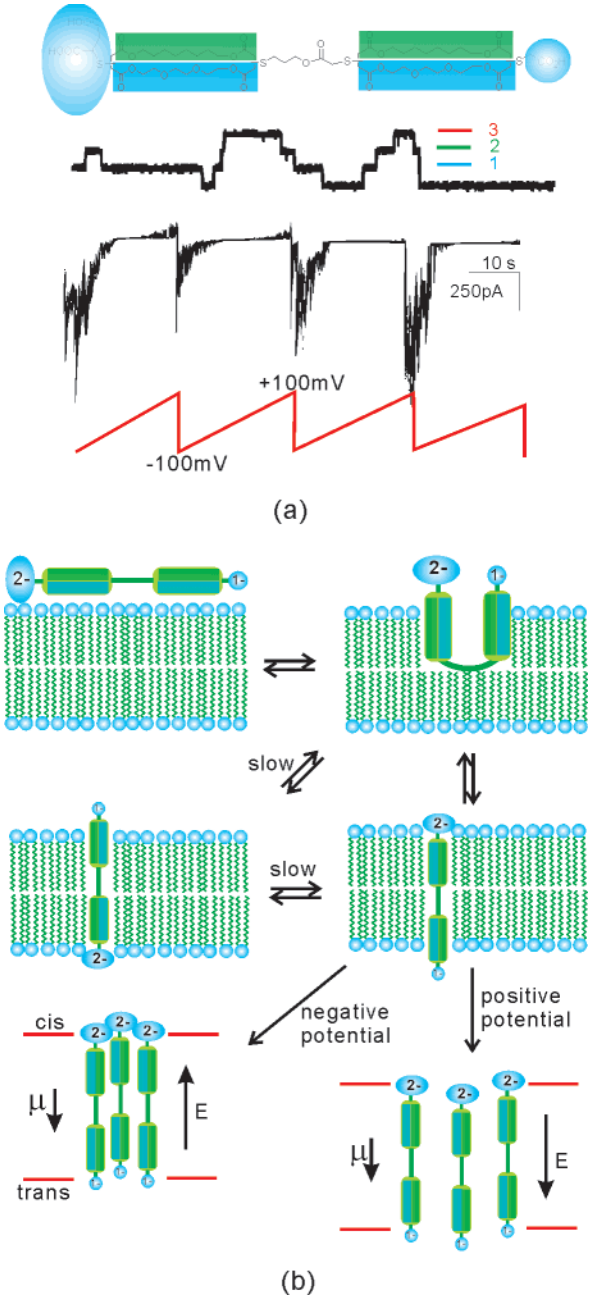

Figure 38. (a) Typical trans-membrane CsCl currents after addition of the diacetic acid bola to a planar lipid bilayer after application of a potential. (b) Proposed mechanism for a voltage-dependent ion channel made of the acetate−succinic acid bola. μ indicates the alignment of bola dipoles; E is the applied electric field.

properties of membranes: they become partly hydrophilic and the entrapped water volume is connected to bulk water.

Cation transport across lipid membranes is usually studied in planar bilayers across an aperture in a polystyrene barrier between two aqueous salt solutions. Transmembrane ion currents can be measured then when a potential of about 100 mV is applied. This worked, for example, when a bola-edge-amphiphile was added to a diphytanoyl phosphatidyl choline bilayer. At first the bilayer was nonconducting, but 15 min after the addition of the pore, former picoampère currents became measurable. No continuous current occurred, but step conductance

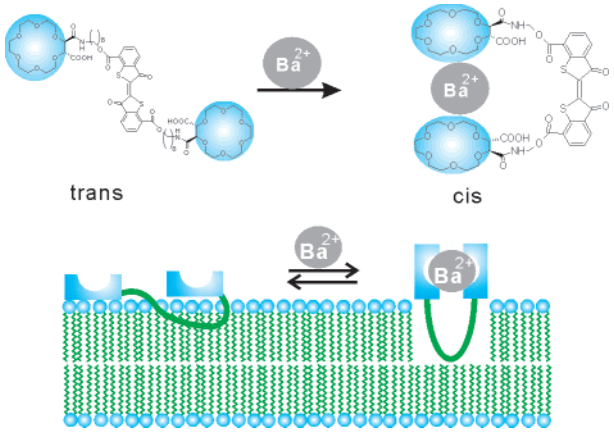

Figure 39. Ba^{2+} ions change the conformation of a di-crown ether bola, and the U-shaped conformer opens the bilayer membrane for the transport of carboxyfluorescein.

changes consistent with the closing and opening of the pore were observed. Some openings lasted a second or longer; others were much shorter. The pore also showed some selectivity of NaCl over CsCl. Opening and closing of the gap may either be caused by aggregation of the U-shaped molecules in both parts of the monolayer or by side-on dimerization of stretched bolas (Figure 38a).[123]

Unsymmetric bola-edge-amphiphiles have also been used to achieve rectified current−voltage responses in which current only flowed at cis-negative potentials. The bolas carried thioacetic acid on one side and thiosuccinic acid or thioglucoside on the other.[124] These arrangements were similar to those used earlier to construct unsymmetric vesicles.[14] The acetate−succinate bola was then added to the cis-compartment of the bilayer clamp and induced bursts of significant KCl currents only at negative applied potentials. The acetate−glucose bola, on the other hand, produced regular step conductance of a single channel. This difference was explained by the spontaneous formation of asymmetric domains in both cases. The less-charged acetate or glucose migrated preferentially through the hydrophobic bilayer, and the more negative side responded to the applied potential. A negative potential would favor anion−anion antiparallel alignments of the molecular dipoles of the bolas and the electric field vector and thereby stabilize the domain, whereas a positive potential would destroy it (Figure 38b). This effect was, however, much less pronounced if electroneutral glucose held the molecules together at the inner side of the membrane. Although strong interactions of an electric field with partly charged membrane surfaces in the presence of 1 M KCl is surprising, so is the positive effect of Ba^{2+}. One may expect closure rather than opening of pores here.

Bis-(crown ether) bolas were used to release vesicle-entrapped 5[6]-carboxyfluorescein. Only a domain formation with divalent ions, in particular with Ba^{2+} and Si^{2+}, led to the membrane's disruption. A thioindigo-connected dimer was 10 times more active as a cis-isomer than in the trans-configuration.[125a] In this case it was clearly stated that a membrane disruption process by ∩-shaped bolas was responsible

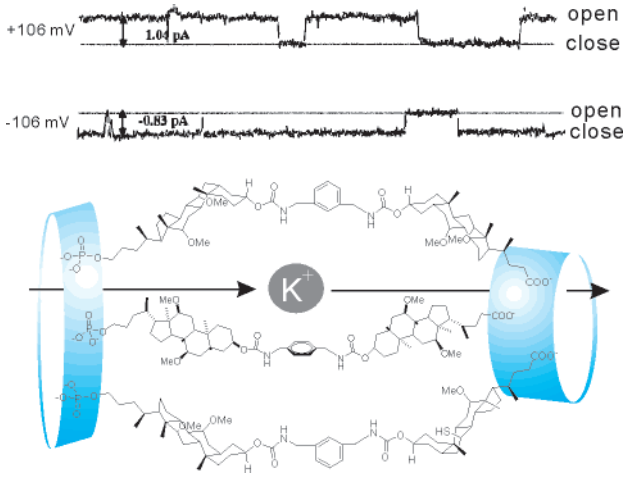

Figure 40. Bola-type cholic acid dimer with methoxy-substituted edges was dissolved in a lipid bilayer membrane. It opened potassium channels after the application of a 100 mV voltage.

for the anticipated dye release (Figure 39). In general, only metal ions are supposed to flow through pores, not dye molecules.[125b]

A similar behavior, namely, the inactivation and activation of channels by applied potentials, was already observed with 1:1 mixtures of oligoethylene glycol ethers with a carboxylate end and octadecylammonium salts. Aggregation−deaggregation processes were postulated, but no additional evidence for such a process was provided.[126,127] Covalent cholic acid dimers with cationic[128] or anionic[128] end groups showed perfect single-channel behavior. In this case the hydrophilic edge only contained two axial methoxy groups, while a hydrophilic channel across the bilayers was not obvious. The "very stable open state" which was proposed might be nothing more than a disrupted membrane here, and the observed currents were very similar to those observed upon application of a high disrupting potential. The destabilization by rigid solutes and their fixation by two end groups only rendered the membrane much more vulnerable to such fields (Figure 40).[129] A 100 mV/5 nm voltage corresponds to 2000 V/cm!

Noncovalent pores in fluid membranes may, however, grow to diameters of 20 Å and more. This depends on the number of edge amphiphile molecules within one vesicle membrane. Thus far no flexible channel for the passage of dyes has, however, been described. Only the disruptive "harpoon" mechanism introduced by Regen seems to work here (see Figure 42). The disruption of fluid bilayers by membrane-spanning bolas is certainly not equivalent to a hydrated pore. It might also happen that single-edge amphiphiles provided hydration spheres on their surface, which allowed temporary ion transport on their surface. The metal ion's hydration sphere might combine with that of the bola's hydrophilic egde and then drag a large number of ions through the membrane.

The only experimental proof for an ion pore, which provides an ion channel, consists of the reversible opening and closing of such pores with chemical

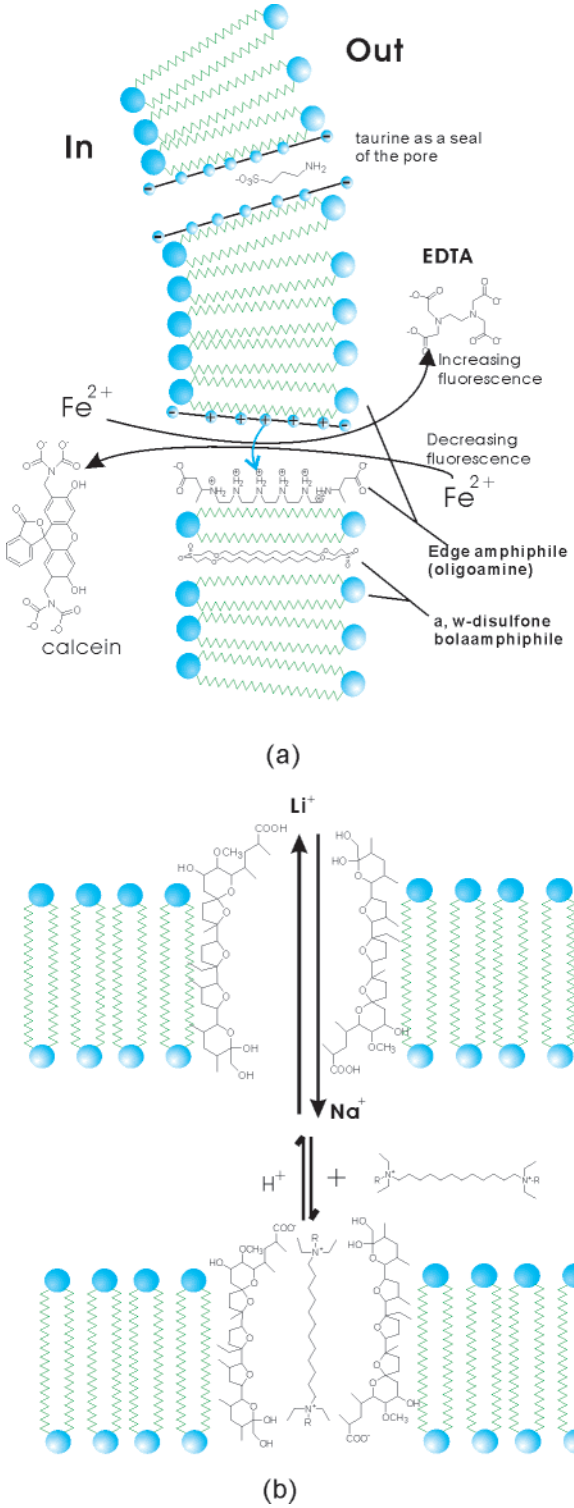

Figure 41. (a) Model of a vesicle pore made of an oligoamine edge amphiphile, which is also an α,ω-dicarboxylate bola. The pore is passed by Fe^{2+} ions which quench the fluorescence of entrapped calcein molecules. Addition of EDTA to the bulk aqueous medium reverses the effect; Taurine seals the pore for ion transport. (b) A monensin-derived bola also produces pores for ion transport. They have been irreversibly sealed by a dicationic bola.

stoppers. Changes of potentials and geometries along the surface of single molecules may just help sliding along polar surfaces. In protein-based pores, chemical stoppers are well known and act as poisons. Curare and tetradotoxin are prominent examples for cationic

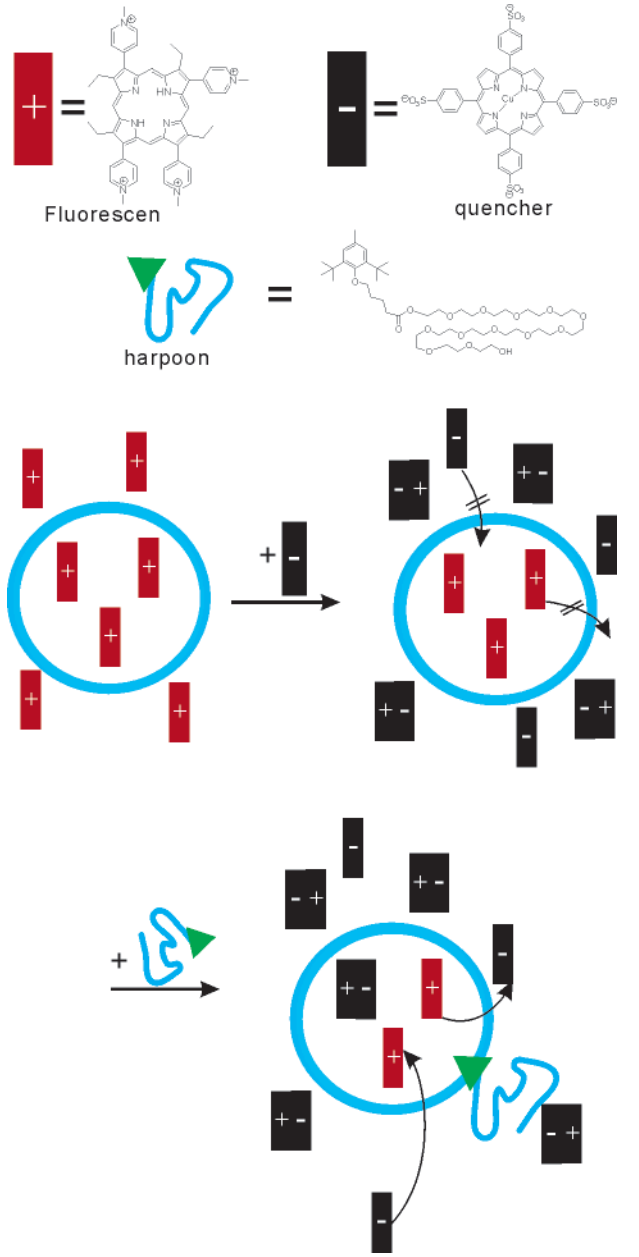

Figure 42. Membranes become leaky for dye molecules if they are treated with "harpoon" amphiphiles, carrying a hydrophobic end with bulky *tert*-butyl groups. Water-soluble porphyrins containing copper ions pass a "harpoonized" membrane.

stoppers of anionic gates. In artificial systems, only one example is known. If a cyclic oligoamine with a hydrophobic edge and two carboxylate end groups was integrated into a monolayer lipid membrane vesicle, the membrane became permeable for iron(II) ions, which quenched the fluorescence of calcein, which was entrapped with the vesicles water volume. EDTA could not pass this noncovalent pore either because it was too large or because it was tightly bound to the oligoamine. It removed, however, the iron(II) ions from the vesicle's water volume. The calcein fluorescence was restored. Addition of excessive iron(II) salts first complexed the EDTA and then migrated again through the pore to react with calcein (Figure 41). This cycle could be repeated several times and stopped at once when an anionic stopper,

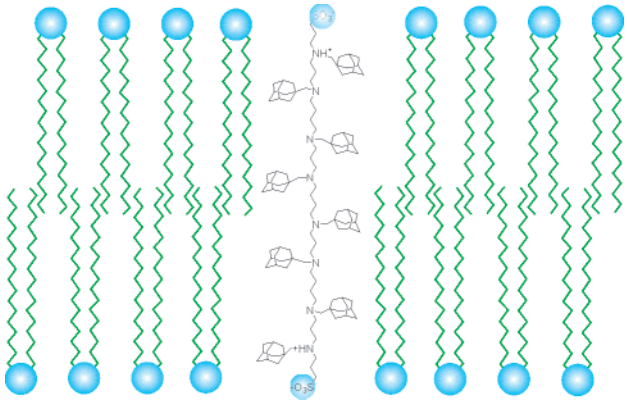

Figure 43. Spermine with adamantane substituents and sulfonate headgroups acted as a permanent harpoon.

e.g., camphor sulfonate, was added. This system involves, however, no bilayer membrane.[130] Thus, there is so far no other controllable pore available which is not based on proteins. Similar results have been reported for anionic monensin derivatives in MLM vesicles, which were closed by a dicationic bola.[131,132]

The most efficient artificial mechanisms to disrupt bilayer lipid without the formation of defined pores are also based on bolas called "harpoon" bolas, which work in bilayer lipid membrane systems.[133] The harpoon mechanism works best with fluid lecithin or DPPC membranes, when they are rigidified with 50% cholesterol. An anionic copper(II) porphyrinate in the bulk water volume was, for example, quickly combined with a cationic porphyrin entrapped in a vesicle's interior after addition of an oligoethylene carrying a membrane-disrupting 2,5-di-*tert*-butyl group (Figure 42).[134] Harpoons thus constitute the opposite of membrane-spanning bolas, which strongly stabilize vesicle membranes. Their bulky second "headgroup" is hydrophobic and cannot leave the membrane's interior bulky.

Fluid lipid membranes also act as barriers for proton transport. A gradient of one pH unit is stable for several hours around neutral pH. Addition of membrane-spanning oligoamines or amides with bulky substituents led to a rapid breakdown of such gradients if it was held by two terminal sulfonate groups (Figure 43).[135] Ion flux was also promoted by tetraphenylporphyrins carrying four heptapeptide units.[136] Attachment of alkyl groups of various sizes to the hydrophobic skeletons of the lipid also created defects in the bilayer.[137] It is always the same motif which returns in artificial "pores" or "channels" in fluid bilayers: any disturbance of the fluidity or of the headgroups' mobility will let ions leak through it. The presence of water channels in membranes cannot be proven by the detection of statistical current fluctuations and voltage effects. If the pore consists of a defined entrance, an entrapped water volume, and an outlet, it must be controllable by stopper molecules and/or movement of its walls.

Synthetic transmembrane channels containing 18-crown-6 or β-cyclodextrin units, which integrate holes within membranes, have been reviewed by Gokel.[138] A tris(macrocyclic) channel model system and a

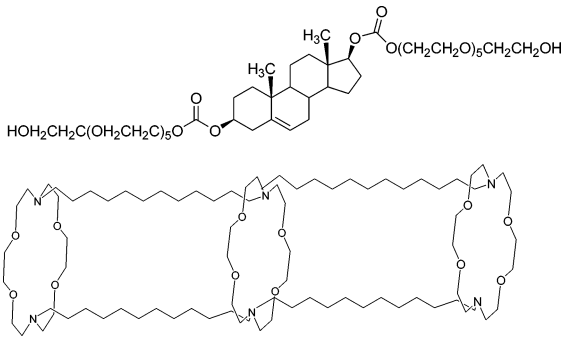

Figure 44. Steroidal and crown-ether bolas also produce channels, which could not be closed.

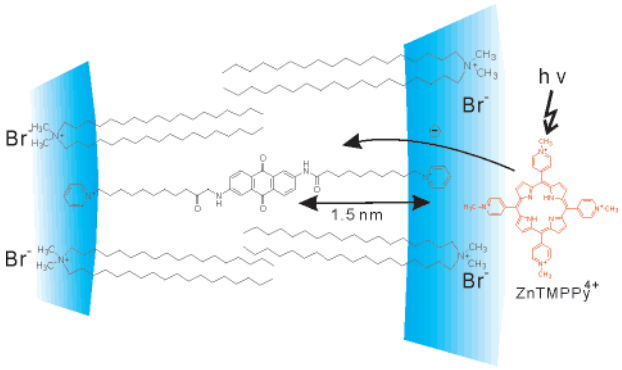

Figure 45. Light-induced charge separation was observed between a quinone bola entrapped in a bilayer vesicle membrane and a zinc porphyrinate in bulk solution. Recombination of charges was, however, as fast as the separation.

steroid bola which is placed at the bilayer membrane midplane and stretches OEG arms to the inner and outer surface are reproduced in Figure 44.

5.3. Electron Conductors

Mono- and bilayer lipid membranes of fluid vesicles are perfect insulators with respect to electron transport. The macrocycle with two quinone moieties in the center formed vesicles in water and was readily reduced to the semiquinone radical and to the hydroquinone with dithionite, but reoxidation with persulfate did not occur (Figure 45). Hydroxyl ions also did not react with the semiquinone. This indicates that electrons cannot jump over a distance of about 1.0 nm. The same holds true for bis-pyridinium-ended quinones coupled with a zinc porphyrin on the vesicle's surface. The porphyrins photoreduce the membrane-integrated quinones within microseconds, but the back-reaction is equally fast.[139]

Disulfonato indigo dissolved in the entrapped water volume is also reduced by borohydride or dithionite in the bulk water when stiff polyene bolas are dissolved in the bilayer lipid membrane. Dithionite or hydride reduction gave, however, the same two different reduction products which are found in homogeneous solution. This is a clear indication that "electron conduction" by the polyene "wire" does not take place. The stiff membrane-spanning polyene bola just disturbs the fluidity of the membrane and allows ion transport.[140] The same phenomenon is obviously caused by another bola polyene called

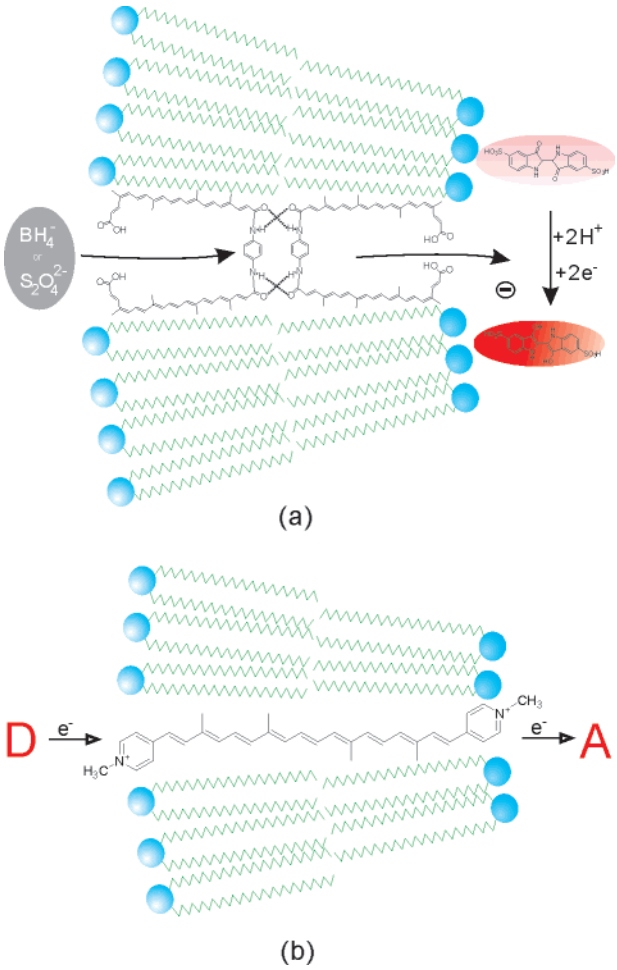

Figure 46. Polyene bolas with electron-withdrawing headgroups should transport electrons via reversible Michael addition of the electrons. In the case of the phenylenediamine−bixin bola (a), only ion transport was observed; in the caroviologen (b), the mechanism of the observed electron transport is not known.

caroviologen.[141] Both systems, bixin and caroviologen carry electron-withdrawing headgroups. Introduction of elections by Michael-type addition to the polyene is a plausible reaction, but it does obviously not occur to a measurable extent (Figure 46).

6. Fibers

Spherical monolayer membranes convert to linear or helical fibers, e.g., long rods or tubules, when rigid segments establish an ordered packing or hydrogen-bond chains are formed between the headgroups or amide bonds in the hydrophobic core.

The vesicle → fiber conversion may be caused by a more rigid hydrophobic core. A phenyl(bissalicylideneimine) unit, for example, gave vesicles, whereas the oxydiphenylene analogue only produced fibers (Figure 47).[142]

α,ω-Diamido bolas with tetraalkylammoniumbromide and glucofuranose headgroups gave beautiful circular vesicles after freeze-fracture cutting in electron microscopy. The observed cross-fracture across the membrane clearly indicated a monolayer membrane made of stretched bolas. Above 60 °C disks were formed instead of vesicles (Figure 48). It was

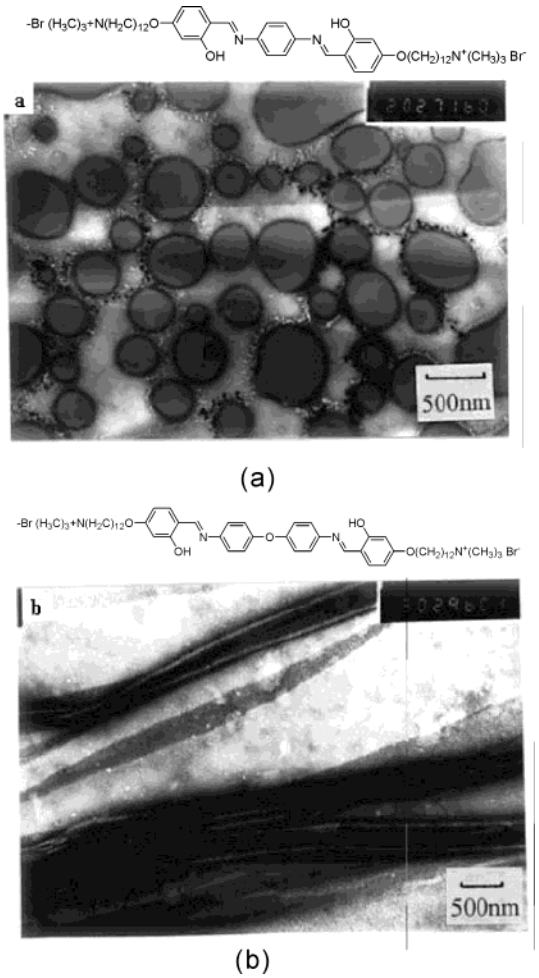

Figure 47. Rigid bolas with long fluid segments either form vesicles (phenyl linker) or extended ribbons (oxy−diphenylene linker).

assumed that the hydration of the glucon units decreased at higher temperatures and the U-shaped form of the bola became more frequent: such folded conformers would then form the edges of the disks as well as planar lamellae.[143]

Bis-glucoside bolas with a stiff diazobenzene bis-amido core form fibers in concentrated DMSO water solutions. The chiral headgroups cause weak CD activity of the 350 nm band (called erroneously a "Soret" band in the publication).[144] Furthermore, the fibers are converted to vesicles by a boronic acid−poly(DL-lysine) salt.[145] The nature of this conversion is not known, although five publications deal with the subject of poly(L-lysine)boronate interactions with carbohydrate amphiphiles.[146] The boronate ions may split hydrogen bonds between the glycoside headgroups; the role of poly(L-lysine) in the formation of giant carbohydrate vesicles (diameter $\approx 1-2$ μm) remains unclear (Figure 49).

The most common conversion of spherical vesicles to linear rods or tubules is caused by formation of linear hydrogen-bond chains between the functional groups of the hydrophilic parts or secondary amide linkages in the hydrophobic core. It is controlled by the size of substituents in the neighborhood of the CONH bond and by temperature. If the distance between the amide groups becomes too large to form

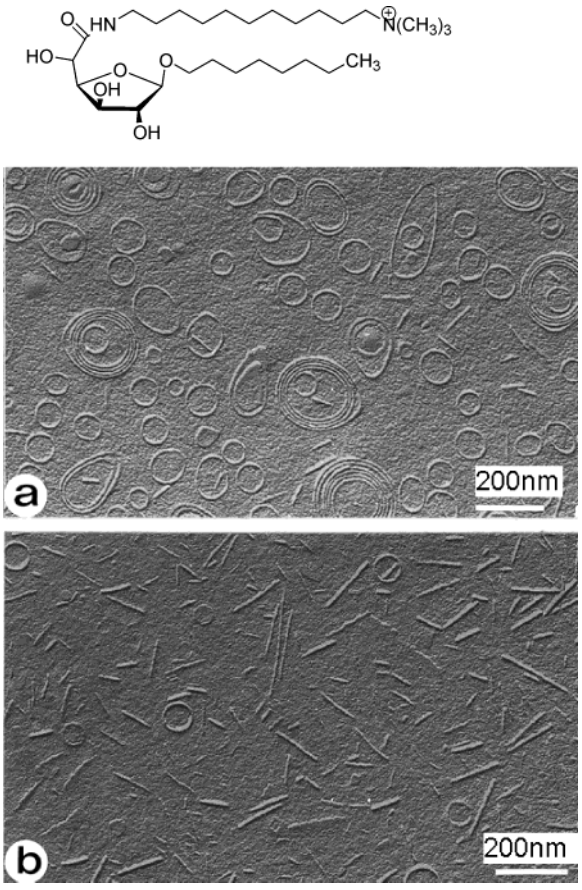

Figure 48. Freeze-fracture TEMs of the same bola may show vesicles if the probe was frozen at a starting temperature of 20° C (a) and rods at 60° C (b). Scale: 100 nm.

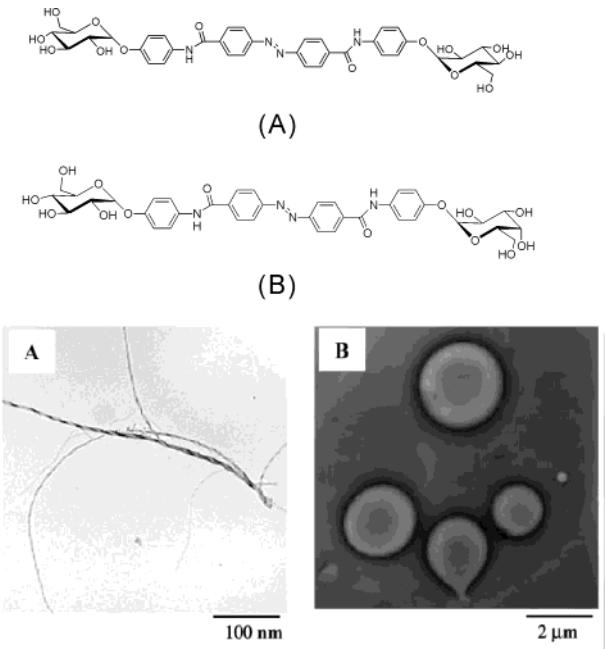

Figure 49. Slight changes in the headgroup stereochemistry may charge the structure of the molecular assembly. The rigid glucose bola A, for example, produced well-organized rods; the glucose−galactose analogue B gave vesicles. Addition of polylysine converted the rods to vesicles (not shown).

stable hydrogen bonds or if curvature does not allow linear chains, crystallization or dissolution of the

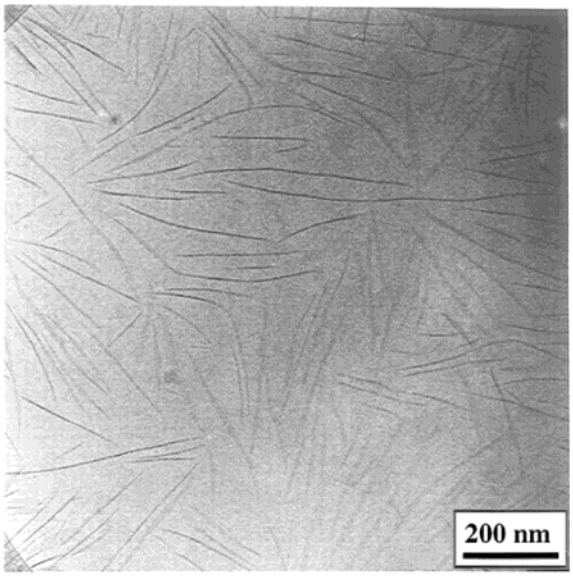

Figure 50. Cryo-TEM of the given α-ammonium-ω-carboxy bola, which was vitrified at pH 6.8 and from 65 °C.

fibers occurs. No bilayer fiber survives a temperature of about 80 °C. This is, however, not true if the fiber is part of a columnar liquid crystal (see at the end of this section).

The most simple case is given by (16-carboxy hexadecyl)trimethylammonium bromide, which forms ribbons of irregular curvature at pH 6.8 with lengths of up to 1 μm and 3−4 nm thickness corresponding roughly to the length of one molecule. Carboxyl−carboxylate hydrogen binding and a charge interaction leading to a U-conformation were made responsible for fiber formation (Figure 50).[147]

Whereas dicarboxyl or diamino bolas appear as linear conformers in crystals, α-carboxyl-ω-pyridinium bolas prefer cyclic conformations. Intramolecular N^+-O distances are close to 3 Å.[148] The situation changes if stiff diazobenzene units intervene. Linear conformers prevail, and long fibers of light microscopic dimensions are formed in water (Figure 51). Upon irradiation with visible or UV light, they irreversibly break up to form short fragments of the same thickness.[149]

The breakthrough to a large variety of bola-derived rods and tubules of molecular dimensions came with the introduction of chiral headgroups based on carbohydrates or amino acids. Chirality is closely related to curvature because it often induces the formation of helices, which may intertwine to form multihelical rods or ribbons. Even tubules with a smooth nonhelical surface are much more stable against rearrangement to planar layers and crystallization if their surface molecules are chiral.

In this case the detailed conformation of the open-chain gluconamide in various crystals and fibers was determined. The crystal structure showed a linear conformation and a strong homodromic hydrogen-bond cycle between neighboring headgroups as well as a head-to-tail arrangement.[150] A 2-gauche conformation at C-2 allowed the entrapment of water molecules in the headgroup. Open-chain glyconamides were first applied as headgroups in single-headed amphiphiles to yield quadruple helices.[150−154] Bolas with two open-chain gluconamide headgroups on the ends of an octamethylene chain, however, crystallized and did not form fibers. No homodromic hydrogen-bond cycles stabilized the crystals.[155] The situation changes with cyclic glucosamides: bis-1-glucosamides with a connecting C_6 chain give bundles of needles, with a C_{10} chain twisted ribbons of light microscopic dimensions (diameter ≤ 3 μm, length ≈ 1 mm; Figure 52) results, whereas the odd-numbered C_{11} bola gives crystals (see section 3.1).[38]

The corresponding diastereomeric 2-glucosamides, made of 2-deoxy-2-amino-glucose instead of the 1-aminoglucoside, also gave twisted ribbons with even-numbered carbon chains. The diasteromeric 1-galactosamide bolas, on the other hand, produced only rigid needles. Introduction of stiff diacetylene groups in the center of a C_{10} chain led to ill-defined, non-

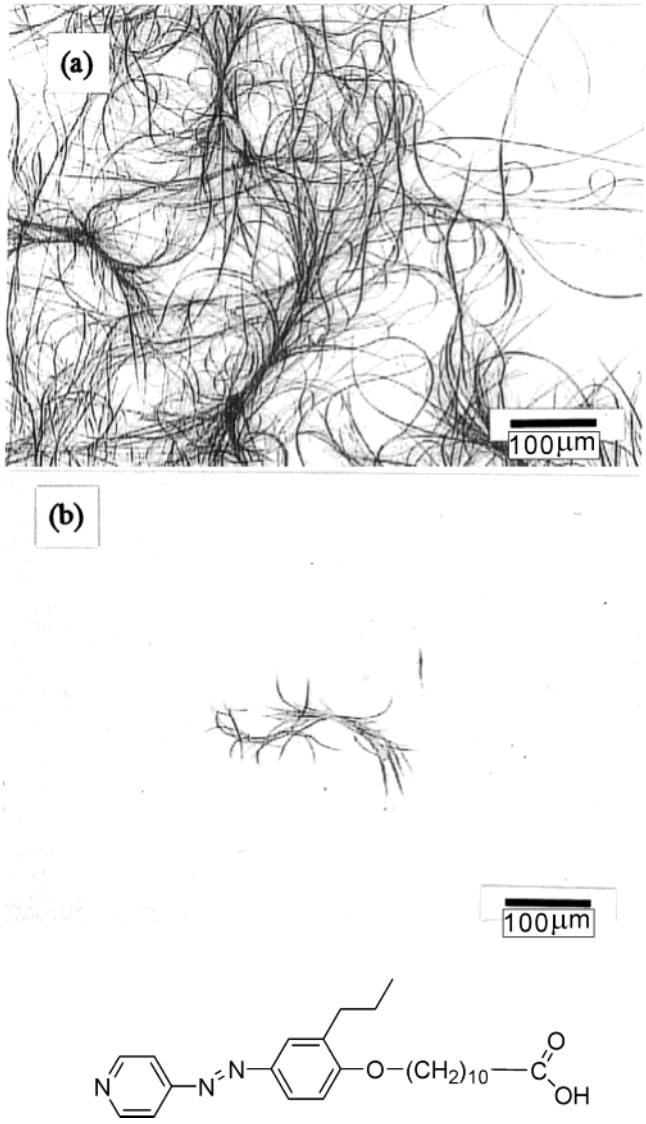

Figure 51. (a) TEM of the fibers made of a rigid pyridyl-*trans*-diazobenzene unit and a fluid $(CH_2)_{11}$ chain. Upon UV irradiation the cis-isomer was formed and the fibers broke up (b).

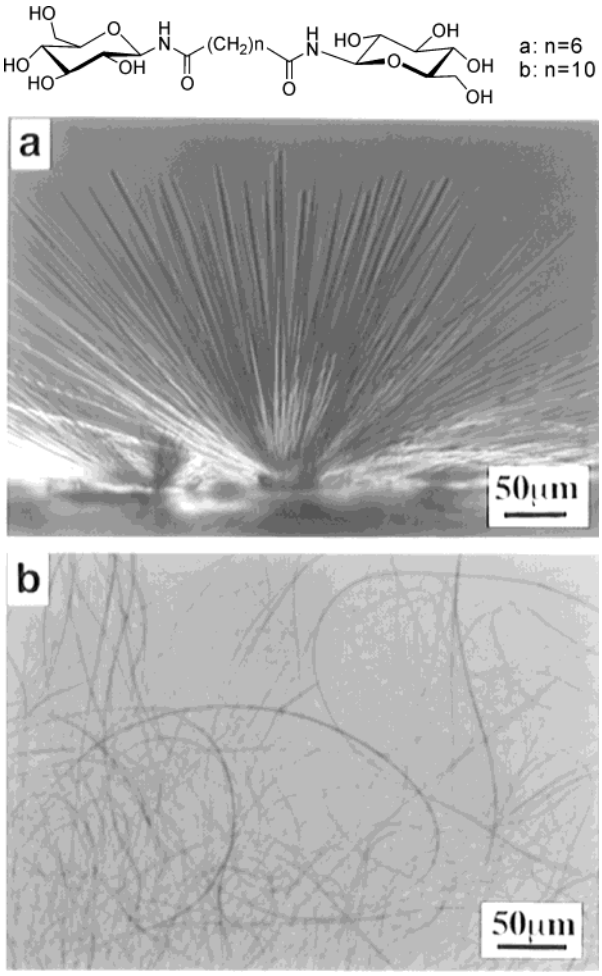

Figure 52. TEM of needlelike fibers made of α,ω-bis-1-aminoglucosides with (a) a $(CH_2)_6$ and (b) a $(CH_2)_{10}$ connecting chain. The short-chain bola crystallizes; the longer-chain bola behaves like a flexible amphiphile (compare with Figure 11; nonlinear alkyl chains produce soft crystals rather than fibers).

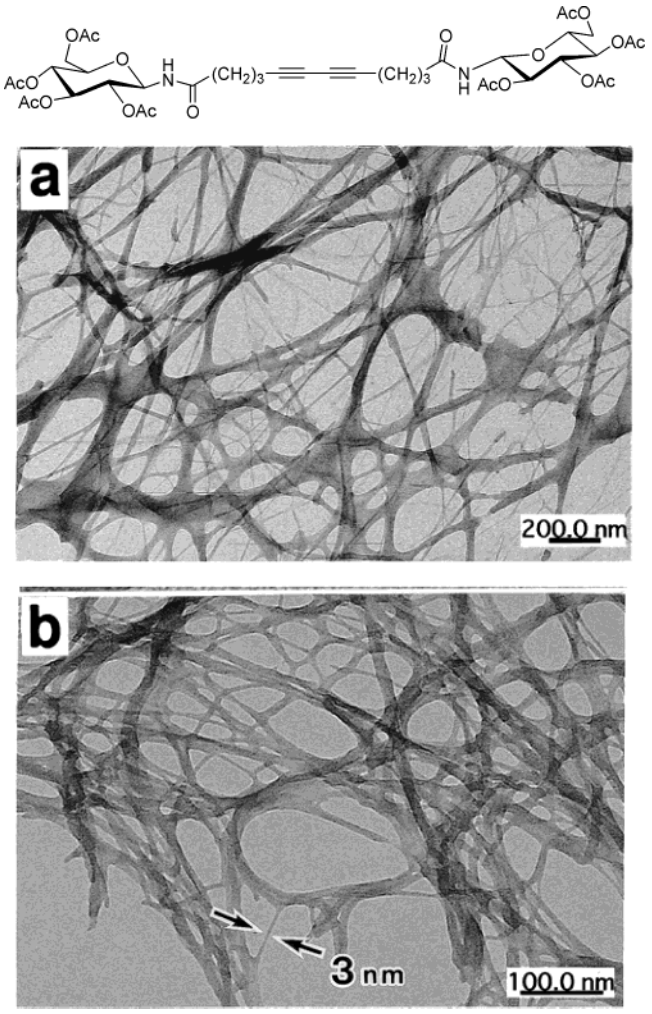

Figure 53. (a) TEM of a typical organogel as obtained from an ethyl acetate/*n*-hexane mixture. The bis-glucoside-tetraacetate contained diacetylene units. (b) Irradiation with γ-rays produced the polymer without changing the fiber's appearance drastically.

helical ribbons, which produced colorless gels. Upon UV irradiation the gel turned red (λ_{max} = 506 and 546 nm), indicating covalent polymerization (~40 mers) without much change of the fiber's appearance in TEMs (Figure 53).[156]

The best aqueous and organo gels with glucosamides were obtained with phenol-glucose and -galactose amides also carrying two secondary amide groups (Scheme 8). These gels were formed in water as well as in several organic solvents. The aqueous bola gels (0.05 wt %) were completely transparent and stable; its CD spectrum shows strong peaks at 245 and 280 nm. SEM pictures show lamellar structures with a thickness of 50−100 nm (Figure 54).[157]

The glucosamide bolas thus produce only disappointingly coarse fibers. Chiral fibers with a diameter of a single molecule were obtained only from amino acids. The N^6-acylated lysine with terminal α-amino acid and amino headgroups produced long rods in water at pH 10.5 with a diameter of 2 nm. Elongation of the bola by 11 methylene groups and introduction of an extra primary amide link gave monolayered, tubular vesicles with a uniform inner diameter of 50 nm and lengths of several micrometers (Figure 55).[158]

Symmetric glycylglycin bolas gave tubes with 100 nm walls and a uniform diameter of about 2 μm. They entrapped a large number of vesicles made of the same material (Figure 56).[159,160] Introduction of proline units gave similar tubules (not shown).[161] The same molecule with a C_7 chain in the center gave nanotubule clusters (Figure 56b) in the presence of Ni(II), which disassembled upon addition of EDTA.[162] Metal-coated wires were obtained from such tubules at pH 6 in citrate buffer solution by treatment with copper or nickel salts and reduction with 0.1 M hypophosphite solution.[163] Bis-bolas also gave gels in water at pH 3−5.[164]

An α-glutamic acid-ω-carboxylate bola with a diacetylenic center assembled in water in the form of helical ribbons made of monomers as well as after UV-induced polymerization. Contact-mode AFM of the polymer showed beautiful hexagonal cells on the surface of the polymeric helical ribbons, allowing detailed analysis of the packing of the three carboxyl groups. The polymer solution was blue at pH < 6 and red at pH > 7.5. Electrostatic repulsion between the carboxylate groups presumably caused strain and

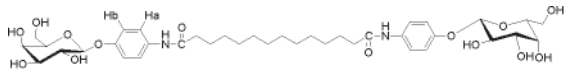

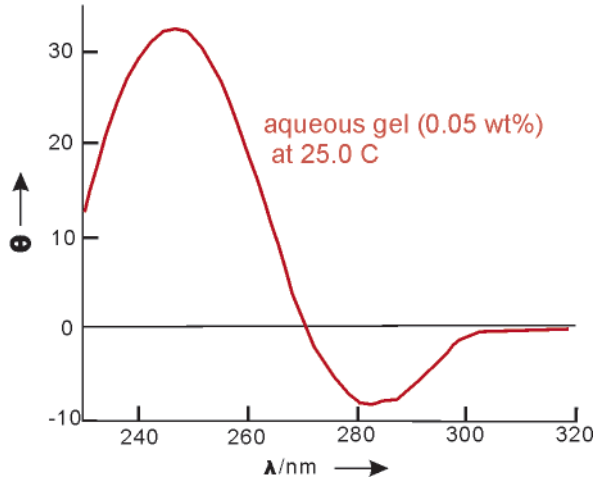

Figure 54. Very stable gels were formed from bolas with stiff extended rigid headgroups at a concentration of 0.2 wt %. CD spectra.

distortion of backbone, resulting in a shorter conjugation pathway and a blue shift (Figure 57). Dense networks were observed in TEM. Extra hydrophobic side chains favored the formation of β-sheets.[166]

Urocanic acid (Scheme 9) is a photoprotective imidazole−acrylate. Its trans-isomer was used as a headgroup in long-chain diesters, diamides, and diamines. Vesicles and rods were observed in water, but no changes upon irradiation with UV light were reported.[163]

Nucleotide-appended bolas with 3′-phosphorylated thymidine moieties at each end gave double-helical ribbons with a width of 1−2 μm (Figure 58) and several hundred micrometers in length. A 0.2 wt % solution formed a rigid gel. Such low concentrations are obviously typical for bola fibers: their networking efficiency is very high. The thymidine units partly photodimerized upon irradiation.[168] The corresponding adenine and asymmetric α-thymine, ω-adenine bolas were also synthesized but formed only ill-defined ribbons in water.[169]

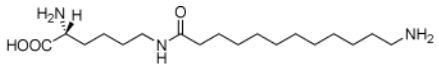

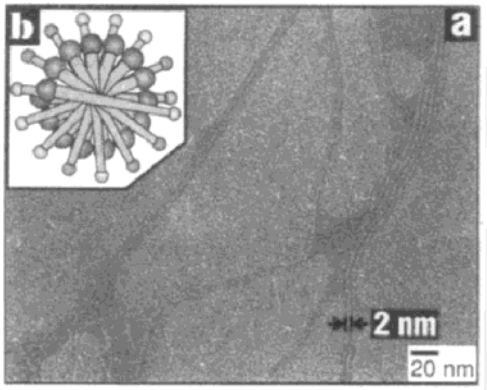

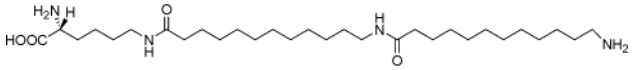

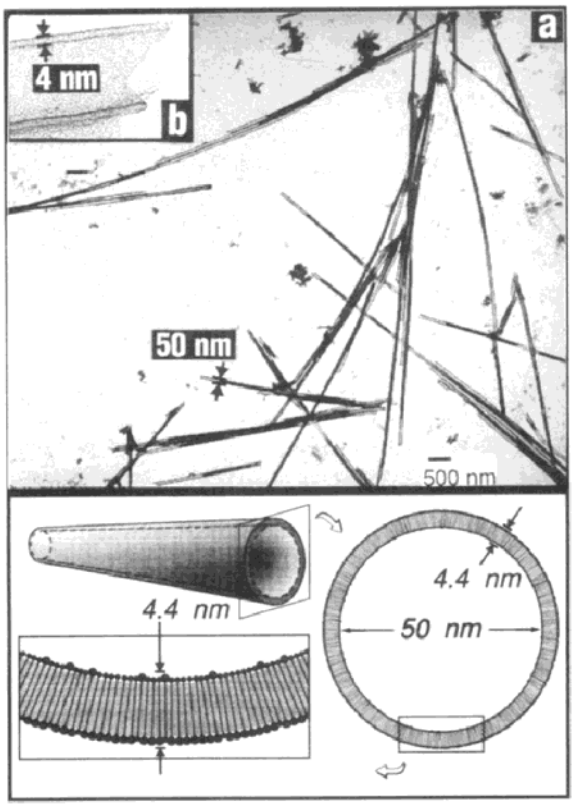

Figure 55. Micellar rods as well as vesicular tubules were obtained from α-amino-ω-lysine bolas with different chain lengths. The micrograph corresponds to the uppermost bola.

A large variety of β-substituted amphiphilic proto- and octaethylporphyrin amphiphiles and bolas have been converted to fibers showing strong excitonic interactions (split of Soret band) of the chromophores.[170−174] *meso*-Tetraphenylporphyrins (TPPs) with a hydrophilic headgroup on each phenyl group can, on the other hand, be considered as a bola as well as an edge amphiphile. They form linear stacks,[175−180] such as those observed in phthalocyanines.[181] TPP stacks show, in general, no exciton effect and are not as good in energy transfer as β-substituted porphyrins. β-Tetrapyridylporphyrins assemble to water-soluble leaflets with a very strong

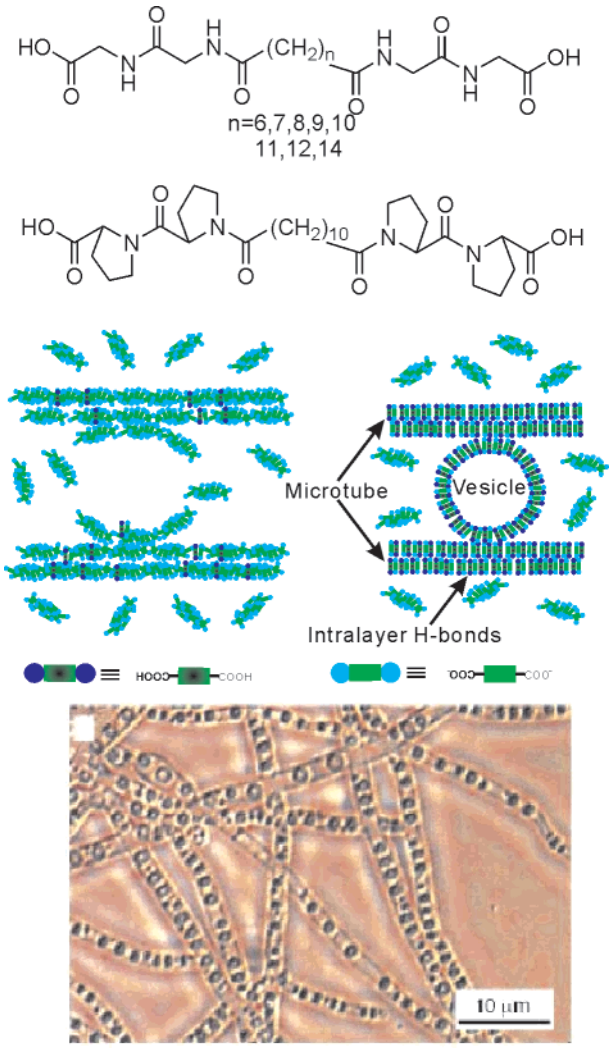

Figure 56. Several peptide bolas with connecting alkane chains produced tubules which entrapped vesicles made of the same material upon acidification.

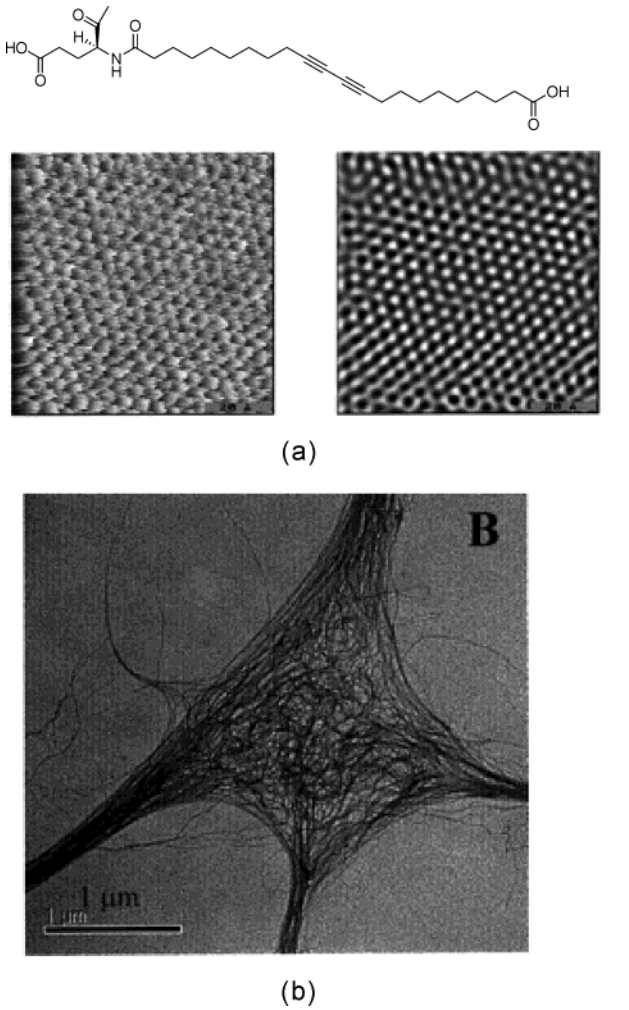

Figure 57. (a) Cross-linked diacetylene bolas with a glutamic acid and a carboxyl headgroup produced ribbons with beautifully ordered surfaces (AFM; contact mode). (b) TEMs showed networks of fibers.

splitting of the Soret band (Figure 59).[174] The exciton effect strongly depends on the angles at which the porphyrins pack: the planes should orient in parallel, and the lateral shift should be around 40°. The chromophores in *meso*-TPP stacks twist should be 45° in order to avoid the neighbors phenyl groups, and they undergo very little lateral shift for the same reason.

Some of the TPP stacks have also been silanized in water.[179] An α,ω-bispyridinium bola formed macaroni-type nanotubes upon TiO_2 formation from $Ti[OCH-(CH_3)_2]$ (Figure 60).[182]

Bolaamphiphiles have also been used in the construction of columns which aggregate to form liquid crystals. Such crystals were made of "triblock" bolas: a hydrophobic core consisted of stiff biphenyl units (first block) with a mobile alkyl side chain (second block). Two hydrophilic glycerol-type headgroups with one phenol ether oxygen atom formed the third block. Upon heating to 135 °C, hexagonal columnar phases were formed and characterized by an X-ray diffraction pattern. The arrangement of all three blocks is fuzzy; all parts are highly mobile

Scheme 9

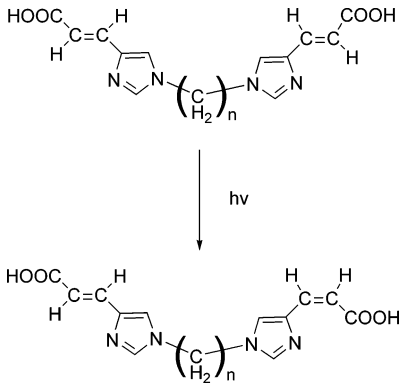

(Figure 61). Different arrangements (micelles, columns, planes) prevail at different temperatures. At 135 °C, the material consisted of micellar disks with the alkyl chains in the center, and six biphenylene units on the surface were formed and connected by hydrogen bonds between the diol headgroups. Stacking of several such disks then leads to columnar liquid crystals. Similar columnar liquid crystals can also be obtained with mesogens containing fluorinated side chains, and the hydrophilic groups are not

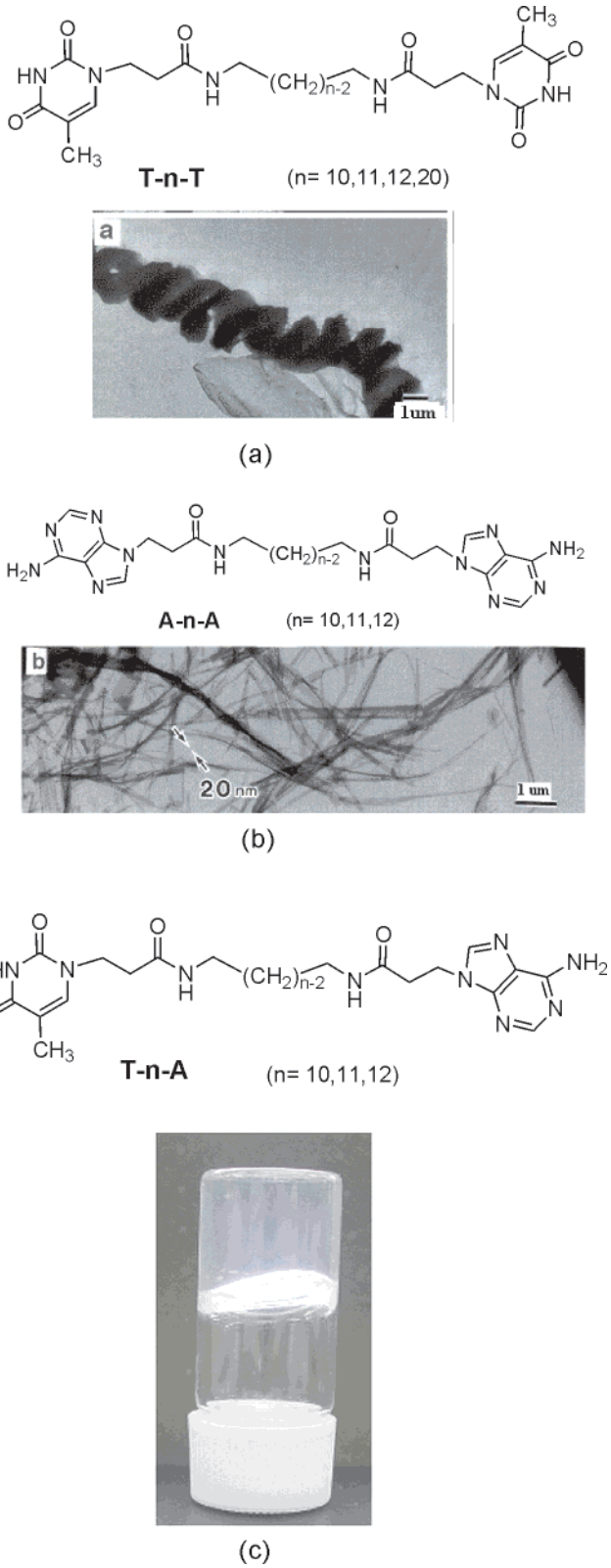

Figure 58. TEM image of (a) a double-helical T−10−T rope and (b) nanofibers made of T−12−A. 0.2 wt % T−20−T solutions gave again strong gels.

necessary. They provide, however, an unmatched variability of texture and phase behavior.[183−185]

7. Recognition

The molecular selectivity of the adsorption process of proteins on solid surfaces has an impact on fields as different as laundry, chromatography, immunoassays, and biocompatibility. Protein adsorption is often not reversible but selective. A negatively charged fragment of cytochrome b_5, for example, was added quickly and irreversibly to a poly(allylamine) surface, slowly and reversibly to an anionic stearate bola surface, and very slow and irreversibly to an electroneutral phospholipid bilayer[186] (Figure 61). Bola SAMs of COOH-terminated alkane thiols $(CH_2)_n$-COOH immobilized cytochrome *c* in a stable, electroactive form. With $n \geq 8$, the electron transfer from the gold electrode occurs by tunneling only. In a mixed monolayer with $HS-(CH_2)_n-OH$, the surface pk_a shifts from 8 to more acidic values and the electron-transfer rate is increased by a factor of 1000. A less dense packing of $-COOH\cdots{}^{-}OCC-$ groups obviously enhances the number of COO^- groups and leads to tighter binding of cationic cytochrome *c*

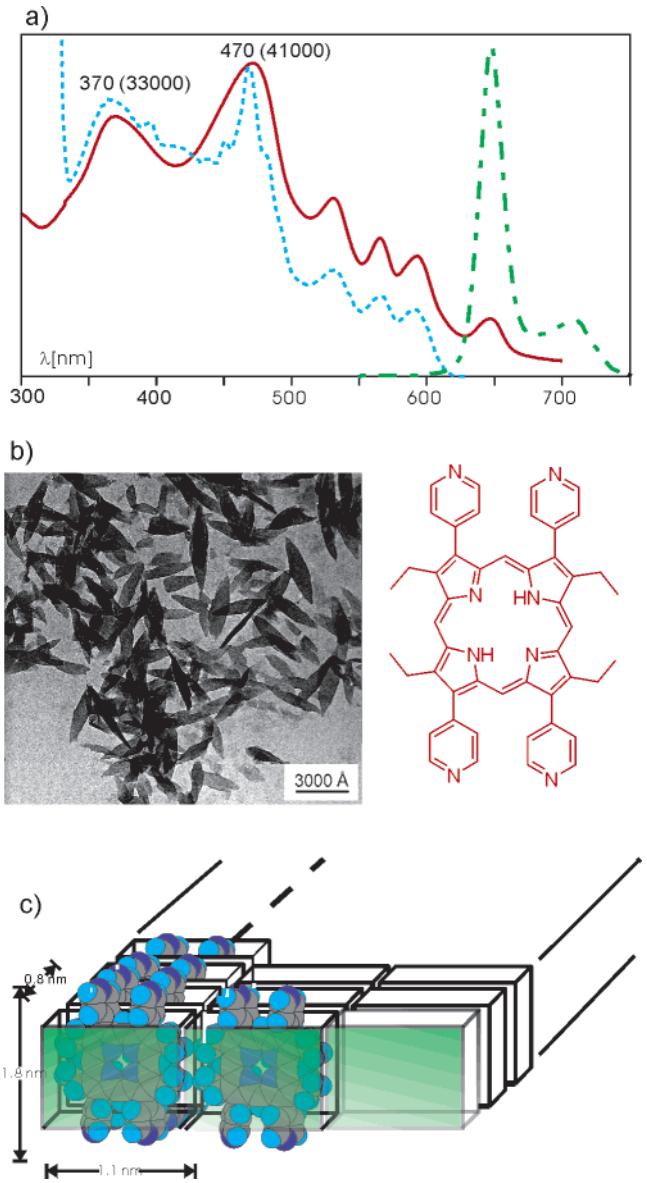

Figure 59. Monolayer porphyrin leaflets in water made of the β-tetraethyl-β'-tetrapyridylporphyrin bola at pH 2. The leaflets are rolled up here because of salt effects: (a) Absorption (···), fluorescence excitation (—), and fluorescence spectra (- - -), (b) electron micrograph, and (c) model.

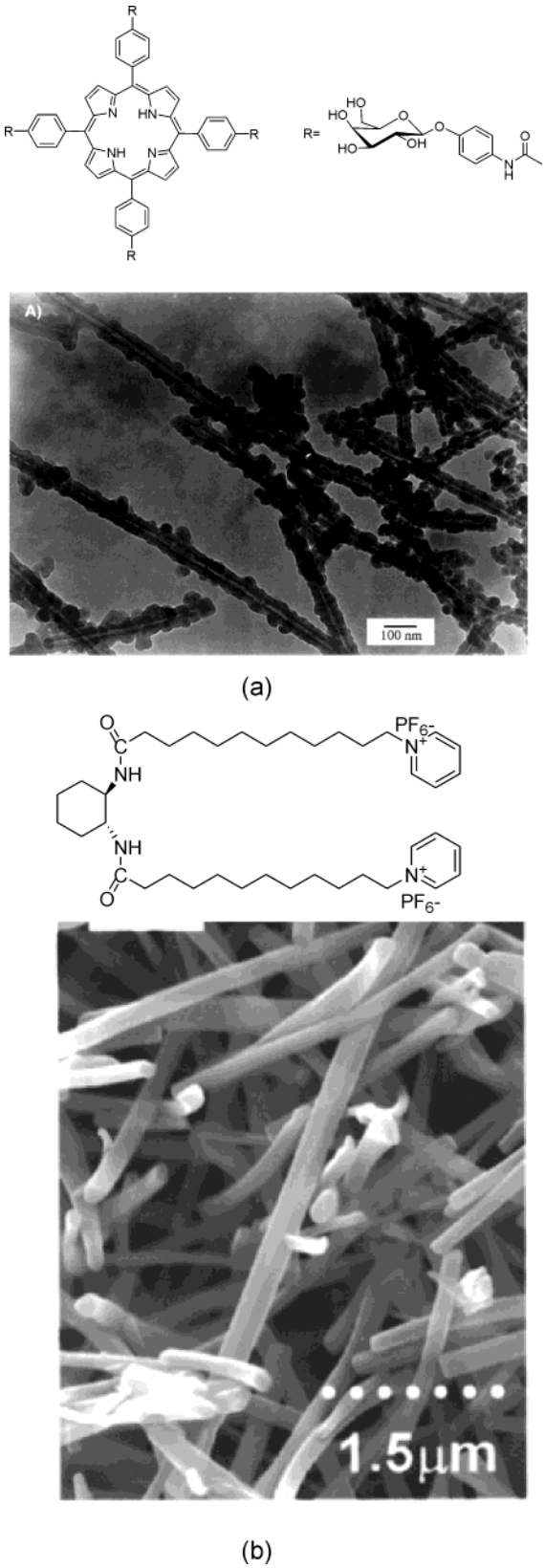

Figure 60. SEMs of (a) a silica-coated porphyrin−glucoside bola and (b) of a bis-pyridinium bola assembly which was treated with titanium(IV)−isopropylate.

(Figure 61).[187] The active center of amine oxidase is only accessible to substrates through a hydrophobic nanowell that is 20 Å deep. The kinetics of a planar electrode would be sluggish at best over such a distance. An α-SH bola with a terminal aniline end

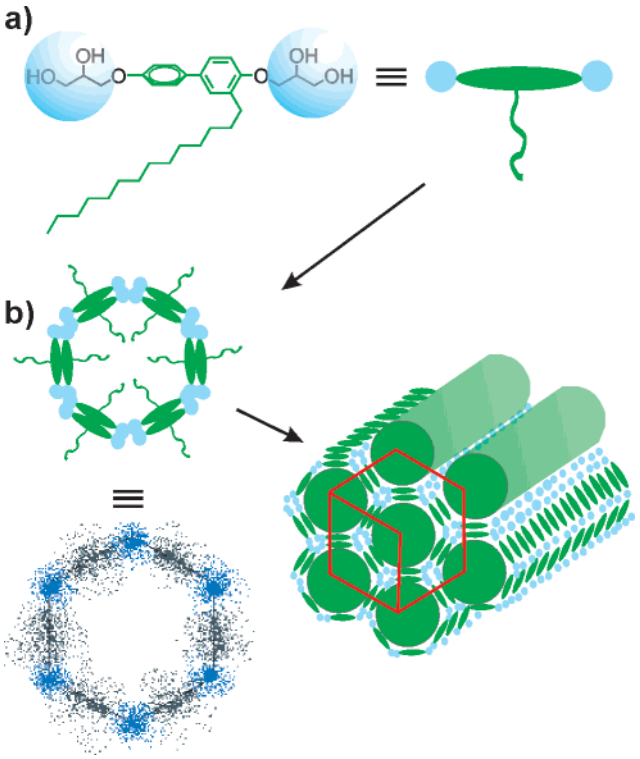

Figure 61. (a) Bola with a rigid biphenyl and fluid alkyl (= bi-block) core and two diol headgroups (= third block) arranges upon heating to form (b) liquid crystals. Models often imply defined ordering of the components. This is, however, not the case in liquid crystals. The diffuse cross-section on the lower left gives a more realistic picture than the other outlined models. (The items of this figure were kindly provided by Professor C. Tschierske, Halle).

entered, however, the channel from a gold electrode (Figure 61b). A perfect cyclic voltammogram was obtained.[188]

SH amphiphiles on gold with polar bolas and nonpolar (single-headed amphiphiles) end groups adsorb proteins at the water/air and water/solvent interfaces. Small proteins only adsorb strongly to hydrophobic surfaces. Larger proteins, however, adsorb to almost any surface, again with some preference for less wettable surfaces (Figure 62).[189]

A single exception concerns oligoethylene (OEG) surfaces. The deeply penetrating ordered water−OEG structure does not allow for hydrophobic protein−monolayer interactions. They behave too much like water. If, however, the OEG surface is coupled with receptor peptides, e.g., Arg-Gly-Arg-Asp-COOH, selective recognition takes place on an otherwise nonadhesive surface. Bola monolayers with OEG end groups were thus derivatized with the cationic−anionic tetrapeptide Arg-Gly-Arg-Asp and became active in cell adhesion by binding to receptor proteins, whereas other proteins were still rejected. α-SH-ω-oligoethylene-coated gold electrodes loose their coat at high potentials and may then absorb proteins. After a cathodic voltage pulse of 30 s, protein islands are formed and cells may grow in these areas. Drugs which inhibit the mobility of the cells lead to smaller spots.[190] AFM imaging of proteins, e.g., fibrinogen, with an OEG bola ($CH_3O-(CH_2-CH_2O)_3-CH=CH_2$) added to the tip by hydrosilylation led to a much

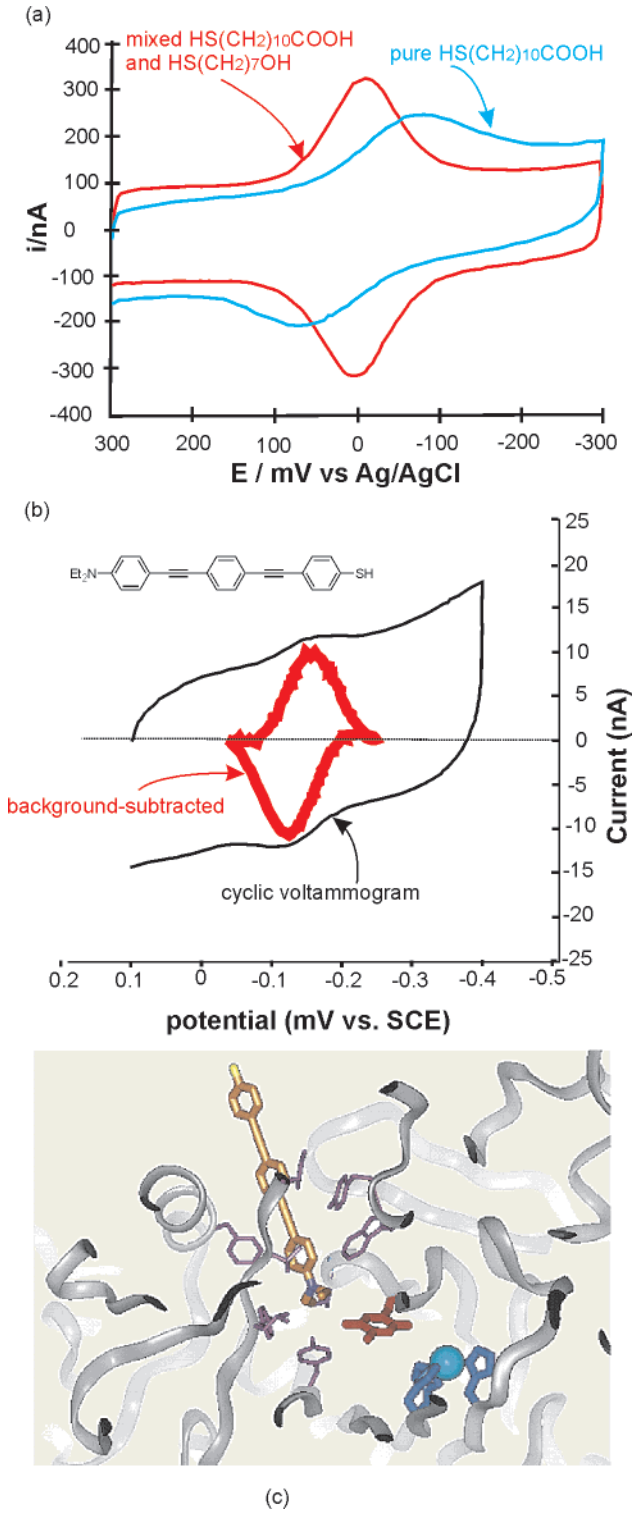

Figure 62. Cyclic voltammograms of (a) yeast cytochrome *c* on gold electrodes coated with $HS(CH_2)_{10}COOH$ or (b) a mixture of the same acid with $HS-(CH_2)_7OH$. The electron-transfer rate was 10^3 times faster in the mixed SAM; (b) an amino oxidase on gold before (outer line) and after (inner line) derivatization of the gold surface with the electron-conducting phenyl-acetylene bola. The model indicates the intrusion of the bola into the enzyme cleft.

better resolution than with a bare silicon tip, which tended to destroy soft adhesive samples (Figure 63).[191]

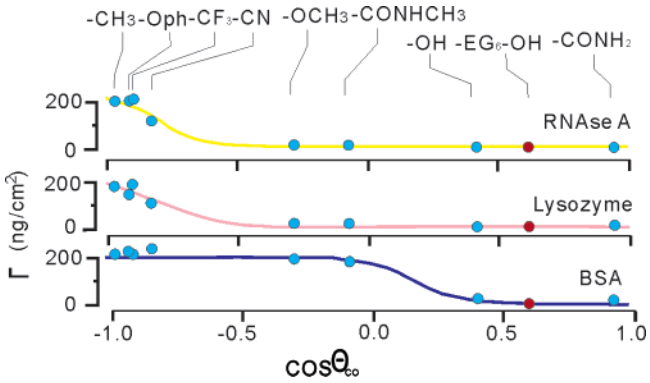

Figure 63. Surface density of adsorbed films of two proteins on a variety of SAMs as a function of the contact angle of water on the SAM under cyclooctane (CO). Low cos θ values indicate high hydrophobicity.

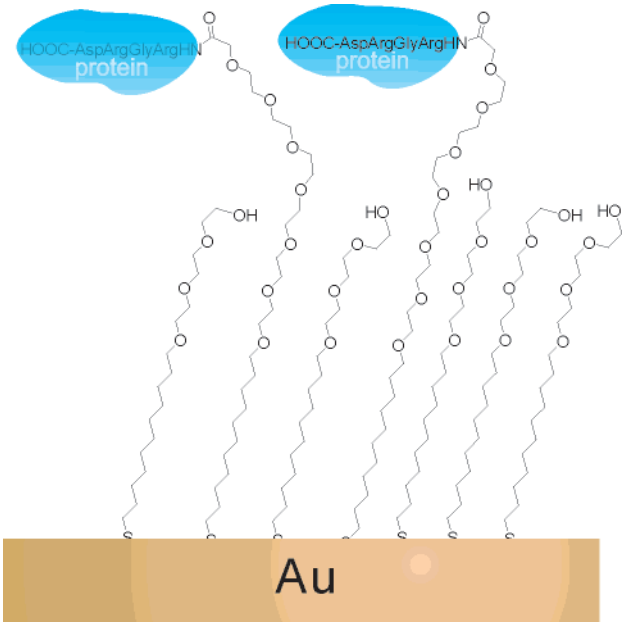

Figure 64. Schematic picture of a SAM with triethyleneglycol areas, which repulse proteins and cells and a receptor peptide, which promotes cell and protein adhesion.

Bolas have also been used routinely as a flexible connecting link between haptens and membranes or between gold and membranes or between haptens and proteins. All three types of linkers were applied in a molecular machinery in which a gramicidine pore is closed for ion transport if an antigen arrives. Gramicidine pores open if two helices combine end-on in both parts of a fluid bilayer lipid membrane. The pore closes if one of the gramicidine molecules diffuses away. Immobilization of the inner gramicidine as an end group of a gold-bound bola still allows the outer membrane α-gramicidine-*ω*-biotin-streptavidin bola to move freely and to open the ion pore. If, however, the streptavidin is bound twice via a biotin-binding peptide bola to an antigen molecule, the gramicidine molecule becomes totally immobilized and the ion flow stops (Figure 64).[192]

Protein tubules were synthesized by binding protein molecules on amino acid−carboxylate bola tubules, which acted as templates. *N*-α-Amidoglycyl-

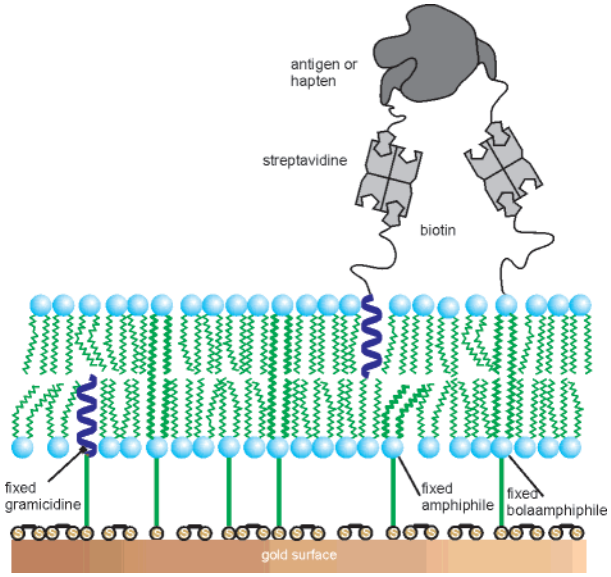

Figure 65. Sensor device for antigens and haptens attached to a gold electrode via a membrane-spanning bola.

glycine)-1,7-heptane dicarboxylate tubules (see Figure 51) contain a free amide group on the surface of the tubules and binds thereby to proteins.[193−195] Both tubules are of light microscopic dimensions (up to 1 μm) and ill-defined in shape, but fluorescence micrographs show that dye-labeled poly(L-lysine), avidin, albumin, and even biotin are strongly adsorbed to these tubules. The biotin-coated fibers may thus be used for binding assays of avidin and vice versa (Figure 65).[194] Furthermore, biotin-coated gold electrodes deposited on glass have been used to immobilize protein-coated fibers. The same procedure was applied to fixate protein tubules on gold electrodes, which had been coated with biotin−SH bola.

Gold substrates functionalized with long-chain α,ω-aminothiols and reacted with 3-maleimidoproponate *N*-hydrosuccinimide ester (MPS). Freshly reduced cow pea mosaic virus (SH−CPMV) was then attached to the maleimido function, and a printing process with the virus on gold particles was developed (Figure 66).[196]

A fluorenyl polymer with dicationic bola-type side chains binds strongly to a pentaanionic oligostilbene as well as to single-stranded DNA. This was shown by fluorescence resonance energy transfer (FRET) from the fluorene polymer to pyrene labels on the anions. DNA hybridization enhances the long-wavelength emission drastically (Figure 67).[197] The bola polymer is efficient because two cations work cooperatively. Hydrophobic interactions hold them together (Figure 68).

We conclude with a short α,ω-diammonium bola with a photoreactive bis-phenol core. It is water soluble and cross links DNA upon UV irradiation. It provides an example that clearly demonstrates what bolas essentially are, extended cross-linkers (Scheme 10).[198]

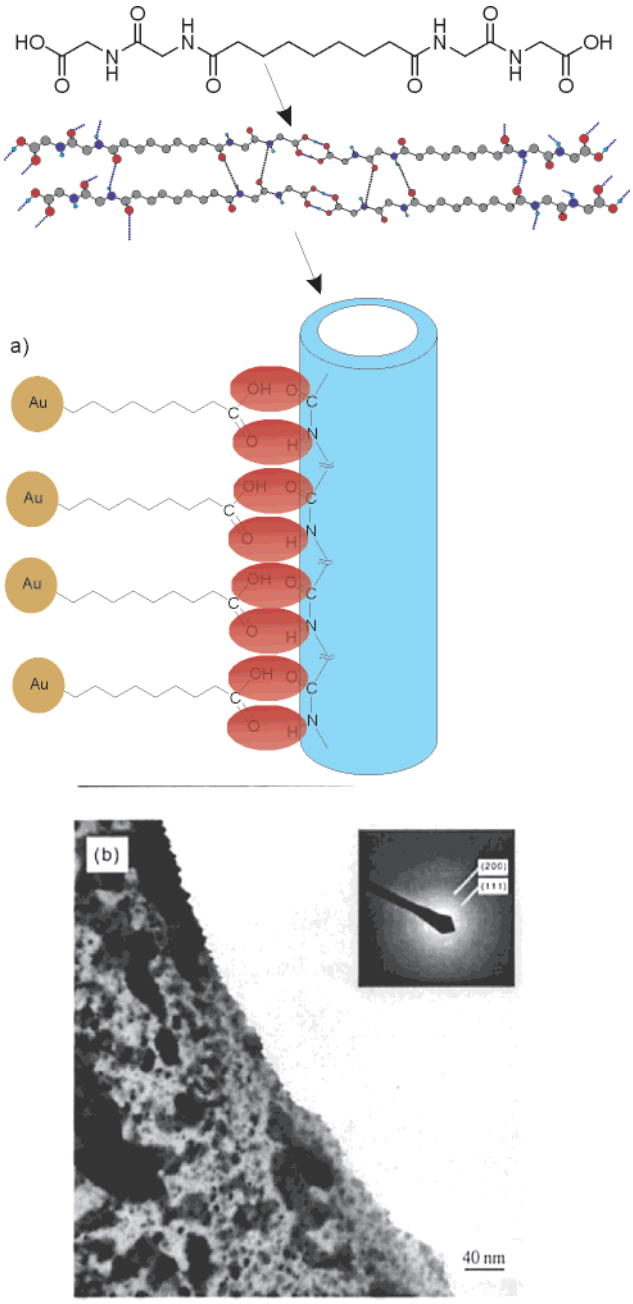

Figure 66. Model of bola−peptide tubules which attach bolas on their surface by hydrogen bonds. The gold particles bound to the end of the thiol bolas are visible in TEMs.

8. Conclusion

The classical application of bolas is the formation of monolayer membrane (MLM) vesicles. These vesicles are robust with respect to fusion and flip−flop of headgroups, and their membrane may be one-half as thick as a bilayer. Synthetic pores are more easily achieved in MLMs than in BLMs, because 2-nm-long edge amphiphiles are easier to synthesize and more soluble than 4-nm analogues.

The major contribution of bolas to supramolecular chemistry lies in the combination of asymmetric arrangements of α,ω-headgroups and the formation of cooperative hydrogen-bond or $\pi-\pi$ interaction chains. The headgroups differentiate between binding to a solid surface and interactions with solvents

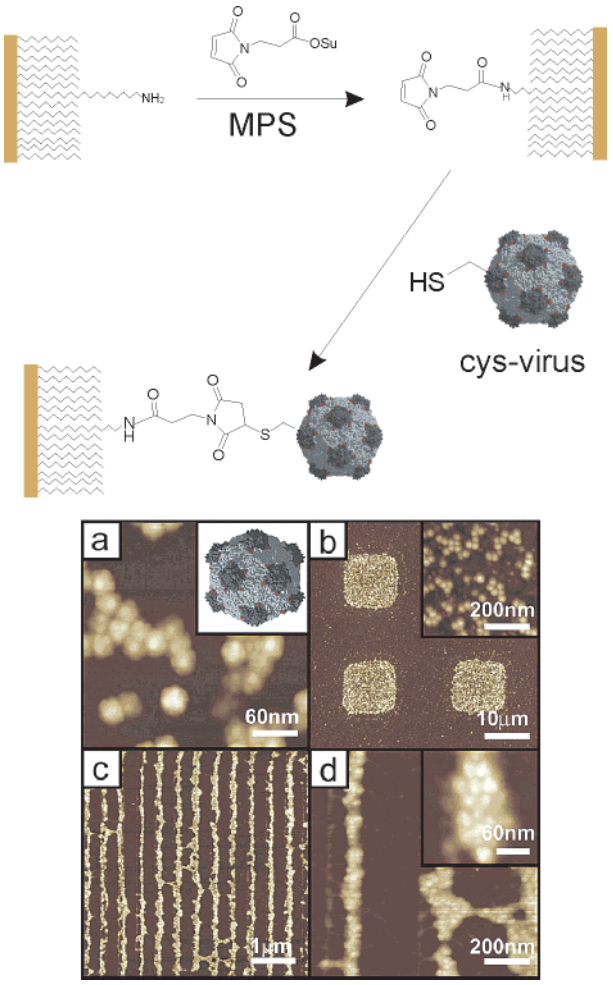

Figure 67. Thiol bolas with a "virus headgroup" have been used as an ink for the formation of virus stripes with a height of 30 nm on gold.

or solutes; the internal connectivity produces an astonishing chemical and physical stability of solid surfaces. Inorganic silica gel and gold particles, for example, become much more stable under an organic bola monolayer. Very strong odd−even and chain-length effects allow one to manipulate the rigidity of the molecular assemblies. **Bolaamphiphiles are molecules for the plain.** Formation of fluid or rigid monolayers on smooth surfaces of low overall curvature and the selective interactions with molecules in the environment via the outer headgroups cooperate to create useful surface properties. Perfect protection against corrosion, form-stable nanowells which may be filled with water or chloroform and nanosized printings are typical bola success stories.

Curvature and flexibility, on the other hand, are not so characteristic for bola assemblies. Quadruple helices, fluid vesicle membranes, and solubilizing micelles are better made from single-headed amphiphiles. Molecular bilayers adjust better to specific interactions between chiral headgroups, and they also allow for solutes within the membrane. Bola fibers tend to have large diameters (≥30 nm) far above molecular dimensions and to be sticky. A technical advantage of the bolas may be the low concentration at which aqueous or organic gels are

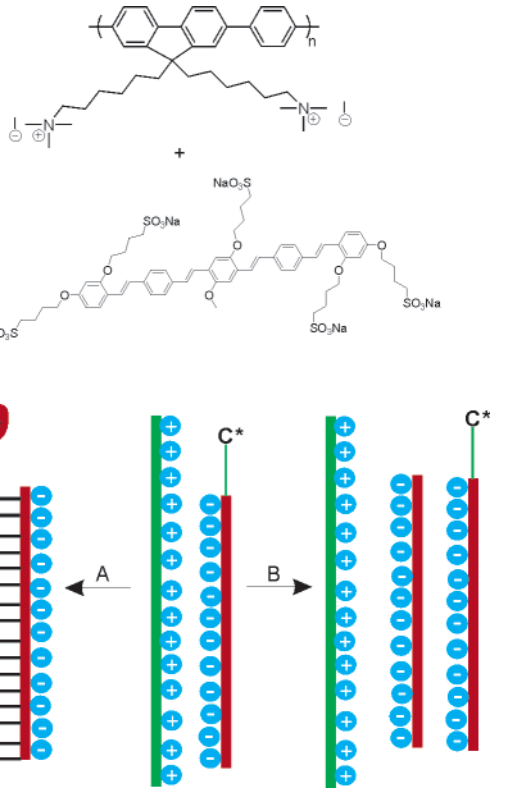

Figure 68. DNA and a pentasulfonated dye reacted with a polymeric bis-ammonium bola to stable molecular complexes in water. An emission band of the dye was considerably enhanced upon hybridization with double-helical DNA.

Scheme 10

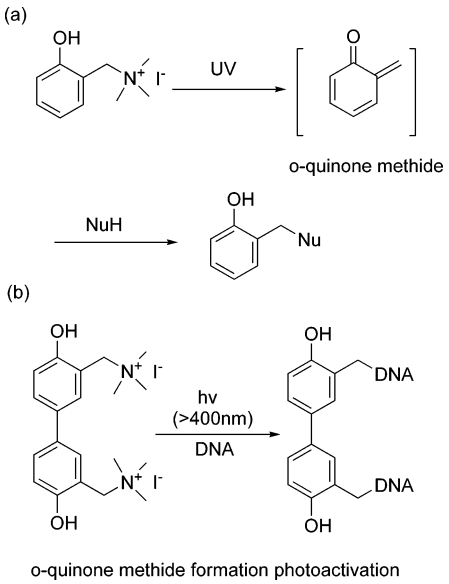

formed (∼0.1 wt %). Only in three-dimensional crystals or liquid crystal helices do columns of very high curvature appear.

It should also be stated that attempts to produce circular conformers by intramolecular interactions between α- and ω-headgroups (e.g., A−T, anion−cation) usually failed if the connecting alkyl chains were long. Bolas tend to remain straight, allowing for a small bend here and there.

9. Acknowledgments

We thank our mentors, collaborators, colleagues, and students who have contributed to our activities and have made research with bolas enjoyable and stimulating. For financial support of our research, we thank the Deutsche Forschungsgemeinschaft (SFB 448 "Mesoscopic Systems"), the European Mobility Program (Network Carbohydrate Nucleotide Recognition), and the FNK of the Free University.

10. References

(1) Fuhrhop, J.-H.; Mathieu, J. *Angew. Chem.* **1984**, *96*, 124−137; Fuhrhop, J.-H.; Mathieu, J. *Angew. Chem., Int. Ed. Engl.* **1984**, *23*, 100.
(2) Fuhrhop, J.-H.; Fritsch, D. *Acc. Chem. Res.* **1986**, *19*, 130.
(3) Escamilla, G. H.; Newkome, G. R. *Angew. Chem., Int. Ed. Engl.* **1994**, *33*, 1937.
(4) Zahna, R. In *Specialist Surfactants*; Robb, I. D., Ed.; Chapman & Hall: Glasgow, 1996, p 81.
(5) Fuhrhop, J.-H.; Koening, J. *Molecular Assemblies and Membranes, Monographs in Supramolecular Chemistry*; Stoddart, J. F., Ed.; Royal Society of Chemistry: London, 1994; Vols. i−xiii, pp 1−227.
(6) Fuhrhop, J.-H.; Endisch, C. *Molecular and Supramolecular Chemistry of Natural Products and Model Compounds*; Marcel Dekker: New York, 2000; 606 pages.
(7) Sprott, G. D. *J. Bioenerg. Biomembr.* **1992**, *24*, 555.
(8) Gambacorca, A.; Gliozzi, A.; De Rosa, M. *World J. Microbiol. Biotechnol.* **1995**, *11*, 115.
(9) Yamauchi, K.; Kinoshita, M. *Prog. Polym. Sci.* **1993**, *18*, 763.
(10) Ulman, A. *An Introduction to Ultrathin Organic Films, from Langmuir−Blodgett to Self-Assembly;* Jovanovich, H. B., Ed.; Academic Press: New York, 1991.
(11) Siggel, U.; Hungerbühler, H.; Fuhrhop, J.-H. *J. Chim. Phys.* **1987**, *84*, 1055.
(12) (a) Quesada, E.; Acuña, A. U.; Amat-Guerri, F. *Angew. Chem.* **2001**, *113*, 2153. (b) Quesada, E.; Acuña, A. U.; Amat-Guerri, F. *Eur. J. Org. Chem.* **2003**, 1308.
(13) Liang, K.; Hui, Y. *J. Am. Chem. Soc.* **1992**, *114*, 6588.
(14) Fuhrhop, J.-H.; Mathieu, J. *J. Chem. Soc., Chem. Commun.* **1983**, 144.
(15) Fuhrhop, J.-H.; David, H. H.; Mathieu, J.; Liman, U.; Winter, H.-J.; Boekema, E. *J. Am. Chem. Soc.* **1986**, *108*, 1785.
(16) Fuhrhop, J.-H.; Fritsch, D. *Systematic Appl. Microbiol.* **1986**, *7*, 272.
(17) Fyles, T. M.; James, T. D.; Pryhitka, A.; Zojaji, M. *J. Org. Chem.* **1993**, *58*, 7456.
(18) Fyles, T. M.; James, T. D.; Kaye, K. C. *J. Am. Chem. Soc.* **1993**, *115*, 12315.
(19) Fyles, T. M.; Loock, D.; van Straaten-Nijenhuis, W. F.; Zhou, X. *J. Org. Chem.* **1996**, *61*, 8866.
(20) Fyles, T. M.; Zeng. B. *J. Org. Chem.* **1998**, *63*, 8337.
(21) Fyles, T. M.; Loock, D.; Zhou, X. *J. Am. Chem. Soc.* **1998**, *120*, 2997.
(22) Fyles, T. M.; Hu, C.-W.; Knoy, R. *Org. Lett.* **2001**, *3*, 1335.
(23) Eggers, K.; Fyles, T. M.; Montoya-Pelaez, P. J. *J. Org. Chem.* **2001**, *66*, 2966.
(24) Cameron, L. M.; Fyles, T. M.; Hu, C.-W. *J. Org. Chem.* **2002**, *67*, 1548.
(25) Eggers, P. K.; Fyles, T. M.; Mitchell, K. D. D.; Sutherland, T. *J. Org. Chem.* **2003**, *68*, 1050.
(26) Autenrieth, W.; Geyer, A. *Chem. Ber.* **1908**, *41*, 4249.
(27) Marvel, C. S.; Sienicki, E. A.; Passer, M.; Robinson, C. N. *J. Am. Chem. Soc.* **1954**, *76*, 933.
(28) Marvel, C. S.; Farrar, R. C. *J. Am. Chem. Soc.* **1957**, *79*, 986.
(29) Delfino, J. M.; Schreiber, S. L.; Richards, F. M. *J. Am. Chem. Soc.* **1993**, *115*, 3458.
(30) Fuhrhop, J.-H.; Liman, U.; Koesling, V. *J. Am. Chem. Soc.* **1988**, *110*, 6840.
(31) (a) Kim, J.-M.; Thompson, D. H. *Langmuir* **1992**, *8*, 637. (b) Thompson, D. H.; Svendsen, C. B.; Di Meglio, C.; Anderson, V. C. *J. Org. Chem.* **1994**, *59*, 2945.
(32) Visscher, I.; Engberts, B. F. N. *Langmuir* **2000**, *16*, 52.
(33) Descotes, G.; Ramza, J. *Tetrahedron Lett.* **1994**, *35*, 7379.
(34) Descotes, G.; Ramza, J.; Basset, J.-M.; Pagano, S. *Tetrahedron Lett.* **1994**, *35*, 7379.
(35) Masuda, M.; Shimizu, T. *Chem. Commun.* **2001**, 2442.
(36) (a) Masuda, M.; Shimizu, T. *Carbohydr. Res.* **2000**, *326*, 56. (b) Masuda, M.; Vill, V.; Shimizu, T. *J. Am. Chem. Soc.* **2000**, *122*, 12327.
(37) Masuda, M.; Shimizu, T. *Carbohydr. Res.* **1997**, *302*, 139.
(38) Shimizu, T.; Masuda, M. *J. Am. Chem. Soc.* **1997**, *119*, 2812.
(39) Schneider, J.; Messerschmidt, C.; Schulz, A.; Gnade, M.; Schade, B.; Luger, P.; Bombicz, P.; Hubert, V.; Fuhrhop, J.-H. *Langmuir* **2000**, *16*, 8575.
(40) Housty; J.; Michel, H. *Compt. Rend* **1964**, *259*, 2437.
(41) Sintes, A.; Housty, J. *Acta Crystallogr.* **1966**, *21*, 965.
(42) Chadha, M.; Dunnigan, M. E.; Sahyun, M. R. V.; Ishida, T. *J. Appl. Phys.* **1998**, *84*, 887.
(43) Kim, Y. J.; Lee, E. W.; Jung, D.-Y. *Chem. Mater.* **2001**, *13*, 2684.
(44) Rueff, J.-M.; Masciocchi, N.; Rabu, P.; Sironi, A.; Skoulios, A. *Eur. J. Inorg. Chem.* **2001**, *11*, 2843.
(45) Rueff, J.-M.; Masciocchi, N.; Rabu, P.; Sironi, A.; Skoulios, A. *Chem. Eur. J.* **2002**, *8*, 1813.
(46) Yeo, L.; Harris, K. D. M.; Guillaume, F. *J. Solid State Chem.* **1997**, *128*, 273.
(47) Makedonopoulou, S.; Mavridis, I. M. *Acta Crystallogr.* **2000**, *B56*, 322.
(48) Miyaji, H.; Dudic, M.; Tucker, J. H. R.; Prokes, I.; Light, M. E.; Hursthouse, M. B.; Stibor, I.; Lhotak, P. *Tetrahedron Lett.* **2002**, *42*, 873.
(49) Gotthardt, R.; Fuhrhop, J.-H.; Buschmann, J.; Luger, P. *Acta Crystallogr.* **1997**, *C53*, 1715.
(50) McNeil, R.; Scheidt, W. R.; Thomas, J. K. *Mol. Cryst. Liquid Cryst.* **1991**, *78*, 85.
(51) Dall'Acqua, L.; Della Gatta, G.; Nowicka, B.; Ferloni, P. *J. Chem. Thermodyn.* **2000**, *34*, 1.
(52) Rontoyianni, A.; Mavridis, I. M. *Supramol. Chem.* **1999**, *10*, 213.
(53) Tsubaki, K.; Tanaka, H.; Furuta, T.; Kinoshita, T.; Fuji, K. *Tetrahedron Lett.* **2000**, *41*, 6089.
(54) Tsubaki, K.; Tanaka, H.; Furuta, T.; Tanaka, K.; Kinoshita, T.; Fuji, K. *Tetrahedron Lett.* **2002**, *58*, 5611.
(55) Neve, F.; Crispini, A. *Cryst. Growth Des.* **2001**, *1*, 387.
(56) Desiraju, G. R. *Crystal Engineering: The Design of Organic Solids*; Elsevier: Amsterdam, 1989.
(57) Braga, D.; Grepioni, F.; Desiraju, G. R. *Chem. Rev.* **1998**, *98*, 1375.
(58) Sim, G. A. *Acta Crystallogr.* **1955**, *8*, 833.
(59) Aigouy, P. T.; Costeseque, P.; Sempere, R.; Senac, T. *Acta Crystallogr.* **1995**, *B51*, 55.
(60) Escudero, E.; Subirana, J. A. *Biopolymers* **2000**, *54*, 365.
(61) Escudero, E.; Subirana, J. A. *Macromolecules* **2001**, *34*, 837.
(62) Li, L.; Koch, M. H. J.; de Jeu, W. H. *Macromolecules* **2003**, *36*, 1626.
(63) Jones, N. A.; Atkins, E. D. T.; Hill, M. J.; Cooper, S. J.; Franco, L. *Macromolecules* **1997**, *30*, 3569.
(64) Tsutsumi, N.; Muzutani, T.; Sakai, W. *Macromolecules* **1997**, *30*, 1637.
(65) Gao, Q.; Scheinbeim, J. I. *Macromolecules* **2000**, *33*, 7564.
(66) (a) Ramesh, C. *Macromolecules* **1999**, *32*, 3721. (b) Ramesh, C. *Macromolecules* **1999**, *32*, 5704.
(67) Lewis, F. D.; Wu, Y.; Liu, X. *J. Am. Chem. Soc.* **2002**, *124*, 12165.
(68) Chabinyc, M. L.; Chem. X.; Holmlin, R. E.; Jacobs, H.; Skulason, H.; Frisbie, C. D.; Mujica, V.; Ratner, M. A.; Rampi, M. A.; Whitesides, G. M. *J. Am. Chem. Soc.* **2002**, *124*, 11730.
(69) Li, G.; Fuhrhop, J.-H. *Langmuir* **2002**, *18*, 7740.
(70) Li, G.; Bhosale, V.; Wang, T.; Hackbarth, S.; Roeder, B.; Siggel, U.; Fuhrhop, J.-H. *J. Am. Chem. Soc.* **2003**, *125*, 10693.
(71) Bain, C. D.; Whitesides, G. M. *J. Am. Chem. Soc.* **1988**, *110*, 5897.
(72) Bain, C. D.; Troughton, E. B.; Tao, Y.-T.; Evall, J.; Whitesides, G. M.; Nuzzo, R. G. *J. Am. Chem. Soc.* **1989**, *111*, 321.
(73) Allara, D. L.; Atre, S. V.; Elliger, C. A.; Snyder, R. G. *J. Am. Chem. Soc.* **1991**, *113*, 185.
(74) Laibinis, P. E.; Whitesides, G. M. *J. Am. Chem. Soc.* **1992**, *114*, 1990.
(75) Colvin, V. L.; Goldstein, A. N.; Alivisatos, A. P. *J. Am. Chem. Soc.* **1992**, *114*, 5221.
(76) Obeng, Y. S.; Laing, M. E.; Friedli, A. C.; Yang, H. C.; Wang, D.; Thulstrup, E. W.; Bard, A. J.; Michl, J. *J. Am. Chem. Soc.* **1992**, *114*, 9943.
(77) Sun, L.; Crooks, R. M.; Ricco, A. J. *Langmuir* **1993**, *9*, 1175.
(78) Zhang, L.; Lu, T.; Gokel, G. W.; Kaifer, A. E. *Langmuir* **1993**, *9*, 786.
(79) Naito, K.; Miura, M.; Azuma, M. *J. Am. Chem. Soc.* **1991**, *113*, 6386.
(80) Obeng, Y. S.; Bard, A. J. *J. Am. Chem. Soc.* **1991**, *113*, 6279.
(81) Maliszewskyj, N. C.; Heiney, P. A.; Jones, D. R.; Strongin, R. M.; Cichy, M. A.; Smith, A. B., III *Langmuir* **1993**, *9*, 1439.
(82) Caldwell, W. B.; Chen, C. A.; Mirkin, S. J. *Langmuir* **1993**, *9*, 1945.
(83) Li, D. Q.; Swanson, B. I.; Robinson, J. M.; Hoffbauer, M. A. *J. Am. Chem. Soc.* **1993**, *115*, 6975.
(84) (a) van Blaaderen, A.; Vrij, A. J. *Colloid Interface Sci.* **1993**, *156*, 1. (b) Tanev, P. T.; Liang, Y.; Pinnavaia, J. *J. Am. Chem. Soc.* **1997**, *119*, 8616.
(85) Li, G.; Fudickar, W.; Skupin, M.; Klyszcz, A.; Draeger, C.; Lauer, M.; Fuhrhop, J.-H. *Angew. Chem.* **2002**, *114*, 1906−1931. Li, G.; Fudickar, W.; Skupin, M.; Klyszcz, A.; Draeger, C.; Lauer, M.; Fuhrhop, J.-H. *Angew. Chem., Int. Ed.* **2002**, *41*, 1828.

(86) Böhme, P.; Hicke, H.-G.; Böttcher, C.; Fuhrhop, H.-J. *J. Am. Chem. Soc.* **1995**, *117*, 5824.
(87) Fudickar, W.; Zimmermann, J.; Ruhlmann, L.; Roeder, B.; Siggel, U.; Fuhrhop, J.-H. *J. Am. Chem. Soc.* **1999**, *121*, 9539.
(88) Skupin, M.; Li, G.; Fudickar, W.; Zimmermann, J.; Röder, B.; Fuhrhop, J.-H. *J. Am. Chem. Soc.* **2001**, *123*, 3454.
(89) Maoz, R.; Cohen, H.; Sagiv, J. *Langmuir* **1998**, *14*, 5988.
(90) Chailapakul, O.; Crooks, R. M. *Langmuir* **1993**, *9*, 884.
(91) Chechik, V.; Crooks, R. M.; Stirling, C. J. M. *Adv. Mater.* **2000**, *12*, 1161.
(92) Sabatani, E.; Cohen-Boulakia, J.; Bruening, M.; Rubinstein, I. *Langmuir* **1993**, *9*, 2974.
(93) Kang, J. F.; Ulman, A.; Liao, S.; Jordan, R. *Langmuir* **1999**, *15*, 2095.
(94) Kang, J. F.; Ulman, A.; Liao, S.; Jordan, R.; Yand, G.; Liu, G.-Y. *Langmuir* **2001**, *17*, 95.
(95) Zehner, R. W.; Sita, L. R. *Langmuir* **1997**, *13*, 2973.
(96) Cygan, M. T.; Dunbar, T. D.; Arnold, J. J.; Bumm, L. A.; Shedlock, N. F.; Burgin, T. P.; Jones, L., II; Allara, D. L.; Tour, J. M.; Weis, P. S. *J. Am. Chem. Soc.* **1998**, *120*, 2721.
(97) Li, X.-M.; Paraschiv, V.; Huskens, J.; Reinhoudt, D. N. *J. Am. Chem. Soc.* **2003**, *125*, 4279.
(98) Green, S. J.; Le-Poul, N.; Edwards, P.; Peacock, G. *J. Am. Chem. Soc.* **2003**, *125*, 3686.
(99) Rampi, M. A.; Schueller, O. J. A.; Whitesides, G. M. *Appl. Phys. Lett.* **1998**, *72*, 1781.
(100) Haag, R.; Rampi, M. A.; Holmlin, R. E.; Whitesides, G. M. *J. Am. Chem. Soc.* **1999**, *121*, 7895.
(101) Wold, D. J.; Haag, R.; Rampi, M. A.; Frisbie, C. D. *J. Phys. Chem. B* **2002**, *106*, 2813.
(102) Holmlin, R. E.; Haag, R.; Chabinyc, M. L.; Ismagilov, R. F.; Cohen, A. E.; Terfort, A.; Rampi, M. A.; Whitesides, G. M. *J. Am. Chem. Soc.* **2001**, *123*, 5075.
(103) Decher, G. In *Comprehensive Supramolecular Chemistry;* Lehn, J.-M., Ed.; Pergamon: Oxford, 1996; Vol. 9, pp 507−528.
(104) Decher, G.; Hong. J. *Makromol. Chem.. Macromol. Symp.* **1991**, 321.
(105) Decher, G.; Hong, J. *Ber. Bunsen-Ges. Phys. Chem.* **1991**, *95*, 1430.
(106) Saremi, F.; Maassen, E.; Tieke, B. *Langmuir* **1995**, *11*, 1068−1071.
(107) Mao, G.; Tsao, Y.-h.; Tirrell, M.; Davis, H. T.; Hessel, V.; Ringsdorf, H. *Langmuir* **1995**, *11*, 942.
(108) Mao, G.; Tsao, Y.; Tirrell, M.; Davis, H. T.; Hessel, V.; Ringsdorf, H. *Langmuir* **1993**, *9*, 3461.
(109) Lu, Q.; Luo, Y.; Li, L.; Liu, M. *Langmuir* **2003**, *19*, 285.
(110) Auer, F.; Scotti, M.; Ulman, A.; Jordan, R.; Sellergren, B.; Garano, J.; Liu, G.-Y. *Langmuir* **2000**, *16*, 7554.
(111) Buller, R.; Cohen, H.; Jensen, T. R.; Kjaer, K.; Lahav, M.; Leiserowitz, L. *J. Phys. Chem. B* **2001**, *105*, 11447.
(112) Ariga, K.; Lvov, Y.; Kunitake, T. *J. Am. Chem. Soc.* **1997**, *119*, 2224.
(113) Lvov, Y.; Ariga, K.; Ichinose, I.; Kunitake, T. *J. Am. Chem. Soc.* **1995**, *117*, 6117.
(114) Hong, J.-D.; Park, E.-S.; Park, A.-L. *Langmuir* **1999**, *15*, 6515.
(115) Advincula, R. C.; Fells, E.; Park, M.-K. *Chem. Mater.* **2001**, *13*, 2870.
(116) Taulier, N.; Ober, R.; Gouzy, M.-F.; Guidetti, B.; Rico-lattes, I.; Urbach, W. *Langmuir* **2002**, *18*, 68.
(117) Yan, Y.; Hung, J.; Li, Z.; Ma, J.; Fu, H. J. *Phys. Chem. B.* **2003**, *107*, 1379.
(118) (a) Bhattacharya, S.; De, S.; Subramanian, M. *J. Org. Chem.* **1998**, *63*, 7640. (b) Moss, R. A.; Fujita, T.; Okumura, Y. *Langmuir* **1991**, *7*, 2415.
(119) Fuhrhop, J.-H.; Fritsch, D.; Tesche, B.; Schmiady, H. *J. Am. Chem. Soc.* **1984**, *106*, 1998.
(120) Fuhrhop, J.-H.; Fritsch, D. *J. Am. Chem. Soc.* **1984**, *106*, 42.
(121) Sano, M.; Oishi, K.; Ishi-i, T.; Shinkai, S. *Langmuir* **2000**, *16*, 3773.
(122) (a) Weissig, V.; Torchilin, V. P. *Adv. Drug Delivery Rev.* **2001**, *49*, 127. (b) Gilot, D.; Miramon, M.-L.; Benvegnu, T.; Ferrieres, V.; Loreal, O.; Guguen-Guillouzo, C.; Plusquellec, D.; Loyer, P. *J. Gene Med.* **2002**, *4*, 415. (c) Fuhrhop, J.-H.; Kaufmann, W.; Schambil, F. *Langmuir* **1985**, *1*, 387.
(123) (a) Kobuke, Y.; Ueda, K.; Sokabe, M. *J. Am. Chem. Soc.* **1992**, *114*, 7618. (b) Fyles, T. M.; Loock, D.; van Straaten-Nijenhuis, W. F.; Zhou, X. *J. Org. Chem.* **1996**, *61*, 8866.
(124) Fyles, T. M.; Loock, D.; Zhou, X. *J. Am. Chem. Soc.* **1998**, *120*, 2997.
(125) (a) Fyles, T. M.; Zeng. B. *J. Org. Chem.* **1998**, *63*, 8337. (b) Voyer, N.; Potvin, L.; Rousseau, É. *J. Chem. Soc., Perkin Trans.* **1997**, *2*, 1469.
(126) Kobuke, Y.; Ueda, K.; Sokabe, M. *J. Am. Chem. Soc.* **1992**, *114*, 7618.
(127) Kobuke, Y.; Satoh, Y. *J. Am. Chem. Soc.* **1992**, *114*, 789.
(128) Kobuke, Y.; Nagatani, T. *J. Org. Chem.* **2001**, *66*, 5094.
(129) Goto, C.; Yamamura, M.; Satake, A.; Kobuke, Y. *J. Am. Chem. Soc.* **2001**, *123*, 12152.
(130) Fuhrhop, J.-H.; Liman, U.; Koesling, V. *J. Am. Chem. Soc.* **1988**, *110*, 6840.
(131) Fuhrhop, J.-H.; Liman, U.; David, H. H. *Angew. Chem.* **1985**, *97*, 337.
(132) Parola, A. H. In *Biomembranes;* Shinitzky, M., Ed.; VCH: Weinheim, 1993; p 159.
(133) Naka, K.; Sadownik, A.; Regen, S. L. *J. Am. Chem. Soc.* **1993**, *115*, 2278.
(134) Fuhrhop, J.-H.; Endisch, C.; Schulz, A.; Turner, J.; Eaton, M. *Langmuir* **1999**, *15*, 3707.
(135) Dubowchik, G. M.; Firestone, R. A. *Tetrahedron Lett.* **1996**, *37*, 6465.
(136) Akerfeldt, K. S.; Kim, R. M.; Camac, D.; Groves, J. T.; Lear, J. D.; DeGrado, W. F. *J. Am. Chem. Soc.* **1992**, *114*, 9656.
(137) Nomura, S. M.; Yoshikawa, Y.; Yoshikawa, K.; Dannenmuller, O.; Chasserot-Golaz, S.; Ourisson, G.; Nakatani, Y. *Chem.Bio-.Chem.* **2001**, 457.
(138) (a) Gokel, G. W.; Murillo, O. *Acc. Chem. Res.* **1996**, *29*, 425. (b) Murillo, O.; Suzuki, I.; Abel, E.; Murray, C. L.; Meadows, E. S.; Jin, T.; Gokel, G. W. *J. Am. Chem. Soc.* **1997**, *119*, 5540.
(139) Siggel, U.; Hungerbuehler, H.; Fuhrhop, J.-H. *J. Chim. Phys.* **1987**, *84*, 1055.
(140) Fuhrhop, J.-H.; Krull, M.; Schulz, A.; Moebius, L. D. *Langmuir* **1990**, *6*, 497.
(141) Kugimiya, S.-I.; Lazrak, T.; Blanchard-Desce, M.; Lehn, J.-M. *J. Chem. Soc., Chem. Commun.* **1991**, 1179.
(142) Wang, X.; Shen, Y.; Pan, Y.; Liang, Y. *Langmuir* **2001**, *17*, 3162.
(143) Guilbot, J.; Benvegnu, T.; Legros, N.; Plusquellec, D.; Dedieu, J.-C.; Gulik, A. *Langmuir* **2001**, *17*, 613.
(144) (a) Shimizu, T.; Iwaura, R.; Masuda, M.; Hanada, T.; Yase, K. *J. Am. Chem. Soc.* **2001**, *123*, 5947. (b) Iwaura, R.; Yoshida, K.; Masuda, M.; Yase, K.; Shimizu, T. *Chem. Mater.* **2002**, *14*, 3047.
(145) Kobayashi, H.; Koumoto, K.; Jung, J. H.; Shinkai, S. J. *Chem. Soc., Perkin Trans. 2* **2002**, 1930.
(146) (a) Nagasaki, T.; Kimura T.; Arimori, S.; Shinkai, S. *Chem. Lett.* **1994**, 1495. (b) Kimura, T.; Arimori, S.; Shinkai, S. *Tetrahedron Lett.* **1995**, *36*, 559. (c) Kimura, T.; Arimori, S.; Takeuchi, M.; Nagasaki, T.; Shinkai, S. *J. Chem. Soc., Perkin Trans. 2* **1995**, 1889. (d) Kobayashi, H.; Nakashima, K.; Ohshima, E.; Hisaeda, Y.; Hamachi, I.; Shinkai, S. *J. Chem. Soc., Perkin Trans. 2* **2000**, 997. (e) Kobayashi, H.; Amaike, M.; Jung, J. H.; Friggeri, A.; Shinkai, S.; Reinhoudt, D. N. *Chem. Commun.* **2001**, 1038.
(147) Jaeger, D. A.; Li, G.; Subotkowski, W.; Carron, K. T.; Bench, M. W. *Langmuir* **1997**, 13, 5563.
(148) Szafran, M.; Dega-Szafran, Z.; Katrusiak, A.; Buczak, G.; Głowiak, T.; Sitkowski, J.; Stefaniak, L. *J. Org. Chem.* **1998**, *63*, 2898.
(149) Aoki, K.; Nakagawa, M.; Ichimura, K. *J. Am. Chem. Soc.* **2000**, *122*, 10997.
(150) Fuhrhop, J.-H.; Schnieder, P.; Rosenberg, J.; Boekema, E. *J. Am. Chem. Soc.* **1987**, *109*, 3387.
(151) Koening, J.; Boettcher, C.; Winkler, H.; Zeitler, E.; Talmon, Y.; Fuhrhop, J.-H. *J. Am. Chem. Soc.* **1993**, *115*, 693.
(152) Svenson, S.; Koening, J.; Fuhrhop, J.-H. *J. Phys. Chem.* **1994**, *98*, 1022.
(153) Svenson, S.; Schaefer, A.; Fuhrhop, J.-H. *J. Chem. Soc., Perkin Trans. 2* **1994**, 1023.
(154) Svenson, S.; Kirste, B.; Fuhrhop, J.-H. *J. Am. Chem. Soc.* **1994**, *116*, 11969.
(155) Mueller-Fahrnow, A.; Saenger, W.; Fritsch, D. *Carbohydr. Res.* **1993**, *242*, 11.
(156) Masud, M.; Hanada, T.; Yase, K.; Shimizu, T. *Macromolecules* **1998**, *31*, 9403.
(157) Jung, J. H.; Shinkai, S.; Shimizu, T. *Chem. Eur. J.* **2002**, *8*, 2684.
(158) Fuhrhop, J.-H.; Spiroski, D.; Boettcher, C. *J. Am. Chem. Soc.* **1993**, *115*, 1600.
(159) Shimizu, T.; Ohnishi, S.; Kogiso, M. *Angew. Chem.* **1998**, *110*, 3509.
(160) Shimizu, T.; Kogiso, M.; Masuda, M. *Nature* **1996**, *383*, 487.
(161) Kogiso, M.; Ohnishi, S.; Yase, K.; Masuda, M.; Shimizu, T. *Langmuir* **1998**, *14*, 4978.
(162) Matsui, H.; Douberly, G. E., Jr. *Langmuir* **2001**, *17*, 7918.
(163) Matsui, H.; Pan, S.; Gologan, B.; Jonas, S. H. *J. Phys. Chem. B* **2000**, *104*, 9576.
(164) Kogiso, M.; Hanada, T.; Yase, K.; Toshimi, S. *Chem. Commun.* **1998**, 1791.
(165) Song, J.; Cheng, Q.; Kopta, S.; Stevens, R. C. *J. Am. Chem. Soc.* **2001**, *123*, 3205.
(166) Sirieix, J.; Lauth-de Viguerie, N.; Riviere, M.; Lattes, A. *Langmuir* **2000**, *16*, 9221.
(167) Bhattacharya, S.; Acharya, S. N. G. *Chem. Mater.* **1999**, *11*, 3121.
(168) Shimizu, T.; Iwaura, R.; Masuda, M.; Hanada, T.; Yase, K. *J. Am. Chem. Soc.* **2001**, *123*, 5947.
(169) Schall, O. F.; Gokel, G. W. *J. Am. Chem. Soc.* **1994**, *116*, 6089.
(170) Fuhrhop, J.-H.; Demoulin, C.; Boettcher, C.; Koening, J.; Siggel, U. *J. Am. Chem. Soc.* **1992**, *114*, 4159.
(171) Fuhrhop, J.-H.; Bindig, U.; Siggel, U. *J. Am. Chem. Soc.* **1993**, *115*, 11036.
(172) Fuhrhop, J.-H.; Bindig, U.; Siggel, U. *Chem. Comm.* **1994**, 1583.

(173) Siggel, U.; Bindig, U.; Schulz, A.; Fuhrhop, J.-H. *New J. Chem.* **1995**, *19*, 427.
(174) Endisch, C.; Boettcher, C.; Fuhrhop, J.-H. *J. Am. Chem. Soc.* **1995**, *117*, 8273.
(175) Tsuchida, E.; Komatsu, T.; Arai, K.; Yamada, K.; Nishide, H.; Boettcher, C.; Fuhrhop, J.-H. *Chem. Comm.* **1995**, 1063.
(176) Komatsu, T.; Yamada, K.; Tsuchida, E.; Siggel, U.; Boettcher, Fuhrhop, J.-H. *Langmuir* **1996**, *12*, 6242.
(177) Komatsu, T.; Yanagimoto, T.; Furubayashi, Y.; Wu, J.; Tsuchida, E.; *Langmuir* **1999**, *15*, 4427.
(178) Tamaru, S.; Nakamura, M.; Takeuchi, M.; Shinkai, S. *Org. Lett.* **2001**, *3*, 3631.
(179) Tamaru, S.-i.; Takeuchi, M.; Sano, M.; Slhinkai, S. *Angew. Chem.* **2002**, *114*, 881.
(180) Behrens, P.; Glaue, A. M. *Monatsh. Chem.* **2002**, *133*, 1405.
(181) Kimura, M.; Muto, T.; Takimoto, H.; Wada, K.; Ohta, K.; Hanabusa, K.; Shirai, H.; Bobayashi, N. *Langmuir* **2002**, *16*, 2078.
(182) Kobayashi, S.; Hanabusa, K.; Hamasaki, N.; Kimura, M.; Shirai, H. *Chem. Mater.* **2000**, *12*, 1523.
(183) Kölbel, M.; Beyersdorff, T.; Chen, X. H.; Tschierske, C.; Kain, J.; Diele, S. *J. Am. Chem. Soc.* **2001**, *123*, 6809.
(184) Cheng, X.; Prehm, M.; Das, M. K.; Kain, J.; Baumeister, U.; Diele, S.; Leine, D.; Blume, A.; Tschierske, C. *J. Am. Chem. Soc.* **2003**, *125*, 10977.
(185) Kölbel, M.; Beyersdorff, T.; Sletvold, I.; Tschierske, C.; Kain, J.; Diele S. *Angew. Chem.* **1999**, *111*, 1146−1149. Kölbel, M.; Beyersdorff, T.; Sletvold, I.; Tschierske, C.; Kain, J.; Diele S. *Angew. Chem., Int. Ed. Engl.* **1999**, *38*, 1077.
(186) Ramsden, J. J.; Roush, D. J.; Gill, D. S.; Kurrat, R.; Willson, R. C. *J. Am. Chem. Soc.* **1995**, *117*, 8511.
(187) El Kasmi, A.; Wallace, J. M.; Bowden, E. F.; Binet, S. M.; Linderman, R. J. *J. Am. Chem. Soc.* **1998**, *120*, 225.
(188) Hess, C. R.; Juda. G. A.; Dooley, D. M.; Amii, R. N.; Hill, M. G.; Winkler, J. R.; Gray, H. B. *J. Am. Chem. Soc.* **2003**, *125*, 7156.
(189) Sigal, G. B.; Mrksich, M.; Whitesides, G. M. *J. Am. Chem. Soc.* **1998**, *120*, 3464.
(190) Roberts, C.; Chen, C. S.; Mrksich, M.; Martichonok, V.; Ingber, D. E.; Whitesides, G. M. *J. Am. Chem. Soc.* **1998**, *120*, 6548.
(191) Yam, C.-M.; Xiao, Z.; Gu, J.; Boutet, S.; Cai, C. *J. Am. Chem. Soc.* **2003**, *125*, 7498.
(192) Cornell, B. Al; Braach-Maskvytis, V. L. B.; King, L. G.; Osman, P. D. J.; Raguse, B. *Nature* **1997**, *387*, 580.
(193) Douberly, G. E.; Pan, S.; Walters, D.; Matsui, H. *J. Phys. Chem. B* **2001**, *105*, 7612.
(194) Matsui, H.; Pan, S.; Douberly, G. E., Jr. *J. Phys. Chem. B.* **2001**, *105*, 1683.
(195) Matsui, H.; Porrata, P.; Douberly, G. E., Jr. *Nano Lett.* **2001**, *1*, 461.
(196) Cheung, C. L.; Camarero, J. A.; Woods, B. W.; Lin, T.; Johnson, J. E.; De Yoreo, J. J. *J. Am. Chem. Soc.* **2003**, *125*, 6848.
(197) Liu, B.; Gaylord, B. S.; Wang, S.; Bazan, G. C. *J. Am. Chem. Soc.* **2003**, *125*, 6705.
(198) Wang, P.; Liu, R.; Wu, X.; Ma, H.; Cao, X.; Zhou, P.; Zhang, J.; Wenig, X.; Zhang, X.-L.; Qi, J.; Zhou, X.; Wenig, L. *J. Am. Chem. Soc.* **2003**, *125*, 1116.

CR030602B